universität wien

MASTER'S THESIS

Title of the Master's Thesis

"Plane wave-based approximation methods for the Helmholtz equation"

submitted by
Paul Stocker, BSc

in partial fulfillment of the requirements for the degree of
Master of Science (MSc)

Vienna, 2017

degree programme code as it appears on the student record sheet:	A 066 821
degree programme as it appears on the student record sheet:	Mathematics
Supervisor:	Univ.-Prof. Ilaria Perugia, PhD

Contents

1 Introduction **3**

2 Helmholtz Equation **7**

3 Plane wave approximation of the homogeneous Helmholtz solution **9**
3.1 Vekua's Theory . . . 9
3.1.1 Continuity of the Vekua Operators . . . 14
3.2 Approximation by Harmonic Polynomials . . . 18
3.2.1 Approximation of Harmonic Functions . . . 19
3.2.2 Approximation of Homogeneous Helmholtz Solutions . . . 21
3.3 Approximation by Plane Waves . . . 23
3.3.1 A Stable Basis for the Plane Wave Space . . . 23
3.3.2 Approximation of Generalized Harmonic Polynomials . . . 24
3.3.3 Approximation of Homogeneous Helmholtz Solution by Plane Waves . . . 28

4 Plane Wave Methods **32**
4.1 Finite Element Spaces . . . 32
4.2 Virtual Element Method . . . 33
4.2.1 The projection operator Π . . . 33
4.2.2 The PW-VEM formulation . . . 34
4.2.3 Convergence Results . . . 35
4.2.4 Choice for the Stabilization Term . . . 36
4.2.5 Matrix Representation . . . 37
4.3 Discontinuous Galerkin Method . . . 41
4.3.1 PW-DG formulation . . . 41
4.3.2 Convergence Results . . . 43

5 Notes on Implementation **44**
5.1 PW-VEM . . . 44
5.1.1 Reconstructing the Solution . . . 44
5.2 PW-DG . . . 45

6 Numerical Results **47**
6.1 Effects of approximating the stabilization term in the PW-VEM . . . 47
6.2 The case of Triangular Meshes . . . 48
6.3 The case of Voronoi Meshes . . . 49
6.3.1 Smooth Solution . . . 49
6.3.2 Singular Solution . . . 51
6.3.3 Pollution Effect . . . 53
6.4 Non-Convex Mesh . . . 53
6.5 Escher Mesh . . . 54

7 Conclusions **55**

A Appendix **56**
A.1 Properties of the Bessel Function . . . 56
A.2 Matlab Code . . . 56

Notation

Denote $\mathbb{N} = \{0, 1, 2, 3, \dots\}$ the natural numbers including zero and let $n, N \in \mathbb{N}$. For multi-indices $\alpha \in \mathbb{N}^N, \alpha = (\alpha_1, \dots, \alpha_N)$ with length $|\alpha| := \sum_{j=1}^N \alpha_j$ we define

$$\boldsymbol{x}^\alpha := x_1^{\alpha_1} \cdots x_n^{\alpha_N} \qquad \boldsymbol{x} \in \mathbb{R}^N.$$

We will write D^α for the corresponding differential operator with respect to the space variable $\boldsymbol{x} \in \mathbb{R}^N$, that is

$$D^\alpha := \frac{\partial^{|\alpha|}}{\partial x_1^{\alpha_1} \cdots x_N^{\alpha_N}},$$

and use the common half-order $\alpha \leq \beta \Leftrightarrow \alpha_i \leq \beta_i,\ i = 1, \dots, N$.

For a domain $\Omega \subset \mathbb{R}^N$ we denote by $W^{n,p}(\Omega)$ the Sobolev spaces with regularity index n and summability index p. In the special case of $p = 2$ we write for the resulting Hilbert space $H^n(\Omega) := W^{n,2}(\Omega)$. The corresponding norms are defined as

$$\begin{aligned}
|u|_{W^{n,p}(\Omega)} &= \left(\sum_{\alpha \in \mathbb{N}^N, |\alpha| = n} \int_\Omega |D^\alpha u(\boldsymbol{x})|^p dx \right)^{\frac{1}{p}} \\
\|u\|_{W^{n,p}(\Omega)} &= \left(\sum_{j=1}^n |u|^p_{W^{j,p}(\Omega)} \right)^{\frac{1}{p}} \\
|u|_{n,\Omega} &= |u|_{W^{n,2}(\Omega)} \\
\|u\|_{n,\Omega} &= \|u\|_{W^{n,2}(\Omega)} \\
|u|_{W^{n,\infty}(\Omega)} &= \max_{\substack{\alpha \in \mathbb{N}^N \\ |\alpha| = n}} \|D^\alpha u(\boldsymbol{x})\|_{L^\infty(\Omega)} \\
\|u\|_{W^{n,\infty}(\Omega)} &= \max_{j=0,\dots,n} |u|_{W^{j,\infty}(\Omega)} \\
\|u\|^2_{s,\omega,\Omega} &= \sum_{j=0}^s \omega^{2(s-j)} |u|^2_{j,\Omega}.
\end{aligned}$$

We define the ω-weighted Sobolev norm by

$$\|u\|^2_{s,\omega,\Omega} := \sum_{j=0}^s \omega^{2(s-j)} |u|^2_{j,\Omega} \qquad \forall u \in H^s(\omega),\ \omega > 0.$$

1 Introduction

Standard polynomial finite element methods, require high degree polynomials to approximate the highly osculating solutions of the Helmholtz equation. A different approach to the problem is to switch out the polynomial trial space with a Trefftz space, i.e. a space of functions that solve the PDE on each element. Several possible choices are discussed in [17], such as generalized harmonic polynomials, plane waves, fundamental solutions and multi-pole expansions. We will present two methods using plane waves: the Plane Wave Discontinuous Galerkin method (PW-DG) and the Plane Wave Virtual Element Method (PW-VEM). We will describe the methods, discuss convergence properties and give an in depth numerical comparison of the two. Other Trefftz methods for the Helmholtz equation (also reviewed in [17]) include the ultra weak variational formulation (UWVF) see [7, 8], the partition of unity method (PUM) see [19].

The convergence analysis of the methods relies on best approximation estimates for plane waves. These estimates aim to show that there exists a series of functions, such that the approximation error goes to zero as either the mesh size is decreased (h-convergence) or the local approximation space is increased (p-convergence). A first attempt on an h-convergence estimate in two dimension was proved in [8], however the obtained order of convergence is not sharp. [20] delivered a p-estimate using complex analysis techniques and Vekua's theory. A similar approach was used in [24], however sharper estimates are achieved by using a more explicit definition of the Vekua operator. Including algebraic order of p-convergence in two dimensions and sharp algebraic order of h-convergence in 2- and 3-dimensions, made possible by using harmonic analysis instead of complex analysis techniques. On top of that, all bounding constants are explicit in the wave number. We will only review the 2-dimensional results, as they are presented in [24] (see also [22, 23]).

The VEM was first introduced very recently in [3] for the 2D Laplace equation as an evolution of the mimetic finite differences approach. The VEM, in general, consists of a VEM space which provides good approximation qualities for the solution, however its functions are not required to be explicitly computable on the element interior (hence the name 'Virtual'). The next step is to define a local projection onto a space with the main feature, that computation of the bilinear form is possible whenever one of its entries belongs to it. This space still needs to hold good approximation properties. Using the projection operator the bilinear form can be split into a computable term, and term which can be approximated (the stabilization term). The main advantages are, that no volume quadrature is needed for the computation of the bilinear form and the values of the functions in the VEM space are not required in the interior of the elements.

An extension of the VEM to the Helmholtz equation, incorporating plane waves into the trial and test spaces, along side a prove for h-convergence, was presented in [25]. For this PW-VEM, a low order VEM space is enriched with plane wave functions and projected onto the space of discontinuous plane wave functions. We need the restriction to a low order VEM space to guarantee that the enriched space is a partition of unity space (allowing results from the PUM to carry over).

We review this method and the accompanying convergence result. The h-convergence analysis has the standard requirement of a small enough mesh width, and the addition specific requirement that the stabilization term fulfills the discrete Gårding inequality. A sufficient condition and a possible choice are presented.

Since the numeric solution is produced in the VEM space, it is not trivial to reconstruct point wise values. This has been discussed in detail for the standard VEM in [2, 4]. We present and compare two different methods for the reconstruction of the PW-VEM solution.

The DG method was first introduced in 1973 by Reed and Hill. Since then, numerous variations for different problems have been presented. We will focus on the UWVF, which was originally introduced by Cessenat and Despres in [8], separate from the DG framework. However, using a special pair of fluxes in the DG method made it possible cast the UWVF in a DG setting.

We will present the DG approach to the UWVF as in [16] and will use it for numeric testing. A numeric comparison of the UWVF to similar PW-DG methods is already well established in [16]. The recast of the UWVF made it possible to apply DG convergence analysis to the method and prove low order h-convergence for the inhomogeneous Helmholtz problem, and high order h-convergence, as well as p-convergence, in the homogeneous case, see [13, 14, 7]. We will review the results relevant to the homogeneous case, covering algebraic p-convergence under the condition that p is large enough.

The outline of this thesis is as follows. After refreshing the basics of the Helmholtz equation in Section 2 we continue in Section 3 by reviewing the framework needed to present the plane wave best approximation estimates. This includes defining the Vekua operators, proving related important properties, and exploiting their connection to (generalized) harmonic functions to get the best approximation results. We go on to present the PW-VEM and PW-DG method in Section 4, and reviewing their convergence properties. Details on the implementation, are given in Section 5, along side a short discussion on the possible ways to reconstruct the VEM solution. Finally, we give an in-depth numeric comparison of the UWVF and the VEM (including both ways of reconstructing the solution) in Section 6.

At this point, I would like to express my gratitude to Prof. Ilaria Perugia for the countless meetings as well as the supervision and continuous support of my thesis.

Einleitung

Klassische Finite-Element-Methoden benötigen einen hohen Polynomgrad, um die stark oszillierenden Lösungen der Helmholtz-Gleichung ausreichend zu approximieren. Daher bietet es sich an, anstatt der Polynome einen sogenannten Trefftz-Raum zu benutzen. Dieser besteht aus Funktionen, die bereits eine Lösung der Differentialgleichung auf jedem finiten Element sind. Mehrere Möglichkeiten diesen Raum zu wählen wurden in [17] vorgestellt, unter anderem: generelle harmonische Polynome, ebene Wellen, fundamentale Lösungen und Multipolentwicklung. In dieser Arbeit werden zwei numerische Methoden präsentiert, die ebene Wellen implementieren: die ‚Plane Wave Discontinuous Galerkin' (PW-DG) Methode und die ‚Plane Wave Virtual Element Method' (PW-VEM). Es werden beide Methoden und ihre Konvergenzeigenschaften im Detail erläutert. Hauptaugenmerk liegt auf einem ausführlichen numerischen Vergleich der beiden. Andere in [17] besprochene Trefftz-Methoden für die Helmholtz-Gleichung sind die ‚Ultra Weak Variational Formulation' (UWVF), siehe auch [7, 8], und die ‚Partition of Unity Method' (PUM), siehe [19].

Grundlage für die Approximation mit ebenen Wellen bieten die Abschätzungen der besten Approximation. Diese Abschätzungen geben Auskunft über die Existenz einer Folge von Funktionen, die es erlaubt, den Fehler der Approximation gegen Null gehen zu lassen. Die Abschätzung ist gegeben bezüglich der Verfeinerung des Gitters (h-Konvergenz) oder der Vergrößerung des lokalen Approximations-Raumes (p-Konvergenz). In [24] wurde algebraische p-Konvergenz in zwei Dimensionen und algebraische h-Konvergenz in zwei und drei Dimensionen gezeigt, wobei alle Abschätzungen explizit in der Wellenzahl sind. Ein wichtiges Werkzeug für die Analysis stellt der Vekua-Operator dar. In dieser Arbeit werden ausschließlich die zweidimensionalen Resultate aus [24] (siehe auch [22, 23]) präsentiert.

Die VEM wurde erstmals 2013 in [3] für die 2D-Laplace-Gleichung vorgestellt. Damit ist sie noch eine äußerst 'junge' Methode. Allgemein gesprochen besteht die VEM aus einem VEM-Raum, der gute approximative Eigenschaften besitzt, jedoch Funktionen beinhaltet, die im Elementinneren nicht berechenbar sein müssen (daher der Name ‚Virtual'). Ein Schlüsselmerkmal der Methode ist die Definition einer Projektion auf einen weiteren Raum, der die Berechnung der Bilinearform immer dann erlaubt, wenn ein Eintrag zu besagtem Raum gehört. Die Wahl dieses Raumes gehört zu den Herausforderungen der VEM, da dieser ebenfalls gute approximative Eigenschaften besitzen soll. Mithilfe der neu definierten Projektion lässt sich die Bilinearform in einen berechenbaren Term und einen zu approximierenden Term (den sogenannten Stabilisationsterm) aufteilen. Ein Vorteil dieses Prozesses liegt darin, dass die Berechnung der Bilinearform keine Volumsquadratur benötigt.

In [25] wurde die VEM in Kombination mit ebenen Wellen zur Lösung der homogenen Helmholtz-Gleichung eingeführt. Für die daraus resultierende PW-VEM konnte, unter den Annahmen eines genügend feinen Gitters und der Erfüllung der Gårding-Ungleichung durch den Stabilisationsterm, h-Konvergenz bewiesen werden. Diese Resultate werden hier erneut präsentiert.

Ein Manko der VEM besteht darin, dass die numerische Lösung im VEM Raum erzeugt wird und daher nicht punktweise ausgewertet werden kann. Dies wurde bereits für die VEM behandelt, siehe [2, 4]. Für die PW-VEM werden hier zwei mögliche Arten der Rekonstruktion der PW-VEM-Lösung besprochen und numerische Resultate der beiden verglichen.

Die DG-Methode wurde 1973 von Reed und Hill eingeführt. Seither wurden unzählige Varianten für verschiedene Problemstellungen konzipiert. In der Arbeit wird ein Fokus auf die UWVF gelegt. Diese wurde zwar ursprünglich als eigenständige Methode von Cessenat und Despres in [8] erstellt, konnte jedoch später in [16] als Sonderfall der PW-DG-Methode nachgestellt werden. Diese Neufassung der UWVF machte es möglich, unter Beihilfe bestehender DG-Konvergenzanalysen, h-Konvergenz niedriger Ordnung für die inhomogene und h-Konvergenz hoher Ordnung sowie p-Konvergenz für die homogene Helmholtz-Gleichung zu zeigen, siehe [13, 14, 7]. Die Arbeit beschränkt sich auf die Resultate für die homogene Helmholtz-Gleichung.

Der grobe Umriss dieser Masterarbeit ist wie folgt: Nach einer kurzen Wiederholung der Basis zur Helmholtz-Gleichung in Kapitel 2 werden die Abschätzungen der besten Approximation für ebene Wellen in Kapitel 3 vorgestellt. Hierzu gehört die Herleitung wichtiger Werkzeuge wie die Definition der Vekua-Operatoren und deren Eigenschaften sowie deren Beziehung zu allgemeinen harmonischen Funktionen. In Kapitel 4 werden die PW-VEM und die PW-DG Methode präsentiert und ihre Konvergenzeigenschaften besprochen. Details zur Implementierung und Rekonstruktion der PW-VEM-Lösung sind in Kapitel 5 gegeben. Schlussendlich werden in Kapitel 6 beide Methoden ausführlich in numerischen Experimenten verglichen.

An dieser Stelle möchte ich mich sehr herzlich bei Prof. Ilaria Perugia für die zahlreichen Treffen, die anregenden Diskussionen und die Unterstützung beim Verfassen dieser Arbeit bedanken.

2 Helmholtz Equation

The Helmholtz boundary value problem in two dimensions on a domain $\Omega \subset \mathbb{R}^N$, $N \in \mathbb{N}$ states: Find $u : \Omega \to \mathbb{C}$ fulfilling

$$-\Delta u - \omega^2 u = f \qquad \text{in } \Omega \tag{2.1}$$
$$\nabla u \cdot \nu + i\omega\ u = g \qquad \text{on } \partial\Omega \tag{2.2}$$

where $\omega > 0$ is the wave number with corresponding wavelength $\lambda = 2\pi/\omega$, ν is the outer normal vector to $\partial\Omega$ and i is the imaginary unit, with given right hand side $f \in L^2(\Omega)$ and impedance boundary conditions on the whole boundary $\partial\Omega$ with datum $g \in L^2(\partial\Omega)$. We assume that the wavelength is shorter than the diameter of our domain, i.e. $\lambda < h$ or equivalently $\omega > 2\pi/h$. For the domain Ω we make the following assumptions:

Assumption 1. Let $\Omega \subset \mathbb{R}^N$ be a bounded open set such that

- $\partial\Omega$ is Lipschitz
- there exists $\rho \in (0, 1/2]$ such that $B_{\rho h} \subseteq \Omega$
- there exists $0 < \rho_0 < \rho$ such that Ω is star-shaped with respect to $B_{\rho_0 h}$

To find the variational formulation we multiply (2.1) with a test function $v \in H^1(\Omega)$, integrate by parts and plug in the boundary condition. Then the weak solution $u \in H^1(\Omega)$ needs to fulfill

$$b(u, v) = a(u, v) + i\omega \int_{\partial\Omega} u\bar{v}\ dS = \int_\Omega f\bar{v} + \int_{\partial\Omega} g\bar{v} \qquad \forall v \in H^1(\Omega) \tag{2.3}$$

where

$$a(u, v) = \int_\Omega \nabla u \cdot \overline{\nabla v}\ dV - \omega^2 \int_\Omega u\bar{v}\ dV. \tag{2.4}$$

For our analysis we introduce the weighted norm

$$\|u\|^2_{s,\omega,\Omega} := \sum_{j=0}^{s} \omega^{2(s-j)} |u|^2_{j,\Omega} \tag{2.5}$$

where $|.|_{j,\Omega}$ denotes the standard seminorm on $H^j(\Omega)$. Furthermore, let us denote by $\|.\|_{j,\Omega}$ the standard norm on $H^j(\Omega)$. The bilinear form $b(u, v)$ does not fulfill the requirements for Lax-Milgram Theorem as it is not coercive. However, we will now show continuity and a Gårding-type inequality (which turns out to be equal in our case) for the bilinear form $b(u, v)$, with respect to the introduced norm.

Lemma 2.1. *For $b(u, v)$ as in Equation (2.3) the following equalities hold:*

a) $\exists C_{cont} > 0$ such that $|b(u, v)| \le C_{cont}\|u\|_{1,\omega,\Omega}\|v\|_{1,\omega,\Omega}$ (continuity)

b) $Re(b(v, v)) = \|v\|^2_{1,\omega,\Omega} - 2\omega^2\|v\|^2_{0,\Omega}$ (Gårding inequality)

Proof. a) Cauchy-Schwarz inequality gives

$$|b(u, v)| \le \|\nabla u\|_{0,\Omega}\|\nabla v\|_{0,\Omega} + \omega^2\|u\|_{0,\Omega}\|v\|_{0,\Omega} + \omega\|u\|_{0,\partial\Omega}\|v\|_{0,\partial\Omega}.$$

The trace inequality provides an estimate of the third term, stating that $\exists C(\Omega) > 0$ depending on the domain, such that

$$\begin{aligned}\omega\|u\|_{0,\partial\Omega}\|v\|_{0,\partial\Omega} &\le C(\Omega)\omega\sqrt{\|u\|_{0,\Omega}\|v\|_{0,\Omega}\|\nabla u\|_{0,\Omega}\|\nabla v\|_{0,\Omega}} \\ &\le C(\Omega)(\omega^2\|u\|_{0,\Omega}\|v\|_{0,\Omega} + \|\nabla u\|_{0,\Omega}\|\nabla v\|_{0,\Omega}).\end{aligned}$$

Plugging this into the above inequality, the statement follows.

b) follows immediately from

$$Re(b(v,v)) = a(v,v) = \|\nabla v\|_{0,\Omega}^2 - \omega^2\|v\|_{0,\Omega}^2 = \|v\|_{1,\omega,\Omega}^2 - 2\omega^2\|v\|_{0,\Omega}^2.$$

□

Because we are not able to apply Lax-Milgram theorem we now find another way to show existence and uniqueness for the solution.

Proposition 2.2. *The variational problem Equation* (2.3) *is well-posed.*

Proof. Let us first show that the solution is unique. We have to show that if u satisfies

$$\int_\Omega \nabla u \cdot \overline{\nabla v}\, dV - \omega^2 \int_\Omega u\bar{v}\, dV + i\omega \int_{\partial\Omega} u\bar{v}\, dS = 0$$

then $u \equiv 0$. Let u be a solution of the above equation. First, the imaginary part of the equation has to be zero and by setting $u = v$ it follows that $u = 0$ on $\partial\Omega$. Second, notice that for any domain $\tilde{\Omega} \supset \Omega$ the extended function

$$\tilde{u}(\boldsymbol{x}) = \begin{cases} u(x) & \text{if } \boldsymbol{x} \in \Omega \\ 0 & \text{if } \boldsymbol{x} \in \tilde{\Omega} \setminus \Omega \end{cases}$$

satisfies the above equations, with Ω replaced $\tilde{\Omega}$, as well. Then the unique continuation principle [18, Ch. 4.3] states that $\tilde{u} \equiv 0$. Hence, Equation (2.3) has indeed a unique solution. By Fredholm's alternative [18, Ch. 2.2] we get existence of a solution, if we can show uniqueness of the solution of the adjoint problem. The adjoint problem is given by $\overline{b(u,v)} = 0$ and uniqueness can be shown analogous to above. □

In the following we consider the homogeneous Helmholtz equation, which is given by Equation (2.1) with zero source term, i.e.

$$\begin{aligned} -\Delta u - \omega^2 u &= 0 && \text{in } \Omega \\ \nabla u \cdot \nu + i\omega\, u &= g && \text{on } \partial\Omega \end{aligned} \tag{2.6}$$

3 Plane wave approximation of the homogeneous Helmholtz solution

The main goal of this section is to find an error estimate for the approximation of the homogeneous Helmholtz solution by plane waves. This, however, is not a straight forward task. We will take a detour through generalized harmonic functions. In fact, we will use generalized harmonic polynomials to approximate the solution of the Helmholtz equation and then, in turn, we shall approximate generalized harmonic polynomials with plane waves.

Generalized harmonic functions are solutions to the Helmholtz equation that arise naturally as an image of harmonic functions under the Vekua operator. Thus, we start by introducing the Vekua operators in Section 3.1 and discuss important properties that will help us find good error estimates later on.

Once we have set up the link between harmonic functions and solutions of the Helmholtz equation we will introduce (generalized) harmonic functions and polynomials in Section 3.2. The error estimates for approximating harmonic functions by harmonic polynomials are presented in Section 3.2.1 followed by estimates for approximating Helmholtz solutions by generalized harmonic polynomials in Section 3.2.2.

At this point we are done with our detour and are finally ready to introduce plane wave spaces in Section 3.3. After finding an error estimate for the approximation of generalized harmonic polynomials by plane waves, we finish this section by finding error estimates for approximating the Holmholtz solution by plane waves in Theorem 3.20.

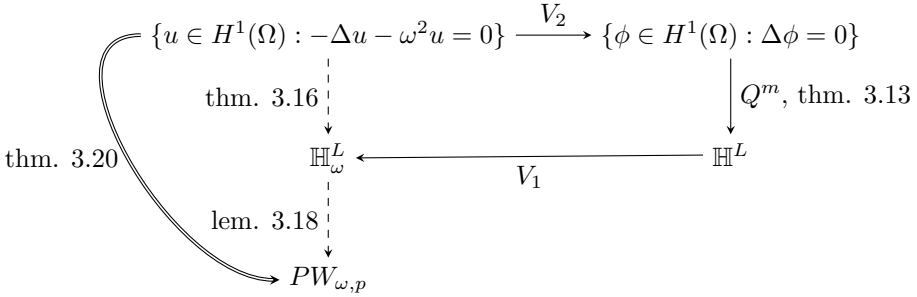

Figure 1: The diagram shows the work we need to do, to approximate homogeneous Helmholtz solution (top left) by plane waves (bottom left). We first follow the solid lines using Vekua operators V_1, V_2, approximation by harmonic polynomials $\mathbb{H}^L$, to approximate the Helmholtz solution by generalized harmonic polynomials $\mathbb{H}^L_\omega$. Second, we approximate those by plane waves, so we can finally combine the two result along the dashed lines in Theorem 3.20.

3.1 Vekua's Theory

A function $u \in H^1(\Omega)$ that fulfills Laplace's equation, i.e. $\Delta u = 0$, is called a *harmonic function*. The Vekua operators build a bridge between harmonic functions and the solutions of the Helmholtz equation. This makes them an important tool for the convergence analysis, as will become apparent later on. Without any further ado let us introduce the Vekua operators.

Definition 3.1. For Ω as in Assumption 1, the Vekua operator V_1 and the inverse Vekua operator V_2 are defined by

$$\begin{aligned} &V_1, V_2 : L^\infty(\Omega) \to L^\infty(\Omega) \\ &V_j[\phi](x) = \phi(x) + \int_0^1 M_j(x,t)\phi(tx)\ dt \qquad \forall \phi \in C(\Omega),\ \forall x \in \Omega,\ j = 1,2 \end{aligned} \tag{3.1}$$

where $M_1, M_2 : \Omega \times [0,1) \to \mathbb{R}$ are continuous functions defined by

$$\begin{aligned} &M_1, M_2 : \Omega \times [0,1) \to \mathbb{R}, \\ &M_1(x,t) = \frac{\omega|x|}{2} \frac{\sqrt{t}^{N-2}}{\sqrt{1-t}}\ J_1(\omega|x|\sqrt{1-t}) \\ &M_2(x,t) = -\frac{i\omega|x|}{2} \frac{\sqrt{t}^{N-3}}{\sqrt{1-t}}\ J_1(i\omega|x|\sqrt{t(1-t)}) \end{aligned}$$

and J_1 denotes the 1-st Bessel function of the first kind.

Let us recall that the Bessel functions of the first kind $J_\nu(z)$ are defined by

$$J_\nu(z) = \sum_{t=0}^{\infty} \frac{(-1)^t}{t!\Gamma(t+\nu+1)} \left(\frac{z}{2}\right)^{2t+\nu}, \qquad \forall \nu, z \in \mathbb{C} \tag{3.2}$$

where Γ denotes the Gamma function.

As the name already gives away the operators are inverse, and as we already mentioned they map harmonic functions to solutions of the Helmholtz equation and vice versa. Let us show these important properties.

Theorem 3.2. *For Ω as in Assumption 1, the Vekua operators satisfy the following:*

i) V_1 and V_2 are inverse, i.e.

$$V_1[V_2[\phi]] = V_2[V_1[\phi]] = \phi \qquad \forall \phi \in L^\infty(\Omega)$$

ii) For harmonic $\phi \in C(\Omega)$, i.e. $\Delta\phi = 0$ in Ω, then

$$-\Delta V_1[\phi] - \omega^2 V_1[\phi] = 0 \qquad \text{in } \Omega$$

iii) For $u \in H^1(\Omega)$ with $-\Delta u - \omega^2 u = 0$ in Ω, we have

$$\Delta V_2[u] = 0 \qquad \text{in } \Omega$$

Proof. i) Substituting $t = \frac{s}{|x|}$ in the definition of V_1 gives

$$\begin{aligned} V_1[\phi](x) &= \phi(x) + \int_0^{|x|} M_1(x, \frac{s}{|x|})\phi(s\frac{x}{|x|})\frac{1}{|x|}\ ds \\ &= \phi(x) - \int_0^{|x|} \frac{\omega|x|}{2} \sqrt{\frac{s}{|x|}}^{N-2} \frac{\sqrt{|x|}}{\sqrt{|x|-s}} \frac{1}{|x|} J_1(\omega\sqrt{|x|(|x|-s)})\phi(s\frac{x}{|x|})\ ds \end{aligned}$$

Similar for V_2

$$\begin{aligned} V_2[\phi](x) &= \phi(x) + \int_0^{|x|} M_2(x, \frac{s}{|x|})\phi(s\frac{x}{|x|})\frac{1}{|x|}\ ds \\ &= \phi(x) - \int_0^{|x|} \frac{i\omega|x|}{2} \sqrt{\frac{s}{|x|}}^{N-3} \frac{\sqrt{|x|}}{\sqrt{|x|-s}} \frac{1}{|x|} J_1(i\omega\sqrt{s(|x|-s)})\phi(s\frac{x}{|x|})\ ds \end{aligned}$$

For convenience we introduce the function

$$\begin{aligned} &g : [0,\infty) \times [0,\infty) \to \mathbb{R} \\ &g(r,s) = \frac{\omega s\sqrt{r}}{2\sqrt{r-s}} J_1(\omega\sqrt{r(r-s)}) \end{aligned}$$

with which we can rewrite the above as

$$V_1[\phi](x) = \phi(x) - \int_0^{|x|} \frac{s^{\frac{N-4}{2}}}{|x|^{\frac{N-2}{2}}} g(|x|, s)\phi(s\frac{x}{|x|})\ ds$$
$$V_2[\phi](x) = \phi(x) + \int_0^{|x|} \frac{s^{\frac{N-4}{2}}}{|x|^{\frac{N-2}{2}}} g(s, |x|)\phi(s\frac{x}{|x|})\ ds$$

Note that in the second equation the arguments in g are swapped, as we made use of $\sqrt{s-|x|} = i\sqrt{|x|-s}$, since $s \leq |x|$ for $t \in [0,1]$.

$$\begin{aligned}
V_1[V_2[\phi]](x) &= V_2[\phi](x) - \int_0^{|x|} \frac{s^{\frac{N-4}{2}}}{|x|^{\frac{N-2}{2}}} g(|x|, s)\ V_2[\phi](s\frac{x}{|x|})\ ds \\
&= \phi(x) + \int_0^{|x|} \frac{s^{\frac{N-4}{2}}}{|x|^{\frac{N-2}{2}}} g(s, |x|)\phi(s\frac{x}{|x|})\ ds \\
&\quad - \int_0^{|x|} \frac{s^{\frac{N-4}{2}}}{|x|^{\frac{N-2}{2}}} g(|x|, s) \left[\phi(s\frac{x}{|x|}) + \int_0^s \frac{z^{\frac{N-4}{2}}}{|x|^{\frac{N-2}{2}}} g(z, s)\phi(z\frac{x}{|x|})\ dz\right]\ ds \\
&= \phi(x) + \int_0^{|x|} \frac{s^{\frac{N-4}{2}}}{|x|^{\frac{N-2}{2}}} \left(g(s, |x|) - g(|x|, s)\right)\phi(s\frac{x}{|x|})\ ds \\
&\quad - \int_0^{|x|} \frac{z^{\frac{N-4}{2}}}{|x|^{\frac{N-2}{2}}} \phi(z\frac{x}{|x|}) \int_z^{|x|} \frac{1}{s} g(z, s)g(|x|, s)\ ds\ dz.
\end{aligned}$$

In the last step we are able to apply Fubini's theorem, as the Bessel function is bounded (Equation (A.2)). Similar calculations show that $V_1[V_2[\phi]] = V_2[V_1[\phi]]$ and therefore we only need to show that V_2 is the right inverse to V_1.

It is left to show that

$$g(t, r) - g(r, t) = \int_t^r \frac{1}{s} g(t, s)g(r, s)\ ds \tag{3.3}$$

then $V_1[V_2[\phi]] = \phi$ follows immediately from the above. To do so, we prepare the following three equalities that will come in handy afterwards.

First, notice that using Equation (3.2) we can write

$$g(r, t) = \frac{\omega^2 rt}{4} \sum_{\ell \geq 0} \frac{(-1)^\ell \omega^{2\ell} r^\ell (r-t)^\ell}{2^{2\ell}\ell!\ (\ell+1)!} \tag{3.4}$$

Second, we use this to calculate

$$g(t, r) - g(r, t) = \frac{\omega^2 rt}{4} \sum_{\ell \geq 0} \frac{(-1)^\ell \omega^{2\ell} (r-t)^\ell ((-t)^\ell - r^\ell)}{2^{2\ell}\ell!\ (\ell+1)!} \tag{3.5}$$

Third, we pre-calculate the following integral using the change of variables $z = \frac{s-t}{r-t}$ and the following property of the Beta function: $B(p, q) = \int_0^1 (1-z)^{p-1} z^{q-1}\ dz = \frac{(p-1)!(q-1)!}{(p+q-1)!}$.

$$\begin{aligned}
\int_t^r s(r-s)^n (t-s)^m\ ds &= (-1)^m (r-t)^{n+m+1} \int_0^1 (1-z)^n z^m (zr + (1-z)t)\ dz \\
&= (-1)^m (r-t)^{n+m+1} \frac{n!m!}{(n+m+2)!} (r(m+1) + t(n+1))
\end{aligned} \tag{3.6}$$

We are ready to prove Equation (3.3),

$$
\begin{aligned}
&\int_t^r \frac{g(t,s)\ g(r,s)}{s}\ ds \\
&\overset{(3.4)}{=} \frac{\omega^2 rt}{4} \sum_{n,m\geq 0} \frac{(-1)^{n+m}\omega^{2(n+m+1)} r^n t^m}{2^{2(n+m+1)} n!(n+1)!m!(m+1)!} \int_t^r \frac{s^2 (r-s)^n (t-s)^m}{s}\ ds \\
&\overset{(3.6)}{=} \frac{\omega^2 rt}{4} \sum_{n,m\geq 0} \frac{(-1)^{n}\omega^{2(n+m+1)} r^n t^m (r-t)^{n+m+1}}{2^{2(n+m+1)} (n+1)!(m+1)!(n+m+2)!} (r(m+1)+t(n+1)) \\
&\overset{\ell=n+m+1}{=} \frac{\omega^2 rt}{4} \sum_{\ell\geq 1} \frac{\omega^{2\ell}(r-t)^\ell}{2^{2\ell}(\ell+1)!}\ \frac{1}{\ell!} \sum_{n=0}^{\ell-1} \ell! \frac{(-1)^n r^n t^{\ell-n-1}}{(n+1)!(\ell-n)!} (r(\ell-n)+t(n+1)) \\
&= \frac{\omega^2 rt}{4} \sum_{\ell\geq 1} \frac{\omega^{2\ell}(r-t)^\ell}{2^{2\ell}(\ell+1)!\ell!} \sum_{n=0}^{\ell-1} \left[-\binom{\ell}{n+1} (-r)^{n+1} t^{\ell-n-1} + \binom{\ell}{n} (-r)^n t^{\ell-n} \right] \\
&= \frac{\omega^2 rt}{4} \sum_{\ell\geq 1} \frac{\omega^{2\ell}(r-t)^\ell}{2^{2\ell}(\ell+1)!\ell!} \left[-(t-r)^\ell + t^\ell + (t-r)^\ell - (-r)^\ell \right] \\
&\overset{(3.5)}{=} g(t,r) - g(r,t)
\end{aligned}
$$

this proves the first part.

ii) Since ϕ is harmonic and therefore satisfies the Laplace's equation we have by [10, Thm.3, Sec. 6.3.1] infinite differentiability in the interior of Ω, i.e. $\phi \in C^\infty(\Omega)$. We start by computing some helpful identities:

$$
\begin{aligned}
\frac{\partial}{\partial|x|} M_1(x,t) &= \omega\sqrt{1-t} \frac{\partial}{\partial(\omega|x|\sqrt{1-t})} \left[-\frac{\sqrt{t}^{N-2}}{2(1-t)} \omega|x|\sqrt{1-t}\ J_1(\omega|x|\sqrt{1-t}) \right] \\
&\overset{(A.1)}{=} -\frac{\omega^2|x|\sqrt{t}^{N-2}}{2} J_0(\omega|x|\sqrt{1-t})
\end{aligned}
$$

We denote with Δ the Laplacian with respect to x. Changing the variable of differentiation from x to $|x|$, since M_1 depends only on $|x|$, and applying the previous result we get

$$
\begin{aligned}
\Delta M_1(x,t) &= \frac{\partial}{\partial|x|} M_1(x,t)\ (\Delta|x|) + \frac{\partial^2}{\partial|x|^2} M_1(x,t)\ (\nabla|x|)^2 \\
&= \frac{\partial}{\partial|x|} M_1(x,t) \frac{N-1}{|x|} + \frac{\partial^2}{\partial|x|^2} M_1(x,t) \\
&= -\frac{\omega^2\sqrt{t}^{N-2}}{2} (N\ J_0(\omega|x|\sqrt{1-t}) - \omega|x|\sqrt{1-t}\ J_1(\omega|x|\sqrt{1-t}))
\end{aligned}
$$

Furthermore, we calculate the following expression that will arise in the integral of $V_1[\phi]$ later on

$$
\begin{aligned}
\Delta\left(M_1(x,t)\phi(tx)\right) &= \Delta M_1(x,t)\phi(tx) + 2\nabla M_1(x,t)\cdot\nabla\phi(tx) + M_1(x,t)\Delta\phi(xt) \\
&= \Delta M_1(x,t)\phi(tx) + 2\frac{\partial}{\partial|x|} M_1(x,t) \frac{x}{|x|}\cdot t\nabla\phi\Big|_{tx} + 0 \\
&= \Delta M_1(x,t)\phi(tx) + 2\frac{t}{|x|}\frac{\partial}{\partial|x|} M_1(x,t)\ \frac{\partial}{\partial t}\phi(tx).
\end{aligned}
$$

since $\frac{\partial}{\partial t}\phi(tx) = x\cdot\nabla\phi\Big|_{tx}$.

For readability we introduce the function $f_1 : [0,h] \times [0,1] \to \mathbb{R}$

$$f_1(r,t) = \sqrt{t}^N \; J_0(\omega r\sqrt{1-t})$$

with the properties

$$\begin{aligned}
&\frac{\partial}{\partial t} f_1(r,t) = \frac{N\sqrt{t}^{N-2}}{2} \; J_0(\omega r\sqrt{1-t}) + \frac{\sqrt{t}^N \omega r}{2\sqrt{1-t}} \; J_1(\omega r\sqrt{1-t}),\\
&f_1(r,0) = 0, \qquad f_1(r,1) = 1.
\end{aligned}$$

We are ready to show that $V_1[\phi]$ solves the homogeneous Helmholtz equation:

$$\begin{aligned}
(\Delta + \omega^2)V_1[\phi](x) &= \Delta\phi(x) + \omega^2\phi(x) + \int_0^1 \Delta\left(M_1(x,t)\phi(tx)\right) \; dt + \int_0^1 \omega^2 M_1(x,t)\phi(tx) \; dt\\
&= \omega^2\phi(x) - \omega^2 \int_0^1 \sqrt{t}^N \; J_0(\omega|x|\sqrt{1-t}) \frac{\partial}{\partial t}\phi(tx) \; dt\\
&\quad - \omega^2 \int_0^1 \left(\frac{N\sqrt{t}^{N-2}}{2} \; J_0(\omega|x|\sqrt{1-t}) - \frac{\omega|x|\sqrt{t}^{N-2}}{2} \frac{1-t}{\sqrt{1-t}} J_1(\omega|x|\sqrt{1-t}) \right.\\
&\quad \left. + \frac{\omega|x|\sqrt{t}^{N-2}}{2\sqrt{1-t}} J_1(\omega|x|\sqrt{1-t}) \right) \phi(tx) \; dt\\
&= \omega^2\phi(x) - \omega^2 \int_0^1 \left(f_1(|x|,t)\frac{\partial}{\partial t}\phi(tx) + \frac{\partial}{\partial t} f_1(|x|,t)\phi(tx) \right) \; dt\\
&= \omega^2 \left(\phi(x) - \left[f_1(|x|,t)\phi(tx) \right]_{t=0}^{t=1} \right) = 0.
\end{aligned}$$

As $t \in [0,1]$ we have that ϕ is only evaluated at values in $[0,x] \subset \Omega$ since Ω is star shaped. Hence the values of the function ϕ and of its derivative are well defined and since $\phi \in C^\infty(\Omega)$, the fundamental theorem of calculus applies.

iii) The prove follows the lines of part ii). The result we used in the beginning of part ii), [10, Thm.3, Sec. 6.3.1], carries over to solutions of the homogeneous Helmholtz equation, therefore $u \in C^\infty(\Omega)$.
We start by computing the same derivatives as above, this time for M_2.

$$\begin{aligned}
\frac{\partial}{\partial|x|} M_2(x,t) &= \frac{\omega^2|x|\sqrt{t}^{N-2}}{2} J_0(i\omega|x|\sqrt{t(1-t)})\\
\Delta M_2(x,t) &= \frac{\omega^2\sqrt{t}^{N-2}}{2}(N \; J_0(i\omega|x|\sqrt{t(1-t)}) - i\omega|x|\sqrt{t(1-t)} \; J_1(i\omega|x|\sqrt{t(1-t)})\\
\Delta\left(M_2(x,t)u(tx)\right) &= \Delta M_2(x,t)u(tx) + 2\frac{t}{|x|}\frac{\partial}{\partial|x|}M_2(x,t) \; \frac{\partial}{\partial t}u(tx) - \omega^2 t^2 M_2(x,t)u(tx).
\end{aligned}$$

We introduce an auxiliary function $f_2 : [0,h] \times [0,1] \to \mathbb{R}$

$$f_2(r,t) = \sqrt{t}^N \; J_0(i\omega r\sqrt{t(1-t)})$$

with the properties

$$\begin{aligned}
&\frac{\partial}{\partial t} f_2(r,t) = \frac{N\sqrt{t}^{N-2}}{2} \; J_0(i\omega r\sqrt{t(1-t)}) + \frac{i\omega r\sqrt{t}^N(1-2t)}{2\sqrt{t(1-t)}} J_1(i\omega r\sqrt{t(1-t)}),\\
&f_2(r,0) = 0, \qquad f_2(r,1) = 1.
\end{aligned}$$

With this preparations we are ready to conclude the prove.

$$\begin{aligned}\Delta V_2[u](x) &= \Delta u(x) + \int_0^1 \Delta \left(M_2(x,t)u(tx)\right)\ dt \\ &= -\omega^2 u(x) + \omega^2 \int_0^1 \sqrt{t}^N\ J_0(i\omega|x|\sqrt{t(1-t)})\frac{\partial}{\partial t}u(tx)\ dt \\ &\quad + \int_0^1 \frac{\omega^2\sqrt{t}^{N-2}}{2}\Big(N\ J_0(i\omega|x|\sqrt{t(1-t)}) \\ &\quad - i\omega|x|\sqrt{t}\frac{1-t}{\sqrt{1-t}}J_1(i\omega|x|\sqrt{t(1-t)} + \frac{i\omega|x|t\sqrt{t}}{\sqrt{1-t}}J_1(i\omega|x|\sqrt{t(1-t)}\Big)\ u(tx)\ dt \\ &= -\omega^2 u(x) + \omega^2 \int_0^1 \left(f_2(|x|,t)\frac{\partial}{\partial t}u(tx) + \frac{\partial}{\partial t}f_2(|x|,t)u(tx)\right)\ dt = 0\end{aligned}$$

□

3.1.1 Continuity of the Vekua Operators

We will show that the Vekua operators are bounded. In general, we say that an operator between two normed spaces $V : X \to Y$ is bounded, if for some $C > 0$ it holds that $\|V[\phi]\|_Y \leq C\|\phi\|_X$ for all $\phi \in X$. Combined with the fact that the Vekua operators are linear we get continuity. Indeed, this holds for any linear bounded operator V, since for any $\phi, \psi \in X$, ψ not equal zero, $\|V[\phi+\psi] - V[\phi]\|_Y = \|V[\psi]\|_Y \leq C\|\psi\|_X \xrightarrow{\psi\to 0} 0$ shows that V is in fact C-Lipschitz.

For us, the continuity results will play a major role in finding error estimates of the approximation of the Helmholtz solution by plane waves, and therefore we aim for explicit continuity constants.

Theorem 3.3. *Let be Ω a domain as in Assumption 1. Let ϕ and u be as in Theorem 3.2 ii) and iii), respectively, and $N \geq 2$. Then the following continuity estimate holds:*

$$\|V_1[\phi]\|_{j,\omega,\Omega} \leq C_1(N)\rho^{\frac{1-N}{2}}(1+j)^{\frac{3}{2}N+\frac{1}{2}}e^j(1+(\omega h)^2)\|\phi\|_{j,\omega,\Omega}. \tag{3.7}$$

Restricting $N = 2, 3$ the following estimates for V_2 hold:

$$\|V_2[u]\|_{j,\omega,\Omega} \leq C_2(N,\omega h,\rho)(1+j)^{\frac{3}{2}N-\frac{1}{2}}e^j\|u\|_{j,\omega,\Omega} \tag{3.8}$$

where $C_1 > 0$ depends on the space dimension N, and $C_2 > 0$ depends on the product ωh of wavenumber and domain size, and the shape parameter ρ. A more explicit estimate for V_2 reads

$$\|V_2[u]\|_{j,\omega,\Omega} \leq C_3\rho^{\frac{1-N}{2}}(1+j)^{\frac{3}{2}N-\frac{1}{2}}e^j(1+(\omega h)^4)e^{\frac{3}{4}(1-\rho)\omega h}\|u\|_{j,\omega,\Omega} \tag{3.9}$$

for $C_3 \geq 0$ depending on the space dimension N. In the L^∞-norm we have continuity with

$$\|V_2[u]\|_{L^\infty(\Omega)} \leq \left(1 + \frac{((1-\rho)\omega h)^2}{4}e^{\frac{1}{2}(1-\rho)\omega h}\right)\|u\|_{L^\infty(\Omega)}. \tag{3.10}$$

In order to prove Theorem 3.3 the following preliminary results are necessary. All proves of which, and a detailed discussion, can be found in [24, Sec 1.2] (see also [23, 24]). In the following we will present [24, Lemma 1.2.3-12], often in reduced form, only keeping the parameters relevant for our analysis.

Lemma 3.4 ([24, Lemma 1.2.2])**.** *For $\xi = 1, 2$, $n \geq 0$ and $\phi \in H^n(\Omega)$, we have*

$$|V_\xi[\phi]|^2_{n,\Omega} \leq 2|\phi|^2_{n,\Omega} + 2(1+n)^{3N-2}e^{2n}\sum_{j=0}^{n}\sup_{t\in[0,1]}|M_\xi(\cdot,t)|^2_{W^{n-j,\infty}(\Omega)}\sum_{|\beta|=j}\int_0^1\int_\Omega |D^\beta\phi(tx)|^2\ dx\ dt \tag{3.11}$$

Next, we review bounds to treat each term in Equation (3.11). The supremum term in (3.11) can be bounded using the following result: For $n \geq 0$ the functions M_1, M_2 fulfill

$$\sup_{t\in[0,1]} |M_1(\cdot,t)|_{W^{n,\infty}}(\Omega) \leq \omega^n(n+(\omega h)^2) \tag{3.12}$$

$$\sup_{t\in[0,1]} |M_2(\cdot,t)|_{W^{n,\infty}}(\Omega) \leq \omega^n(1+\omega h)e^{\frac{3}{4}(1-\rho)\omega h} \tag{3.13}$$

$$\sup_{t\in[0,1]} |M_2(\cdot,t)|_{W^{0,\infty}(\Omega)} \leq \frac{((1-\rho)\omega h)^2}{4} e^{\frac{1}{2}(1-\rho)\omega h} \tag{3.14}$$

$$\tag{3.15}$$

see [24, Lemma 1.2.3] for more detail. For the last term in Equation (3.11) we will use a reduced version of [24, Lemma 1.2.4] stating: For $\phi \in H^{\omega}(\Omega, \beta \in \mathbb{N}^2$ multi-index of length $|\beta| = j$ and D^{β} the corresponding differentiable operator in the variable x, we have that

$$\int_0^1 \int_{\Omega} |D^{\beta}\phi(tx)|^2 \, dx \, dt \leq \left(\frac{2}{\rho}\right)^{N-1} \|D^{\beta}\phi\|^2_{0,\Omega} + \left(\frac{2}{\rho}\right)^{2j+1} \frac{|\Omega|}{2\omega+1} \|D^{\beta}\phi\|^2_{L^{\infty}(B_{\frac{\rho h}{2}})} \tag{3.16}$$

where $|\Omega|$ denotes the measure of Ω.

In order to estimate the last term in Equation (3.16) we need estimates for $\|D^{\beta}\phi\|$ in the interior of Ω (see [24, Lemma 1.2.8-13]).We will consider the cases where ϕ is a harmonic function, then the bound follows immediately from the mean value theorem for harmonic functions, and the case where ϕ is a solution to the Helmholtz equation.

Lemma 3.5 (Interior estimates for harmonic functions)**.** *Let the function ϕ be harmonic in $B_R(x_0)$, with $R > 0$. Then*

$$|\phi(x)|^2 \leq \frac{1}{R^N|B_1|} \|\phi\|^2_{0,B_r(x_0)} \tag{3.17}$$

where $|B_1| = \frac{\pi^{\frac{N}{2}}}{\Gamma(\frac{N}{2}+1)}$ is the volume of the unit ball in $\mathbb{R}^N$. If $\phi \in H^n(\Omega)$ and $\beta \in \mathbb{N}^N$, $|\beta| \leq n$ then

$$\|D^{\beta}\phi\|^2_{L^{\infty}(B_{\frac{\rho h}{2}})} \leq \frac{1}{|B_1|} \left(\frac{2}{\rho h}\right)^N \|D^{\beta}\phi\|^2_{0,\Omega} \tag{3.18}$$

Lemma 3.6 (Interior estimate for Helmholtz solutions)**.** *Let $u \in H^1(B_R(x_0))$ be a solution of the inhomogeneous Helmholtz equation with right hand side $f \in H^1(B_R(x_0))$ and $N \geq 2$, then there exists a constant $C > 0$ depending only on the space dimension N, such that*

$$\begin{aligned}
&\text{if } N = 2: \\
&\|u\|_{L^{\infty}(B_{\frac{R}{2}}(x_0))} \leq CR^{-1}\Big[\left(1+\omega^2R^2\right)\|u\|_{0,B_R(x_0)} + R\|\nabla u\|_{0,B_R(x_0)} + R^2\|f\|_{0,B_R(x_0)}\Big] \\
&\text{if } N = 3,4,5: \\
&\|u\|_{L^{\infty}(B_{\frac{R}{2}}(x_0))} \leq CR^{-\frac{N}{2}}\Big[\left(1+\omega^2R^2\right)\|u\|_{0,B_R(x_0)} + R\|\nabla u\|_{0,B_R(x_0)} + R^2\|f\|_{0,B_R(x_0)} \\
&\qquad\qquad + R^3\|\nabla f\|_{0,B_R(x_0)}\Big] \\
&\text{if } N = 2,3: \\
&\|\nabla u\|_{L^{\infty}(B_{\frac{R}{2}}(x_0))} \leq CR^{-\frac{N}{2}}\Big[\left(1+\omega^2R^2\right)\|\nabla u\|_{0,B_R(x_0)} + \omega^2R\|u\|_{0,B_R(x_0)} + R\|f\|_{0,B_R(x_0)} \\
&\qquad\qquad + R^2\|\nabla f\|_{0,B_R(x_0)}\Big]
\end{aligned}$$

Remark 3.7. For the homogeneous Helmholtz equation the bounds in Lemma 3.6 can be reduced to

$$\begin{aligned} &\text{if } N = 2,3,4,5: \\ &\|u\|_{L^\infty(B_{\frac{R}{2}}(x_0))} \leq CR^{-\frac{N}{2}} \Big[\left(1+\omega^2 R^2\right) \|u\|_{0,B_R(x_0)} + R\|\nabla u\|_{0,B_R(x_0)} \Big] \end{aligned} \tag{3.19}$$

$$\begin{aligned} &\text{if } N = 2,3: \\ &\|\nabla u\|_{L^\infty(B_{\frac{R}{2}}(x_0))} \leq CR^{-\frac{N}{2}} \Big[\left(1+\omega^2 R^2\right) \|\nabla u\|_{0,B_R(x_0)} + \omega^2 R\|u\|_{0,B_R(x_0)} \Big] \end{aligned} \tag{3.20}$$

where C only depends on the space dimension N.

Now that we collected all important results, we are ready to proof the continuity bounds of the Vekua operators.

Proof of Theorem 3.3. We start with Equation (3.7). Using Equation (3.11) with $\xi = 1$. We start by inserting Equations (3.12) and (3.16)

$$\begin{aligned} |V_1[\phi]|^2_{n,\Omega} &\overset{(3.11)}{\leq} 2|\phi|^2_{n,\Omega} + 2(1+n)^{3N-2}e^{2n} \sum_{j=0}^{n} \sup_{t\in[0,1]} |M_1(\cdot,t)|^2_{W^{n-j,\infty}(\Omega)} \sum_{|\beta|=j} \int_0^1 \int_\Omega |D^\beta \phi(tx)|^2 \, dx \, dt \\ &\overset{(3.12),\,(3.16)}{\leq} 2|\phi|^2_{n,\Omega} + 2(1+n)^{3N-2}e^{2n} \sum_{j=0}^{n} \omega^{2(n-j)}(n-j+(\omega h)^2)^2 \\ &\quad \cdot \left(\left(\frac{2}{\rho}\right)^{N-1} |\phi|^2_{j,\Omega} + \left(\frac{\rho}{2}\right)^{2j+1} \frac{|\Omega|}{2j+1} \sum_{|\beta|=j} \|D^\beta \phi\|^2_{L^\infty(B_{\frac{\rho h}{2}})} \right) \\ &\overset{(3.18)}{\leq} 2|\phi|^2_{n,\Omega} + 2(1+n)^{3N-2}e^{2n} \sum_{j=0}^{n} \omega^{2(n-j)}(n-j+(\omega h)^2)^2 \\ &\quad \cdot \left(\left(\frac{2}{\rho}\right)^{N-1} |\phi|^2_{j,\Omega} + \left(\frac{\rho}{2}\right)^{2j+1} \frac{|\Omega|}{2j+1} \frac{1}{|B_1|} \left(\frac{2}{\rho h}\right)^N \sum_{|\beta|=j} \|D^\beta \phi\|^2_{0,\Omega} \right) \\ &\leq C_1(1+n)^{3N-2+2}e^{2n}(1+(\omega h)^2)^2 \sum_{j=0}^{n} \omega^{2(n-j)} \left(\rho^{1-N} + \rho^{2j+1}\frac{|\Omega|}{h^2} \right) |\phi|^2_{j,\Omega} \end{aligned}$$

for $C_1 > 0$ depending only on N. Recall that we assumed that ϕ is harmonic, and we can therefore apply the interior estimate (3.18). Finally, we use $|\Omega| \leq h^N$ and $\rho < 1$ and by taking the square root we get

$$|V_1[\phi]|_{n,\Omega} \leq C_1 \rho^{\frac{1-N}{2}} (1+n)^{\frac{3}{2}N} e^n (1+(\omega h)^2) \|\phi\|_{n,\omega,\Omega}$$

In order to find the bound for the complete Sobolev norm, we sum up the bounds for the seminorms, giving the additional factor of $(1+n)^{\frac{1}{2}}$ on the right hand side.

To prove Equations (3.8) and (3.9) we first need to bound $\|D^\beta u\|_{L^\infty(B_{\frac{\rho h}{2}})}$ on the full domain, for a solution of the homogeneous Helmholtz equation $u \in H^n$ and multi index β, $|\beta| = n$. To this end we will use the interior estimates for Helmholtz solutions. In the case $n = 0$ we use Equation (3.19) and get

$$\begin{aligned} \|D^\beta u\|_{L^\infty(B_{\frac{\rho h}{2}})} &= \|u\|_{L^\infty(B_{\frac{\rho h}{2}})} \\ &\leq C(\rho h)^{-\frac{N}{2}} \Big[\left(1+(\omega\rho h)^2\right) \|u\|_{0,\Omega} + \rho h \|\nabla u\|_{0,\Omega} \Big]. \end{aligned} \tag{3.21}$$

For $n \geq 1$ we want to apply Equation (3.20) and therefore we use that there exists another multi-index α, with $|\alpha| = n-1$, such that

$$\begin{aligned}\|D^\beta u\|_{L^\infty(B_{\frac{\rho h}{2}})} &\leq \|\nabla D^\alpha u\|_{L^\infty(B_{\frac{\rho h}{2}})} \\ &\leq C(\rho h)^{-\frac{N}{2}}\left[\omega^2\rho h\|D^\alpha u\|_{0,\Omega} + \left(1+(\omega\rho h)^2\right)\|\nabla D^\alpha u\|_{0,\Omega}\right].\end{aligned} \tag{3.22}$$

Note that Equation (3.20) is only valid for $N = 2, 3$. To estimate the sum over all multi-indices β, let us first look at the sets of multi-indices that we will deal with. On one hand we have all multi-indices $\beta = (\beta_1, \dots, \beta_N)$ with length $j \geq 1$, that is $\{(\beta_1, \dots, \beta_N) : |\beta| = j\}$, on the other hand ∇D^α will alter the multi-index $\alpha = (\alpha_1, \dots, \alpha_N)$ such that it can be written in the form $\cup_{n=1,\dots,N}\{(\alpha_1, \dots, \alpha_n+1, \dots, \alpha_N) : |\alpha| = j-1\}$. The two sets contain the same elements, however considering the second set as a multi set, it contains $N\binom{N+j-2}{N-2}$ elements with a maximum of N repetitions. Thus we can estimate

$$\begin{aligned}\sum_{|\alpha|=j-1}\|\nabla D^\alpha u\|_{0,\Omega}^2 &= \sum_{|\alpha|=j-1}\int_\Omega (D^{(\alpha_1+1,\dots,\alpha_N)}u)^2 + \dots + (D^{(\alpha_1,\dots,\alpha_N+1)}u)^2\, dS \\ &\leq \sum_{|\beta|=j} N\|D^\beta u\|_{0,\Omega}^2 = N|u|_{j,\Omega}^2.\end{aligned}$$

This allows us to conclude

$$\begin{aligned}\sum_{|\beta|=j}\|D^\beta u\|_{L^\infty(B_{\frac{\rho h}{2}})}^2 &\leq \sum_{|\alpha|=j-1}\|\nabla D^\alpha u\|_{L^\infty(B_{\frac{\rho h}{2}})}^2 \\ &\overset{(3.22)}{\leq} \sum_{|\alpha|=j-1} C_N(\rho h)^{-2}\left[\omega^2\rho h\|D^\alpha u\|_{0,\Omega} + \left(1+(\omega\rho h)^2\right)\|\nabla D^\alpha u\|_{0,\Omega}\right]^2 \\ &\leq C_N(\rho h)^{-2}\left[\omega^4\rho^2h^2|u|_{j-1,\Omega}^2 + \left(1+(\omega\rho h)^2\right)^2|u|_{j,\Omega}^2\right],\end{aligned} \tag{3.23}$$

where $C_N > 0$ only depends on N. We are ready to estimate V_2. Similar to the case of V_1, we use Equation (3.11), this time with $\xi = 2$ and insert Equations (3.13) and (3.16)

$$\begin{aligned}|V_2[u]|_{n,\Omega}^2 &\leq C_N|u|_{n,\Omega} + (1+n)^{3N-2}e^{2n}\sum_{j=0}^n \omega^{2(n-j)}(1+\omega h)^2 e^{\frac{3}{2}(1-\rho)\omega h} \\ &\quad\cdot\left(\rho^{1-N}|u|_{j,\Omega} + \rho^{2j+1}\frac{|\Omega|}{2j+1}\sum_{|\beta|=j}\|D^\beta u\|_{L^\infty(B_{\frac{\rho h}{2}})}^2\right) \\ &\leq Ce^{2n}(1+n)^{3N-2}(1+\omega h)^2 e^{\frac{3}{2}(1-\rho)\omega h} \\ &\quad\cdot\sum_{j=0}^n \omega^{2(n-j)}\left(\rho^{1-N}|u|_{j,\Omega}^2 + \rho^{2j+1}|\Omega|\sum_{|\beta|=j}\|D^\beta u\|_{L^\infty(B_{\frac{\rho h}{2}})}^2\right)\end{aligned}$$

Next, we take the square root on both sides and split up the sum into the cases $j = 0$ and $j \geq 0$ where we apply the above results

$$
\begin{aligned}
|V_2[u]|_{n,\Omega} &\overset{(3.21)}{\overset{(3.23)}{\leq}} Ce^n(1+n)^{\frac{3}{2}N-1}(1+\omega h)e^{\frac{3}{4}(1-\rho)\omega h} \\
&\quad \cdot \Bigg[\omega^{2n}\rho^{1-N}\left(\|u\|_{0,\Omega}^2 + \frac{|\Omega|}{h^N}(1+(\omega\rho h)^2)^2\Big(\|u\|_{0,\Omega}+\rho h\|\nabla u\|_{0,\Omega}\Big)^2\right) \\
&\quad + \sum_{j=1}^{n}\omega^{2(n-j)}\rho^{1-N}\left(|u|_{j,\Omega}^2 + \rho^{2j}\frac{|\Omega|}{h^N}\Big(\omega^4\rho^2h^2|u|_{j-1,\Omega}^2 + \big(1+(\omega\rho h)^2\big)^2|u|_{j,\Omega}^2\Big)\right)\Bigg]^{\frac{1}{2}} \\
&\leq Ce^n(1+n)^{\frac{3}{2}N-1}(1+\omega h)e^{\frac{3}{4}(1-\rho)\omega h}\rho^{\frac{1-N}{2}} \\
&\quad \cdot \Bigg[\omega^{2n}(1+\omega h)^2\Big(\|u\|_{0,\Omega}+h\|\nabla u\|_{0,\Omega}\Big)^2 \\
&\quad + \sum_{j=1}^{n}\omega^{2(n-j)}\left(\omega^4h^2|u|_{j-1,\Omega}^2 + \big(1+(\omega h)^2\big)^2|u|_{j,\Omega}^2\right)\Bigg]^{\frac{1}{2}} \\
&\leq Ce^n(1+n)^{\frac{3}{2}N-1}(1+\omega h)e^{\frac{3}{4}(1-\rho)\omega h}\rho^{\frac{1-N}{2}} \\
&\quad \cdot \Bigg[\Big((1+\omega h)^2\omega^{2n}\|u\|_{0,\Omega}^2 + ((\omega h)^2+(\omega h)^6)\omega^{2(n-1)}\|\nabla u\|_{0,\Omega}^2 \\
&\quad + \omega^2h^2\sum_{j=1}^{n}\omega^{2(n-j+1)}|u|_{j-1,\Omega}^2 + \big(1+(\omega h)^2\big)^2\sum_{j=1}^{n}\omega^{2(n-j)}|u|_{j,\Omega}^2\Bigg]^{\frac{1}{2}} \\
&\leq Ce^n(1+n)^{\frac{3}{2}N-1}(1+(\omega h)^4)e^{\frac{3}{4}(1-\rho)\omega h}\rho^{\frac{1-N}{2}}\|u\|_{n,\omega,\Omega}
\end{aligned}
$$

where we used $\frac{|\Omega|}{h^2} \leq 1$. Passing to the complete norm adds a factor of $(1+n)^{\frac{1}{2}}$ on the right hand side. This proves Equation (3.9) and Equation (3.8) follows immediately.

Finally, we prove (3.10) by plugging in the definition of V_2 and using Equation (3.14) we get

$$
\begin{aligned}
\|V_2[u]\|_{L^\infty(\Omega)} &\leq \big(1+\|M_2\|_{L^\infty(\Omega\times[0,1])}\big)\,\|u\|_{L^\infty(\Omega)} \\
&\leq \left(1+\frac{((1-\rho)\omega h)^2}{4}e^{\frac{1}{2}(1-\rho)\omega h}\right)\|u\|_{L^\infty(\Omega)}
\end{aligned}
$$

completing the proof. □

3.2 Approximation by Harmonic Polynomials

From now on out we restrict ourselfs to the two dimensional case. In addition to harmonic functions, that we have already encountered in the beginning of Section 3.1, we now give the following related definitions.

Definition 3.8. For a domain $\Omega \subset \mathbb{R}^2$ we denote with $\mathbb{P}^L(\Omega)$ the space of homogeneous polynomials of degree L on the domain Ω. The subspace of *harmonic polynomials* is then given by

$$\mathbb{H}^L(\Omega) = \{P \in \mathbb{P}^L(\Omega) : \Delta P = 0\}.$$

We define the *generalized harmonic polynomials* $\mathbb{H}_\omega^L(\Omega)$ of degree L, as the image of the harmonic polynomials under V_1, that is

$$\mathbb{H}_\omega^L(\Omega) = V_1[\mathbb{H}^L(\Omega)] = \{Q \in L^2(\Omega) : \exists P \in \mathbb{H}^L(\Omega) \text{ s.t. } Q = V_1[P]\}.$$

The introduced vector spaces are of dimension

$$
\begin{aligned}
\dim \mathbb{P}^0 = \dim \mathbb{H}^0 = \dim \mathbb{H}_\omega^0 &= 1 \\
\dim \mathbb{H}^L = \dim \mathbb{H}_\omega^L &= 2 \qquad \forall L \geq 1.
\end{aligned}
$$

In order to get a better grip on harmonic functions under the Vekua transform we provide the following lemma.

Lemma 3.9 ([24, Lemma 1.3.2])**.** *Let $\phi \in L^2(\Omega)$ be an ℓ-homogeneous function with $\ell \in \mathbb{R},\ \ell > -1$, i.e., there exists $g \in L^2(S^1)$ such that*

$$\phi(\boldsymbol{x}) = g\left(\frac{\boldsymbol{x}}{|\boldsymbol{x}|}\right)|\boldsymbol{x}|^\ell,$$

then its Vekua transform is

$$V_1[\phi](\boldsymbol{x}) = \Gamma(\ell+1)\left(\frac{2}{\omega}\right)^\ell g\left(\frac{\boldsymbol{x}}{|\boldsymbol{x}|}\right) J_\ell(\omega|\boldsymbol{x}|) \qquad a.e.\ \boldsymbol{x} \in \Omega \tag{3.24}$$

Remark 3.10. With the standard identification $\mathbb{R}^2 \cong \mathbb{C}$ and writing the complex variable as $z = re^{i\psi}$ we can apply applying Lemma 3.9 to the special case of the polynomial

$$P(z) = \sum_{\ell=-L}^{L} a_\ell r^{|\ell|} e^{i\ell\psi}$$

which then gives

$$V_1[P](z) = \sum_{\ell=-L}^{L} a_\ell |\ell|! \left(\frac{2}{\omega}\right)^{|\ell|} e^{i\ell\psi} J_{|\ell|}(\omega r). \tag{3.25}$$

3.2.1 Approximation of Harmonic Functions

To approximate harmonic functions by polynomials we proceed similar as in the well-known general case, where we approximate functions with the Taylor polynomial. However, to ensure that the approximating polynomial is also harmonic, we rely on the following definition.

Definition 3.11. Let Ω be a domain as in Assumption 1 and ψ be a smooth cut-off function such that

$$\text{supp } \psi = B_{\rho_0 h}, \qquad \int_{B_{\rho_0 h}} \psi = 1, \qquad \|\psi\|_{L^\infty(B_{\rho_0 h})} \leq C\frac{1}{(\rho_0 h)^2}$$

for some independent $C > 0$.

Let $\phi \in H^{m-1}(\Omega)$ and $\boldsymbol{y} \in B_{\rho_0 h}$. Fot the Taylor polynomial of order m of ϕ centered at $\boldsymbol{y}$ we write $T^m_{\boldsymbol{y}}[\phi](\boldsymbol{x}) = \sum_{|\alpha|<m} \frac{1}{\alpha!} D^\alpha \phi(\boldsymbol{y})(\boldsymbol{x}-\boldsymbol{y})^\alpha$. We then define the *averaged Taylor polynomial* of order m of ϕ as

$$\begin{aligned} Q^m\phi(\boldsymbol{x}) &= \int_{B_{\rho_0 h}} T^m_{\boldsymbol{y}}[\phi](\boldsymbol{x})\psi(\boldsymbol{y})\ d\boldsymbol{y} && (3.26)\\ &= \int_{B_{\rho_0 h}} \sum_{|\alpha|<m} \frac{1}{\alpha!} D^\alpha\phi(\boldsymbol{y})(\boldsymbol{x}-\boldsymbol{y})^\alpha\psi(\boldsymbol{y})\ d\boldsymbol{y} && (3.27)\end{aligned}$$

From Equation (3.26) is immediately follows that $Q^m\phi(\boldsymbol{x})$ is a polynomial of degree at most $m-1$. It is possible to extend the definition to accommodate $\phi \in L^1(B_{\rho_0 h})$, see [6, Proposition 4.1.12].

We can calculate the derivative of for every multi-index β with $|\beta| \leq m-1$ to be

$$\begin{aligned} D^\beta Q^m\phi(\boldsymbol{x}) &= \int_{B_{\rho_0 h}} \sum_{\substack{|\alpha|<m\\ \alpha\geq\beta}} \frac{1}{\alpha!} D^\alpha\phi(\boldsymbol{y}) \frac{\alpha!}{(\alpha-\beta)!}(\boldsymbol{x}-\boldsymbol{y})^{\alpha-\beta}\psi(\boldsymbol{y})\ d\boldsymbol{y}\\ &\overset{\gamma=\alpha-\beta}{=} \int_{B_{\rho_0 h}} \sum_{|\gamma|<m-|\beta|} \frac{1}{\gamma!} D^{\beta+\gamma}\phi(\boldsymbol{y})(\boldsymbol{x}-\boldsymbol{y})^\gamma\psi(\boldsymbol{y})\ d\boldsymbol{y}\\ &= Q^{m-|\beta|}D^\beta\phi(\boldsymbol{x}). \end{aligned} \tag{3.28}$$

This result and the linearity of Q^m allows us to show that if ϕ is harmonic then $Q^m\phi$ is harmonic as well, for every $m \in \mathbb{N}$. Indeed,

$$\Delta Q^m\phi = \left(\frac{\partial^2}{\partial \boldsymbol{x}_1^2} + \frac{\partial^2}{\partial \boldsymbol{x}_2^2}\right) Q^m\phi = Q^{m-2}\left(\frac{\partial^2}{\partial \boldsymbol{x}_1^2} + \frac{\partial^2}{\partial \boldsymbol{x}_2^2}\right)\phi = Q^{m-2}\Delta\phi = 0.$$

Therefore, $Q^m\phi \in \mathbb{H}^{m-1}(\Omega)$ for every harmonic function ϕ.

Proposition 3.12 ([6, Prop. 4.2.8])**.** *The remainder term of the averaged Taylor polynomial $R^m u = u - Q^m u$ is given by*

$$R^m u(\boldsymbol{x}) = m \sum_{|\alpha|=m} \int_{C_{\boldsymbol{x}}} \frac{1}{\alpha!}(\boldsymbol{x}-\boldsymbol{z})^\alpha k(\boldsymbol{x},\boldsymbol{z}) D^\alpha u(u)\ d\boldsymbol{z} \tag{3.29}$$

where $C_{\boldsymbol{x}}$ denotes the convex hull of $\{\boldsymbol{x}\} \cup B_{\rho_0 h}$ and

$$|k(\boldsymbol{x},\boldsymbol{z})| \le C\left(1 + \frac{1}{\rho_0 h}|\boldsymbol{x}|\right)^2 |\boldsymbol{x}-\boldsymbol{z}|^{-2} \le C\left(1+\frac{1}{\rho_0}\right)^2 |\boldsymbol{x}-\boldsymbol{z}|^{-2} \tag{3.30}$$

We now aim for an estimate of the remainder that shows h- and p-convergence of the approximation. Similar to the Bramble-Hilbert lemma, we present in Theorem 3.13 a bound in terms of the Sobolev semi-norm of the harmonic function and the diameter of the domain, thus showing h-convergence.

Theorem 3.13 (Bramble-Hilbert for harmonic functions, h-estimate)**.** *Let Ω be a domain as in Assumption 1 and let $\phi \in H^m(\Omega)$ be a harmonic function for $m \in \mathbb{N}$, then*

$$|\phi - Q^m\phi|_{j,\Omega} \le C(\rho_0)(1+j)^{\frac{1}{2}} h^{m-j} |\phi|_{m,\Omega}, \qquad j = 0,\dots,m \tag{3.31}$$

where $C(\rho_0) > 0$ depends on ρ_0.

Proof. If $j = m$ we have that $|\phi - Q^m\phi|_{m,\Omega} = |\phi|_{m,\Omega}$, since the derivative vanishes. Let us assume $0 \le j < m$.

For $f \in L^2(\Omega)$ let us define

$$g(\boldsymbol{x}) = \int_\Omega |\boldsymbol{x}-\boldsymbol{z}|^{m-2}|f(\boldsymbol{z})|\ d\boldsymbol{z}.$$

We compute

$$\begin{aligned}
\|g\|_{0,\Omega}^2 &= \int_\Omega \left(\int_\Omega |\boldsymbol{x}-\boldsymbol{z}|^{m-2}|f(\boldsymbol{z})|\ d\boldsymbol{z}\right)^2 d\boldsymbol{x} \\
&= \int_\Omega \langle |\boldsymbol{x}-.|^{\frac{m-2}{2}}, |\boldsymbol{x}-.|^{\frac{m-2}{2}}|f|\rangle_{L^2(\Omega)}^2\ d\boldsymbol{x} \\
&\le \int_\Omega \||\boldsymbol{x}-.|^{\frac{m-2}{2}}\|_{0,\Omega}^2\ \||\boldsymbol{x}-.|^{\frac{m-2}{2}}|f|\|_{0,\Omega}^2\ d\boldsymbol{x} \\
&= \int_\Omega \left(\int_\Omega |\boldsymbol{x}-\boldsymbol{z}|^{(m-2)}\ d\boldsymbol{z}\right)\ \left(\int_\Omega |\boldsymbol{x}-\boldsymbol{z}|^{(m-2)}|f(\boldsymbol{z})|^2\ d\boldsymbol{z}\right)\ d\boldsymbol{x} \\
&\le \int_\Omega \left(|\boldsymbol{x}-\boldsymbol{z}|^{m-2}\ d\boldsymbol{x}\right)|f(\boldsymbol{z})|^2\ d\boldsymbol{z}|S^1|\frac{h^m}{m} \\
&\le |S^1|^2\frac{h^{2m}}{m^2}\|f\|_{0,\Omega}^2 = \pi^2\frac{h^{2m}}{m^2}\|f\|_{0,\Omega}^2
\end{aligned} \tag{3.32}$$

using Cauchy-Schwarz inequality and

$$\int_\Omega |\boldsymbol{x}-\boldsymbol{z}|^{m-2}\ d\boldsymbol{x} \le |S^1|\int_0^h r^{m-2} r\ dr = |S^1|\frac{h^m}{m} \qquad \boldsymbol{z} \in \Omega.$$

Without loss of generality we restrict ourselves to a domain with $h = 1$, since we can scale any generic domain in such a way.

We start by computing the inequality for $j = 0$, recall that $C_{\boldsymbol{x}}$ denotes the convex hull of $\{\boldsymbol{x}\} \cup B_{\rho_0 h}$. Therefore $C_{\boldsymbol{x}} \subset \Omega$, since Ω is star shaped with respect to the ball $B_{\rho_0 h}$.

$$\begin{aligned}
\|\phi - Q^m\phi\|_{0,\Omega} &\overset{(3.29)}{\leq} m \sum_{|\alpha|=m} \frac{1}{\alpha!} \left\| \int_{C_{\boldsymbol{x}}} (\boldsymbol{x}-\boldsymbol{z})^\alpha k(\boldsymbol{x},\boldsymbol{z}) D^\alpha \phi(\boldsymbol{z})\, dt \right\|_{0,\Omega} \\
&\overset{(3.30)}{\leq} mC \left(1 + \frac{1}{\rho_0}\right)^2 \sum_{|\alpha|=m} \frac{1}{\alpha!} \left\| \int_{\Omega} |\boldsymbol{x}-\boldsymbol{z}|^{m-2} |D^\alpha \phi(\boldsymbol{z})|\, d\boldsymbol{z} \right\|_{0,\Omega} \\
&\overset{(3.32)}{\leq} mC_{\rho_0} \sum_{|\alpha|=m} \frac{1}{\alpha!} \frac{\pi}{m} \|D^\alpha \phi\|_{0,\Omega} \\
&\leq C_{\rho_0} |\phi|_{m,\Omega} \frac{1+m}{(\lfloor \frac{m}{2} \rfloor !)^2} \\
&\leq C_{\rho_0} |\phi|_{m,\Omega}
\end{aligned} \tag{3.33}$$

since $\alpha! \geq (\lfloor \frac{m}{2} \rfloor !)^2$. For $0 < j < m$ we calculate

$$\begin{aligned}
|\phi - Q^m\phi|_{j,\Omega} &\overset{(3.28)}{=} \left[\sum_{|\beta|=j} \|D^\beta \phi - Q^{m-j} D^\beta \phi\|_{0,\Omega} \right]^{\frac{1}{2}} \\
&\overset{(3.33)}{\leq} C_{\rho_0} \left[\sum_{|\beta|=j} |D^\beta \phi|^2_{m-j,\Omega} \right]^{\frac{1}{2}} \\
&\leq C_{\rho_0} (1+j)^{\frac{1}{2}} |\phi|_{m,\Omega}.
\end{aligned}$$

The statement follows from a scaling argument. □

The above estimate is sharp in h, however does not converge in polynomials degree L. With the additional assumption we introduce below, we are able to get a sharp estimate for *hp*-convergence.

Definition 3.14. A domain Ω satisfies the *exterior cone condition* with angle $\pi\lambda$, $\lambda \in [0,1]$ if for every $z \in \mathbb{C} \setminus \Omega$ there is a cone $C \subset \mathbb{C} \setminus \Omega$ with vertex in z and congruent to

$$C_0(\lambda\pi, r) = \{x \in \mathbb{C} \mid 0 < \arg(x) < \lambda\pi, |x| < r\}.$$

Theorem 3.15 ([21, Theorem 2.9])**.** *Let $\Omega \subset \mathbb{R}^2$ be a domain as in Assumption 1 that satisfies the exterior cone condition with angle $\lambda\pi$ and $\phi \in H^m$ a harmonic function, for an integer $m \geq 0$. Then for every $L \geq m-1$ there exists a harmonic polynomial P_L of degree L such that*

$$|\phi - P_L|_{j,\Omega} \leq C\ h^{m-j} \left(\frac{\log(L+2)}{L+2} \right)^{\lambda(m-j)} |\phi|_{m,\Omega} \qquad j = 0, \ldots, m, \tag{3.34}$$

where the constant $C > 0$ depends only on m and the shape of Ω.

3.2.2 Approximation of Homogeneous Helmholtz Solutions

Now that we have established the error estimates for approximating harmonic functions with harmonic polynomials, we can use the Vekua transform to transfer everything to solutions of the homogeneous Helmholtz equation and generalized harmonic polynomials.

Theorem 3.16. *Let $\Omega \subset \mathbb{R}^2$ be a domain as in Assumption 1, $m \in \mathbb{N}$ and $u \in H^{m+1}$ be a solution of the homogeneous Helmholtz equation. Then the following statements hold true.*

i) (h-estimate, explicit in ωh)

For every $L \leq m$ there exists a generalized harmonic polynomial Q_L of degree at most L such that, for ever $j \leq L+1$ is holds that

$$\|u - Q_L\|_{j,\omega,\Omega} \leq C(L+1)^{6+\frac{1}{2}} e^{L+j}(1+(\omega h)^{j+6}) h^{L+1-j} e^{\frac{3}{4}(1-\rho)\omega h} \|u\|_{L+1,\omega,\Omega} \tag{3.35}$$

where the constant $C > 0$ depends only on ρ, ρ_0 but is independent of h, ω, L, j and u. This holds for $Q_L = V_1[Q^{L+1}V_2[u]]$.

ii) (hp-estimate)

If Ω satisfies the exterior cone condition with angle $\lambda\pi$, then for every $L \geq k$ there exist a generalized harmonic polynomial Q'_L of degree at most L such that, for every $j \leq k+1$, it holds

$$\|u - Q'_L\|_{j,\omega,\Omega} \leq C(1+(\omega h)^{j+6}) e^{\frac{3}{4}(1-\rho)\omega h} \left(\frac{\log(K+2)}{L+2}\right)^{\lambda(k+1-j)} h^{k+1-j} \|u\|_{k+1,\omega,\Omega} \tag{3.36}$$

where $C > 0$ dpeneds only on the shape of Ω, j and k, but is independent of h, ω, L and u. This holds for $Q'_L = V_1[P'^L]$ where P'^L is the polynomials approximating $V_2[u]$ provided by Theorem 3.15.

Proof. i) Set $Q_L = V_1[Q^{L+1}V_2[u]]$ and using the linearity and inverse properties of the Vekua operator, shown in Theorem 3.2, we get

$$\begin{aligned}
\|u - Q_L\|^2_{j,\omega,\Omega} &= \|V_1[V_2[u] - Q^{L+1}V_2[u]]\|^2_{j,\omega,\Omega} \\
&\overset{(3.7)}{\leq} C(1+j)^7 e^{2j}(1+(\omega h)^2)^2 \sum_{\ell=0}^{j} \omega^{2(j-\ell)} |V_2[u] - Q^{L+1}V_2[u]|^2_{\ell,\Omega} \\
&\overset{(3.31)}{\leq} C(1+j)^7 e^{2j}(1+(\omega h)^2)^2 \sum_{\ell=0}^{j} \omega^{2(j-\ell)}(1+\ell) h^{2(L+1-\ell)} |V_2[u]|^2_{L+1,\Omega} \\
&\leq C(1+j)^8 e^{2j}(1+(\omega h)^{j+2})^2 h^{2(L+1-j)} |V_2[u]|^2_{L+1,\Omega} \\
&\overset{(3.9)}{\leq} C(1+j)^8 e^{2j}(1+(\omega h)^{j+2})^2 h^{2(L+1-j)} \\
&\quad \cdot (L+2)^5 e^{2(L+1)}(1+(\omega h)^4)^2 e^{\frac{3}{2}(1-\rho)\omega h} \|u\|^2_{L+1,\omega,\Omega} \\
&\leq C(L+1)^{13} e^{2(L+j)}(1+(\omega h)^{j+6})^2 h^{2(L+1-j)} e^{\frac{3}{2}(1-\rho)\omega h} \|u\|^2_{L+1,\omega,\Omega}.
\end{aligned}$$

ii) Choose $Q'_L = V_1[P'^L]$ where P'^L is the polynomials approximating $V_2[u]$ provided by Theorem 3.15, then

$$\begin{aligned}
\|u - Q'_L\|^2_{j,\omega,\Omega} &\overset{(3.7)}{\leq} C(1+j)^7 e^{2j}(1+(\omega h)^2)^2 \sum_{\ell=0}^{j} \omega^{2(j-\ell)} |V_2[u] - P'^L|^2_{\ell,\Omega} \\
&\overset{(3.34)}{\leq} C(1+(\omega h)^2)^2 \sum_{\ell=0}^{j} \omega^{2(j-\ell)} h^{2(k+1-j)} \cdot \left(\frac{\log(L+2)}{L+2}\right)^{\lambda(k+1-\ell)} |V_2[u]|^2_{k+1,\Omega} \\
&\leq C(1+(\omega h)^{j+2})^2 \left(\frac{\log(L+2)}{L+2}\right)^{\lambda(k+1-\ell)} h^{2(k+1-j)} |V_2[u]|^2_{k+1,\Omega} \\
&\overset{(3.9)}{\leq} C(1+(\omega h)^{j+6})^2 e^{\frac{3}{4}(1-\rho)\omega h} \left(\frac{\log(L+2)}{L+2}\right)^{\lambda(k+1-\ell)} h^{2(k+1-j)} \|u\|^2_{k+1,\omega,\Omega}.
\end{aligned}$$

□

3.3 Approximation by Plane Waves

For wave propagation problems like the homogeneous Helmholtz equation, a non-polynomial trial space has shown to be efficient. Therefore we introduce the space of *plane wave functions* given by

$$PW_{\omega,p}(\mathbb{R}^2) := \left\{ u \in C^\infty(\mathbb{R}^2) : \ u(\mathbf{x}) = \sum_{j=1}^{p} \alpha_l \ e^{i\omega \mathbf{x}\cdot \mathbf{d}_j} \right\} \tag{3.37}$$

spanned by the directions $d_j \in \mathbb{S}^1$, where the unit sphere is denoted by $\mathbb{S}^1 = \{\mathbf{x} \in \mathbb{R}^2 : \ |\mathbf{x}| = 1\}$.

3.3.1 A Stable Basis for the Plane Wave Space

For small wave numbers the basis of the plane wave space $\{e^{i\omega \mathbf{x}\cdot \mathbf{d}_j}\}_{j=1,\dots,p}$ becomes ill-conditioned since the basis functions tend to linearly depend. We therefore start by introducing a different basis that is stable with respect to the limit $\omega \to 0$.

An important tool for this is the Jacobi-Anger expansion, providing an expansion of plane waves into circular waves, given by

$$e^{ir\cos\theta} = \sum_{\ell \in \mathbb{Z}} i^\ell J_\ell(r) e^{i\ell\theta} \qquad \forall r \geq 0, \theta \in [0, 2\pi] \tag{3.38}$$

the proof of this is given in [9, Sec. 2.4].

Lemma 3.17. *Let the plane wave directions be*

$$\boldsymbol{d}_\ell = (\cos\theta_\ell, \sin\theta_\ell) \qquad \ell = -q, \dots, q, \qquad \boldsymbol{d}_\ell \neq \boldsymbol{d}_m \quad \forall \ell \neq m$$

and define the matrix A as

$$A = \{A_{\ell,m}\}_{\substack{\ell=-q,\dots,q \\ m=-q,\dots,q}} = \{e^{-i\ell\theta_m}\}_{\substack{\ell=-q,\dots,q \\ m=-q,\dots,q}} \in \mathbb{C}^{2q+1,2q+1}.$$

Then a stable basis for the plane wave space, defined in Equation (3.37)*, with respect to the limit $\omega \to 0$ is given by*

$$b_\ell(\boldsymbol{x}) := (-i)^\ell \gamma_\ell |\ell|! \left(\frac{1}{\omega}\right)^{|\ell|} \sum_{m=-q}^{q} (A^{-t})_{\ell,m} e^{i\omega \boldsymbol{x}\cdot \boldsymbol{d}_m} \tag{3.39}$$

where

$$\gamma_\ell = \begin{cases} 1 & \text{for } \ell \geq 0 \\ (-1)^\ell & \text{for } \ell < 0. \end{cases}$$

Proof. Switching to polar coordinates we write $\boldsymbol{x} = r(\cos\psi, \sin\psi)$ and calculate

$$\begin{aligned}
b_\ell(\boldsymbol{x}) &= (-i)^\ell \gamma_\ell |\ell|! \left(\frac{1}{\omega}\right)^{|\ell|} \sum_{m=-q}^{q} (A^{-t})_{\ell,m} e^{i\omega \boldsymbol{x}\cdot \boldsymbol{d}_m} \\
&\overset{(3.38)}{=} (-i)^\ell \gamma_\ell |\ell|! \left(\frac{1}{\omega}\right)^{|\ell|} \sum_{n\in\mathbb{Z}} i^n J_n(\omega r) e^{in\psi} \sum_{m=-q}^{q} (A^{-t})_{\ell,m} e^{-in\theta_m} \\
&= (-i)^\ell \gamma_\ell |\ell|! \left(\frac{1}{\omega}\right)^{|\ell|} \left(i^\ell J_\ell(\omega r) e^{i\ell\psi} + \sum_{|m|>q} i^n J_n(\omega r) e^{in\psi} \sum_{m=-q}^{q} (A^{-t})_{\ell,m} e^{-in\theta_m} \right) \\
&\overset{(3.25)}{=} V_1[r^{|\ell|} e^{i\ell\psi}] + O(\omega^{q+1})_{\omega\to 0}
\end{aligned}$$

where γ_ℓ canceled out with the property $J_{-\ell}(z) = (-1)^\ell J_\ell(z),\ \forall \ell \in \mathbb{Z}$. The limit of the first term is given by

$$V_1[r^{|\ell|}e^{i\ell\psi}] = |\ell|!e^{i\ell\psi}\sum_{n=0}^{\infty}\frac{(-1)^n r^{n+|\ell|}\left(\frac{\omega}{2}\right)^n}{(\ell+n)!n!} \xrightarrow{\omega\to 0} r^{|\ell|}e^{i\ell\psi}$$

with uniform convergence on closed sets. Thus the basis does not degenerate with respect to the limit $\omega \to 0$. It is left to show that the matrix A is invertible, which is indeed true since it can be written as a product of a Vandermonde matrix V_A and a diagonal matrix D_A

$$\begin{aligned} A &= \begin{pmatrix} 1 & e^{-i\theta_{-q}} & e^{-2i\theta_{-q}} & \dots & e^{-2qi\theta_{-q}} \\ 1 & e^{-i\theta_{-q+1}} & e^{-2i\theta_{-q+1}} & \dots & e^{-2qi\theta_{-q+1}} \\ 1 & e^{-i\theta_{-q+2}} & e^{-2i\theta_{-q+2}} & \dots & e^{-2qi\theta_{-q+2}} \\ \vdots & \vdots & \vdots & \ddots & \vdots \\ 1 & e^{-i\theta_q} & e^{-2i\theta_q} & \dots & e^{-2qi\theta_q} \end{pmatrix} \cdot \begin{pmatrix} e^{iq\theta_{-q}} & 0 & 0 & \cdots & 0 \\ 0 & e^{iq\theta_{-q+1}} & 0 & \cdots & 0 \\ 0 & 0 & e^{iq\theta_{-q+2}} & \cdots & 0 \\ \vdots & \vdots & \vdots & \ddots & \vdots \\ 0 & 0 & \cdots & 0 & e^{iq\theta_q} \end{pmatrix} \\ &= \{e^{-ij\theta_m}\}_{\substack{j=0,\dots,2q \\ m=-q,\dots,q}} \cdot \operatorname{diag}\{e^{iq\theta_m}\}_{m=-q,\dots,q} = V_A \cdot D_A \end{aligned}$$

□

3.3.2 Approximation of Generalized Harmonic Polynomials

Since we have already established how to approximate the solution of the homogeneous Helmholtz equation by generalized harmonic polynomials, what is left to do is to approximate generalized harmonic polynomials by plane waves.

Lemma 3.18. *Let $\Omega \subset \mathbb{R}^2$ be a domain as in Assumption 1. Take the plane wave space $PW_{\omega,p}$, defined in Equation (3.37), with dimension $p = 2q+1$ and spanned by the different directions*

$$\{\boldsymbol{d}_\ell = (\cos\theta_\ell, \sin\theta_\ell)\}_{\ell=-q,\dots,q}.$$

We assume that there exists a $0 < \delta \leq 1$ such that the angles fulfill

$$\min_{\substack{m,n=-q,\dots,q \\ n\neq m}} |\theta_n - \theta_m| \geq \frac{2\pi}{p}\delta. \tag{3.40}$$

Furthermore, let the indices fulfill

$$0 \leq K \leq L \leq q, \qquad L - K + 1 \leq \lfloor \frac{q+1}{2} \rfloor. \tag{3.41}$$

Let P be a harmonic polynomial of degree L, inducing the generalized harmonic polynomial $V_1[P]$. Then there exists a vector $\alpha \in \mathbb{C}^p$ such that, for every ball with radius $R > 0$, the generalized harmonic polynomials can be approximated by

$$\|V_1[P] - \sum_{n=-q}^{q}\alpha_n e^{i\omega\boldsymbol{x}\cdot\boldsymbol{d}_n}\|_{L^\infty(B_R)} \leq C(\omega,\delta,\rho,h,R,q,K,L)\|P\|_{K,\omega,\Omega} \tag{3.42}$$

where

$$\begin{aligned} C(\omega,\delta,\rho,h,R,q,K,L) = \frac{e^3}{\pi^{\frac{3}{2}}\rho^{\lfloor\frac{q+1}{2}\rfloor}}\left(\frac{e^{\frac{5}{2}}}{2\sqrt{2}\delta^2}\right)^q \left(2^L\sqrt{L+1}\right)e^{\frac{\omega R}{2}} \\ \cdot (\omega R)^{q+1}\left(1+(\omega h)^{-L}\right)h^{K-1}\frac{1}{(q+1)^{\frac{q+1}{2}}}. \end{aligned}$$

Proof. With the usual identification $\mathbb{R}^2 \cong \mathbb{C}$ and writing the complex variable as $z = re^{i\psi}$ we can write the polynomial P of degree L in the general form

$$P(z) = \sum_{\ell=-L}^{L} a_\ell r^{|\ell|} e^{i\ell\psi}. \tag{3.43}$$

We have

$$\begin{aligned}
V_1[P](z) - \sum_{n=-q}^{q} \alpha_n e^{i\omega(r\cos\psi, r\sin\psi)\cdot \boldsymbol{d}_n} \\
&\overset{(3.25)}{=} \sum_{\ell=-L}^{L} a_\ell |\ell|! \left(\frac{2}{\omega}\right)^{|\ell|} e^{i\ell\psi} J_{|\ell|}(\omega r) - \sum_{n=-q}^{q} \alpha_n e^{i\omega r\cos(\psi-\theta_n)} \\
&\overset{(3.38)}{=} \sum_{\ell=-L}^{L} a_\ell |\ell|! \left(\frac{2}{\omega}\right)^{|\ell|} e^{i\ell\psi} \gamma_\ell J_\ell(\omega r) - \sum_{\ell\in\mathbb{Z}} i^\ell J_\ell(\omega r) e^{i\ell\psi} \sum_{n=-q}^{q} \alpha_n e^{-i\ell\theta_n}
\end{aligned}$$

where we choose $\gamma_\ell = 1$ if $\ell \geq 0$ and $\gamma_\ell = (-1)^\ell$ if $\ell < 0$ in order to accommodate for the sign produced by the fact that $J_{-\ell}(z) = (-1)^\ell J_\ell(z),\ \forall \ell \in \mathbb{Z}$. We recall the previously defined $p \times p$ matrix A

$$A = \{e^{-i\ell\theta_m}\}_{\substack{\ell=-q,\dots,q \\ m=-q,\dots,q}} = \{e^{-ij\theta_m}\}_{\substack{j=0,\dots,2q \\ m=-q,\dots,q}} \cdot \operatorname{diag}\{e^{iq\theta_m}\}_{m=-q,\dots,q} = V_A \cdot D_A$$

which we then wrote as the product of the Vandermonde matrix V_A and the diagonal matrix D_A. We would like to choose the vector $\alpha = (\alpha_{-q}, \dots, \alpha_q)$ such that the addends with indices $-q, \dots, q$ cancel out. This is done by setting

$$\beta_\ell = \begin{cases} a_\ell |\ell|! \left(\frac{2}{\omega}\right)^{|\ell|} i^{-\ell}\gamma_\ell & \ell = -L, \dots, L \\ 0 & \ell = -q, \dots, -L-1, L+1, \dots, q \end{cases} \tag{3.44}$$

and choosing α as the solution of the linear system $A\alpha = \beta$. A solution exists since A is non-singular as discussed earlier. With the choice, we get

$$V_1[P](z) - \sum_{n=-q}^{q} \alpha_n e^{i\omega \boldsymbol{x}\cdot \boldsymbol{d}_n} = -\sum_{|\ell|>q} i^\ell J_\ell(\omega r) e^{i\ell\psi} \sum_{n=-q}^{q} \alpha_n e^{i\ell\theta_n}$$

we can bound the L^∞-norm by

$$\left\| V_1[P](z) - \sum_{n=-q}^{q} \alpha_n e^{i\omega \boldsymbol{x}\cdot \boldsymbol{d}_n} \right\|_{L^\infty(B_R)} \leq 2\|A^{-1}\|_1 \|\beta\|_1 \sup_{t\in[0,\omega R]} \sum_{\ell>q} |J_\ell(t)|. \tag{3.45}$$

We will find a bound for each of the three factors on the right hand side.

We start with the easiest, the last term, where we use the bound for the Bessel function Equation (A.2) to find

$$\begin{aligned}
\sup_{t\in[0,\omega R]} \sum_{\ell>q} |J_\ell(t)| &\overset{(A.2)}{\leq} \sup_{t\in[0,\omega R]} \sum_{\ell>q} \left(\frac{t}{2}\right)^\ell \frac{1}{\ell!} \\
&\leq \sup_{t\in[0,\omega R]} \left(\frac{t}{2}\right)^{q+1} \frac{1}{(q+1)!} \sum_{j>0} \left(\frac{t}{2}\right)^j \frac{1}{j!} \\
&= \left(\frac{\omega R}{2}\right)^{q+1} \frac{1}{(q+1)!} e^{\frac{\omega R}{2}}.
\end{aligned}$$

To estimate $\|A^{-1}\|_1$ we use $A^{-1} = V_A^{-1} \cdot D_A^{-1}$ and estimating the inverse of Vandermonde matrices with the help of [11, Theorem 1]. For the diagonal matrix the maximum row sum is 1. Thus,

$$\begin{aligned}\|A^{-1}\|_1 &\leq \|V_A^{-1}\|_1 \|D_A^{-1}\|_1 \leq p\|V_A^{-1}\|_\infty \cdot 1 \\ &\leq p \max_{j=-q,\dots,q} \prod_{\substack{s=-q,\dots,q \\ s\neq j}} \frac{1+|e^{-i\theta_s}|}{|e^{-i\theta_s}-e^{-i\theta_j}|}.\end{aligned}$$

Due to the constraint (3.40) the product is bounded from above. Let us denote the maximizer as θ^*. From the constraint we know that the minimal distance between the angles is $\frac{2\pi}{p}\delta$ and by setting

$$\theta_s^* = \theta^* + \frac{2\pi}{p}|s|\delta \qquad s = -q, \dots, q$$

we can find a lower bound for the denominator. Let us first pre-calculate the distance between the maximizer θ^* and the angles θ_s^*

$$\begin{aligned}|\theta_s^* - \theta^*| &= \left[(\cos(\theta_s^*) - \cos(\theta^*))^2 + (\sin(\theta^*) - \sin(\theta_s^*))^2\right]^{\frac{1}{2}} \\ &= \left[2 - 2(\cos(\theta_s^*)\cos(\theta^*) + \sin(\theta_s^*)\sin(\theta^*))\right]^{\frac{1}{2}} \\ &= \sqrt{2}\sqrt{1-\cos(\theta_s^* - \theta^*)} \\ &\geq \frac{2}{\pi}|\theta_s^* - \theta^*| = \frac{4}{p}\delta|s|,\end{aligned}$$

where we have used $1-\cos t \geq \frac{2}{\pi^2}t^2$, $\forall t \in [-\pi, \pi]$. This gives us a lower bound for the denominator and putting it all together we get

$$\begin{aligned}\|A^{-1}\|_1 &\leq p \max_{j=-q,\dots,q} \prod_{\substack{s=-q,\dots,q \\ s\neq j}} \frac{1+|e^{-i\theta_s}|}{|e^{-i\theta_s}-e^{-i\theta_j}|} \\ &\leq 2p \prod_{\substack{s=-q,\dots,q \\ s\neq 0}} \frac{1}{|e^{-i\theta_s^*}-e^{-i\theta^*}|} \\ &\leq \prod_{\substack{s=-q,\dots,q \\ s\neq 0}} \frac{2p}{4\delta|s|} \leq \frac{p^p}{(2\delta)^{2q}(q!)^2}\end{aligned} \tag{3.46}$$

It is left to estimate $\|\beta\|_1$. With the goal of bounding $|a_l|$ from above by the Sobolev seminorm of the polynomial P, we start in reverse and estimate the norm of P from below. For every $m = 0, \dots, L$ we get

$$\begin{aligned}|P|_{m,\Omega}^2 \geq \left\|\frac{\partial^m}{\partial r^m}P\right\|_{0,B_{\rho h}}^2 &= \left\|\sum_{|j|=m}^{L} a_j \frac{|j|!}{(|j|-m)!} r^{|j|-m} e^{ij\psi}\right\|_{0,B_{\rho h}} \\ &= \int_0^{\rho h} \sum_{|j|,|j'|=m}^{L} \frac{a_j\overline{a_{j'}}\ |j|!\ |j'|!}{(|j|-m)!\ (|j'|-m)!} r^{|j|+|j'|-2m} \int_0^{2\pi} r^{i(j-j')\psi} d\psi\ r\ dr \\ &= 2\pi \sum_{|j|=m}^{L} |a_j|^2 \frac{(|j|!)^2}{((|j|-m)!)^2} \frac{(\rho h)^{2(|j|-m+1}}{2(|j|-m+1)},\end{aligned}$$

where we used

$$\int_0^{2\pi} e^{i(j-j')\psi}\ d\psi = 2\pi\delta_{jj'}.$$

Note that all terms on the right hand side are positive, thus we can loose all but one term of the sum and reverse the inequality to find an estimate for each a_ℓ. For a fixed K as in the statement of the lemma, we consider two cases, if $|\ell| < K$ then we need to use the inequality with the Sobolev seminorm of order $|\ell|$ and only consider the first summand. For $K \le |\ell| \le L$ we will fix the Sobolev seminorm to order K and keep the respective summand. Thus,

$$\begin{aligned}
|a_\ell| &\le \frac{1}{\sqrt{\pi}} \frac{1}{|\ell|!(\rho h)} |P|_{|\ell|,\Omega} \qquad \text{if } |\ell| < K \\
|a_\ell| &\le \frac{1}{\sqrt{\pi}} \frac{(|\ell|-K)!\sqrt{|\ell|-K+1}}{|\ell|!(\rho h)^{|\ell|-K+1}} |P|_{K,\Omega} \qquad \text{if } K \le |\ell| \le L.
\end{aligned}$$

With this we can estimate β by

$$\begin{aligned}
\|\beta\|_1 &= \sum_{\ell=-L}^{L} |a_\ell| \left(\frac{2}{\omega}\right)^{|\ell|} |\ell|! \\
&\le \sum_{\ell=-K}^{K} \frac{1}{\rho h \sqrt{\pi}} \left(\frac{2}{\omega}\right)^{|\ell|} |P|_{|\ell|,\Omega} \\
&\quad + \sum_{|\ell|=K+1}^{L} \frac{1}{\sqrt{\pi}} \left(\frac{2}{\omega}\right)^{|\ell|} \frac{(|\ell|-K)!\sqrt{|\ell|-K+1}}{(\rho h)^{|\ell|-K+1}} |P|_{K,\Omega} \\
&\le \frac{\sqrt{2K+1}}{\rho\sqrt{\pi}} \left(\frac{1}{\omega h}\right)^{K} 2^{K+\frac{1}{2}} h^{K-1} \|P\|_{K,\omega,\Omega} \\
&\quad + \frac{2}{\sqrt{\pi}} \frac{2^L h^{K-1}}{\rho^{L-K+1}} \left(\sum_{\ell=K+1}^{L} \frac{(\ell-K)!\sqrt{\ell-K+1}}{(\omega h)^\ell} \right) |P|_{K,\Omega} \\
&\le \left\{ \frac{2^{L+1}}{\sqrt{\pi}\rho^{L-K+1}} h^{K-1} (1 + (\omega h)^{-L}) \right. \\
&\quad \left. \cdot \left(\sqrt{K+1} + (L-K)\ (L-K)!\ \sqrt{L-K+1} \right) \right\} \|P\|_{K,\omega,\Omega}.
\end{aligned} \tag{3.47}$$

Finally we plug the established bounds into Equation (3.45) and get

$$\begin{aligned}
\left\| V_1[P] - \sum_{n=-q}^{q} \alpha_\omega e^{i\omega \boldsymbol{x}\cdot\boldsymbol{d}_n} \right\|_{L^\infty(B_R)} &\le 2 \left\{ \left(\frac{\omega R}{2}\right)^{q+1} \frac{1}{(q+1)!} e^{\frac{\omega R}{2}} \right\} \cdot \left\{ \frac{p^p}{(2\delta)^{2q}(q!)^2} \right\} \\
&\quad \cdot \left\{ \frac{2^{L+1}}{\sqrt{\pi}\rho^{L-K+1}} h^{K-1} (1 + (\omega h)^{-L}) \sqrt{L+1} (L-K+1)! \right\} \|P\|_{K,\omega,D} \\
&\le \left\{ \left(\frac{1}{8\delta^2}\right)^{q} (\omega R)^{q+1} e^{\frac{\omega R}{2}} \frac{p^p}{(q!)^2(q+1)!} \right\} \\
&\quad \cdot \left\{ \frac{2^{L+1}}{\sqrt{\pi}\rho^{L-K+1}} h^{K-1} (1 + (\omega h)^{-L}) \sqrt{L+1} (L-K+1)! \right\} \|P\|_{K,\omega,D} \\
&\overset{(3.41)}{\le} \frac{2}{\sqrt{\pi}\rho^{\lfloor \frac{q+1}{2} \rfloor}} \left(\frac{1}{8\delta^2}\right)^{q} (2^L \sqrt{L+1}) e^{\frac{\omega R}{2}} (\omega R)^{q+1} \\
&\quad \cdot (1 + (\omega h))^{-L} h^{K-1} \frac{p^p \lfloor \frac{q+1}{2} \rfloor!}{(q!)^2 (q+1)!} \|P\|_{K,\omega,D}.
\end{aligned}$$

We will use the Stirling formula

$$\sqrt{2\pi n} n^n e^{-n} e^{\frac{1}{12n+1}} < n! < \sqrt{2\pi n} n^n e^{-n} e^{\frac{1}{12n}} \qquad \forall n \ge 1$$

to bound the factorials, giving

$$\begin{aligned}\frac{p^p\lfloor\frac{q+1}{2}\rfloor!}{(q!)^2(q+1)!} &\leq (2q+2)^{2q+2}(q+1)^2\frac{\lfloor\frac{q+1}{2}\rfloor!}{((q+1)!)^3}\\ &< \frac{2^{2q+1}}{2\pi}\frac{\left(\frac{q+1}{2}\right)^{\left(\frac{q+1}{2}\right)+\frac{1}{2}}}{(q+1)^{q+\frac{3}{2}}}e^{\frac{5}{2}q+3}e^{-\frac{3}{12(q+1)+1}+\frac{1}{6q}}\\ &\leq \frac{e^3}{2\pi}\left(2\sqrt{2}e^{\frac{5}{2}}\right)^q(q+1)^{-\frac{q+1}{2}}\end{aligned}$$

where the last inequality follows because the exponential fulfils $-\frac{3}{12(q+1)+1}+\frac{1}{6q}<0$ for $q>2$ and in the cases $q=1,2$ is stays less than $\frac{5}{2}q+3$. Thus we obtain for any $q\geq 1$ that

$$\begin{aligned}\left\|V_1[P]-\sum_{n=-q}^{q}\alpha_n e^{i\omega\boldsymbol{x}\cdot\boldsymbol{d}_n}\right\|_{L^\infty(B_R)} &\leq \frac{e^3}{\pi^{\frac{3}{2}}\rho^{\lfloor\frac{q+1}{2}\rfloor}}\left(\frac{e^{\frac{5}{2}}}{2\sqrt{2}\delta^2}\right)^q\left(2^L\sqrt{L+1}\right)e^{\frac{\omega R}{2}}\\ &\quad\cdot(\omega R)^{q+1}\left(1+(\omega h)^{-L}\right)h^{K-1}\frac{1}{(q+1)^{\frac{q+1}{2}}}\|P\|_{K,\omega,\Omega},\end{aligned}$$

finishing the proof. □

3.3.3 Approximation of Homogeneous Helmholtz Solution by Plane Waves

Before we are able to put everything together, we need to link the Sobolev norm to the L^∞-norm so we can apply Lemma 3.18.

Lemma 3.19 ([24, Lemma 3.2.1])**.** *Let Ω be a domain as in Assumption 1 and let ϕ be a harmonic function in $H^j(B_h)$, $j\in\mathbb{N}$ and $\omega>0$. Then*

$$\|V_1[\phi]\|_{j,\omega,\Omega}\leq C(j)\ \rho^{-\frac{1}{2}-j}(1+(\omega h)^{j+4})e^{\frac{1}{2}\omega h}h^{1-j}\|V_1[\phi]\|_{L^\infty(B_h)}, \tag{3.48}$$

where the constant $C>0$ only depends on j.

We finish the section with the final result, giving an approximation estimate for homogeneous Helmholtz solutions by plane waves with respect to the diameter h.

Theorem 3.20 (h-estimate)**.** *Let $u\in H^{m+1}(\Omega)$ be a solution of the homogeneous Helmholtz equation in a domain $\Omega\subset\mathbb{R}^2$, satisfying Assumption 1. Fix $q>0$ and let $p=2q+1$ be the space dimension of the plane wave space, with directions $\{\boldsymbol{d}_k\}_{\{k=1,\dots,p\}}$ satisfying* (3.40)*. Then for every $1\leq L\leq\min(q,m)$, there exists an $\alpha\in\mathbb{C}^p$ such that, for every $j\leq L$,*

$$\left\|u-\sum_{k=1}^{p}\alpha_k e^{i\omega\boldsymbol{x}\cdot\boldsymbol{d}_k}\right\|_{j,\omega,\Omega}\leq C\ e^{(\frac{7}{4}-\frac{3}{4}\rho)\omega h}h^{L+1-j}(1+(\omega h)^{j+q+8})\|u\|_{L+1,\omega,\Omega} \tag{3.49}$$

where the constant $C>0$ depends on q,j,L,ρ,ρ_0 and the directions $\{\boldsymbol{d}_k\}_{\{k=1,\dots,p\}}$, however is independent of ω,h and u.

Proof. Set $Q_L=V_1[Q^{L+1}V_2[u]]$ to be the generalized harmonic polynomial of the averaged Taylor polynomial of the Vekua transformed Helmholtz solution, as in Theorem 3.16.

We start by applying what we have established about approximation of generalized harmonic polynomials by plane wave functions in Lemma 3.18, to approximate Q_L on a ball with radius h.

Using Lemma 3.18 with $K = L$ we get

$$\begin{aligned}
&\left\| Q_L - \sum_{k=1}^{p} \alpha_k e^{i\omega \boldsymbol{x}\cdot \boldsymbol{d}_k} \right\|_{L^\infty(B_h)} \\
&\overset{(3.42)}{\leq} C(\rho, L, q) e^{\frac{\omega h}{2}} ((\omega h)^{q-L} + (\omega h)^q) h^L \omega \|V_2[Q_L]\|_{L,\omega,\Omega} \\
&\leq C(\rho, L, q) e^{\frac{\omega h}{2}} ((\omega h)^{q-L} + (\omega h)^q) h^L \|V_2[Q_L]\|_{L+1,\omega,\Omega} \\
&\leq C(\rho, L, q) e^{\frac{\omega h}{2}} (1 + (\omega h)^q) h^L \left[\|V_2[u]\|_{L+1,\omega,\Omega} + \|V_2[u] - V_2[Q_L]\|_{L+1,\omega,\Omega} \right] \\
&\overset{(3.31)}{\leq} C(\rho, L, q, \rho_0) e^{\frac{\omega h}{2}} (1 + (\omega h)^q) h^L \|V_2[u]\|_{L+1,\omega,\Omega} \\
&\overset{(3.9)}{\leq} C(\rho, L, q, \rho_0) e^{(\frac{1}{2} + \frac{3}{4}(1-\rho))\omega h} (1 + (\omega h)^{q+4}) h^L \|u\|_{L+1,\omega,\Omega}
\end{aligned}$$

where we are able to apply Bramble Hilbert for harmonic functions (3.31), because $V_2[Q_L] = Q^{L+1} V_2[u]$ is the averaged Taylor polynomial approximating the harmonic function $V_2[u]$. Note that we are only able to use Lemma 3.18 by assuming $1 \leq L \leq q$.

Finally, we insert Q_L and use the triangle inequality. The first of the two resulting terms can be treated by Theorem 3.16, the second by Equation (3.48) followed by our calculations above.

$$\begin{aligned}
\left\| u - \sum_{k=1}^{p} \alpha_k e^{i\omega \boldsymbol{x}\cdot \boldsymbol{d}_k} \right\|_{j,\omega,\Omega} &\leq \|u - Q_L\|_{j,\omega,\Omega} + \left\| Q_L - \sum_{k=1}^{p} \alpha_k e^{i\omega \boldsymbol{x}\cdot \boldsymbol{d}_k} \right\|_{j,\omega,\Omega} \\
&\overset{(3.35)}{\overset{(3.48)}{\leq}} C\ e^{\frac{3}{4}(1-\rho)\omega h} h^{L+1-j} (1 + (\omega h)^{j+6}) \|u\|_{L+1,\omega,\Omega} \\
&\quad + C\ e^{\frac{1}{2}\omega h} h^{1-j} (1 + (\omega h)^{j+4}) \left\| Q_L - \sum_{k=1}^{p} \alpha_k e^{i\omega \boldsymbol{x}\cdot \boldsymbol{d}_k} \right\|_{L^\infty(B_h)} \\
&\leq C\ e^{(\frac{7}{4} - \frac{3}{4}\rho)\omega h} h^{L+1-j} (1 + (\omega h)^{j+q+8}) \|u\|_{L+1,\omega,\Omega}
\end{aligned}$$

Theorem 3.16 i) constrains $L \leq m$, thus we indeed need to assume $1 \leq L \leq \min(q, m)$. □

As we used Theorem 3.13 for the above result, it only captures h convergence. Using (3.36) from Theorem 3.16 we are able to derive a *hp* version.

Theorem 3.21 (hp-estimate, [24, Theorem 3.2.3])**.** *Let $u \in H^{m+1}(\Omega)$ be a solution of the homogeneous Helmholtz equation in a domain $\Omega \subset \mathbb{R}^2$ satisfying Assumption 1 and the exterior cone condition with angle $\lambda\pi$. Fix $q \geq 1$, set $p = 2q+1$ and let the directions $\{d_k = (\cos\theta_k, \sin\theta_k)\}_{k=-q,\dots,q}$ satisfy* (3.40)*. Then for every L satisfying*

$$0 \leq m \leq L \leq q \qquad L - m + 1 \leq \left\lfloor \frac{q+1}{2} \right\rfloor$$

there exists a $\alpha \in \mathbb{C}^p$ such that for every $0 \leq j \leq m$,

$$\begin{aligned}
\left\| u - \sum_{k=1}^{p} \alpha_k e^{i\omega \boldsymbol{x}\cdot \boldsymbol{d}_k} \right\|_{j,\omega,\Omega} &\leq C\ e^{(\frac{7}{4} - \frac{3}{4}\rho)\omega h} h^{m+1-j} (1 + (\omega h)^{j+8}) \\
&\cdot \left\{ \left(\frac{\log(L+2)}{L+2} \right)^{\lambda(m+1-j)} + 2^L \sqrt{\frac{L+1}{q+1}} \left(\frac{e^{\frac{5}{2}}}{2\sqrt{2}\delta^2 \rho^{\frac{1}{2}}} \frac{(1+\omega h)}{q+1} \right)^q \right\} \|u\|_{m+1,\omega,\Omega}
\end{aligned} \tag{3.50}$$

Remark 3.22. In Theorem 3.21, we can choose

$$L = m - 1 + \left\lfloor \frac{q+1}{2} \right\rfloor$$

as long $m \leq q+1-\lfloor \frac{q+1}{2} \rfloor = \lceil \frac{q+1}{2} \rceil$. With this, the first term in the curly brackets of Equation (3.50) takes the form

$$\frac{\log(m+1+\lfloor \frac{q+1}{2} \rfloor)}{m+1+\lfloor \frac{q+1}{2} \rfloor}$$

which behaves asymptotically like $\frac{\log(q)}{q}$ for large q. Thus the first term converges to zero algebraically, whereas the second term converges exponentially. If the solution u can be extended analytically to a strictly larger domain then we are able to show exponential convergence, see [15, Section 5.2]. The speed of exponential convergence depends on how far u can be extended analytically.

Remark 3.23. Analysing the above error bounds will give some valuable information on what is the best possible accuracy we can expect from our numerical tests. Note that the above results govern how well any numeric scheme can approximate the homogeneous Helmholtz solution using plane waves.

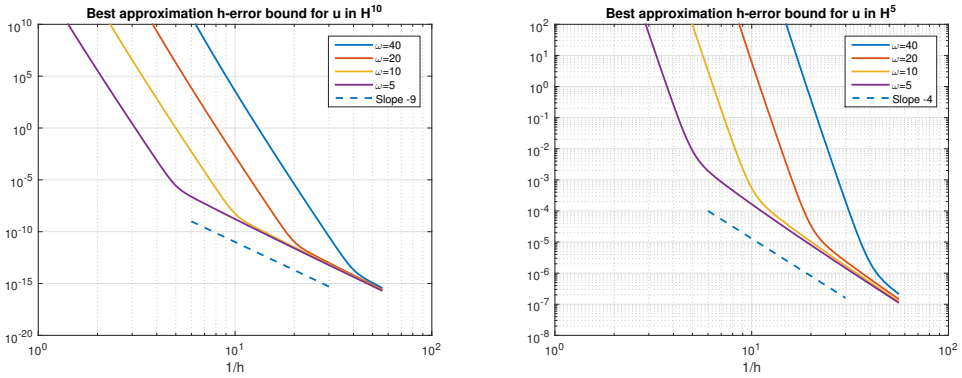

Figure 2: Qualitative plots of the bounds given in Theorem 3.20 for $u \in H^{10}$ (left) and $u \in H^5$ (right).

Theorem 3.20 gives information about h convergence, without any requirement on the number of plane waves, as opposed to Theorem 3.21 which requires $m \leq q$. Thus, for analysing the bound in Equation (3.49) we fix q equal to the space dimension m and vary h. The results are plotted in Figure 2. We observe two cases: a smoother solution $u \in H^{10}$ and a less smooth solution $u \in H^5$.

The main difference is that the bound reaches a smaller value in the first case. Also in the case of $u \in H^{10}$ the point where we can observe the expected convergence is reached slightly earlier.

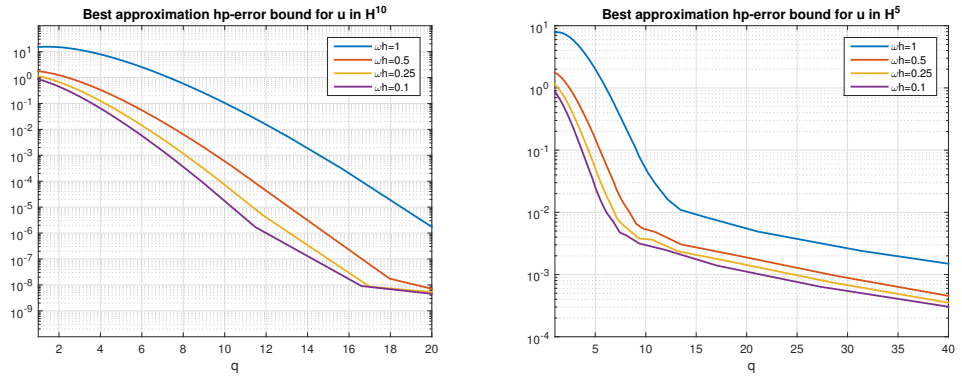

Figure 3: Qualitative plots of the bounds given in Theorem 3.21 for $u \in H^{10}$ (left) and $u \in H^5$ (right)

Other then that, both cases behave the same way: We can observe the expected convergence rate in h (shown by the dotted line), however, we require the product ωh to be small enough. Depending on the choice of ω, the error bound explodes quickly for increasing values of h. This happens earlier for larger wave numbers.

The plots in Figure 3 show the bound of Theorem 3.21 which gives information for $m \leq q$. For small q the bound shows little convergence. Especially for larger ωh the increased error takes up a large interval before showing convergence. This is evidence for a threshold condition, only after which we can expect convergence. Furthermore, the bound for larger ωh never perform as well as for smaller values of ωh.

For $u \in H^5$ the area where the error convergences is small, and it is unable to reach the same low levels as before, which is similar to the behavior of the h case.

We can conclude that in both cases the bounds show evidence for a threshold condition For less smooth solutions u the bounds change rapidly, however settle at a higher error level than in the case of a smoother solution. In case of larger ω it will take stronger requirements on the mesh size or plane waves, before we can expect reasonable convergence. In both cases we require ωh to be small to guarantee convergence to a low error bound.

4 Plane Wave Methods

We recall the homogeneous version of the Helmholtz problem, given by Equation (2.6). Its weak formulation reads: find $u \in H^1(\Omega)$ such that

$$b(u,v) = a(u,v) + i\omega \int_{\partial\Omega} u\bar{v}\ dS = \int_{\partial\Omega} g\bar{v} \qquad \forall v \in H^1(\Omega) \tag{4.1}$$

where

$$a(u,v) = \int_\Omega \nabla u \cdot \overline{\nabla v}\ dV - \omega^2 \int_\Omega u\bar{v}\ dV. \tag{4.2}$$

In this section we assume that the domain $\Omega \subset \mathbb{R}^2$ is a bounded polygon that fulfils Assumption 1. Note that the first point in Assumption 1 is, however, trivial due to Ω being a polygon.

4.1 Finite Element Spaces

We start by introducing spaces of functions that we will use the approximate the solution. Let $\mathcal{T}_h$ be a mesh of the domain Ω, consisting of non-overlapping polygons K. The index h is called the *mesh width*, and is given by $h = \max_{K\in\mathcal{T}_h} h_K$, where h_K denotes the diameter of K. We will take the following assumption on the mesh elements:

Assumption 2. We assume that each $K \in \mathcal{T}_h$ fulfills Assumption 1 and does not have degenerated sides.

Furthermore, let us denote with $\boldsymbol{\nu}_K$ the outer normal vector of K pointing outwards, $\mathbf{x}_K$ the mass center of K, n_K the number of edges e_j, and by $\boldsymbol{v}_j$, $j = 1,\dots,n_K$ the vertices of K and their coordinates. Most of the constructions in this section are only relevant to the VEM. The PW-DG method only makes use of the (global) plane wave spaces defined in Equations (4.5) and (4.7).

For a polygon $K \in \mathcal{T}_h$ we introduce the VEM space

$$V(K) = \{v \in H^1(K) : v|_{\partial K} \in C^0(\partial K),\ v|_e \in \mathbb{P}_1(e)\ \forall e \subset \partial K, \Delta v \equiv 0 \text{ in } K\} \tag{4.3}$$

where $\mathbb{P}_1(D)$ denotes the polynomials on the domain D with degree at most 1. In [3, Prop. 4.1.] it is shown that the functions in $V(K)$ are completely determined by their value in the n_K vertices. Thus the canonical basis $\{\varphi_j\}_{j=1}^{n_K}$ is determined by the condition

$$\varphi_j(\boldsymbol{v}_i) = \delta_{ij} \qquad i,j = 1,\dots,n_K$$

and we immediately see that $\dim(V(K)) = n_K$. Note that [3] introduces the VEM space for higher polynomial degrees. Since we have to approximate oscillating solutions, we adopt a different approach, namely we enrich the space with plane wave functions, resulting in the local PW-VEM space

$$V_{p_K}(K) = \sum_{j=1}^{n_K} \varphi_j V^* = \{v : v = \sum_{j=1}^{n_K}\sum_{\ell=1}^{p_K} a_{j\ell}\varphi_j(\boldsymbol{x}) e^{i\omega \boldsymbol{d}_\ell\cdot(\boldsymbol{x}-\boldsymbol{v}_j)},\ a_{j\ell} \in \mathbb{C}\}, \tag{4.4}$$

where

$$V^*_{p_K}(K) = \{v : v = \sum_{\ell=1}^{p_K} a_\ell e^{i\omega \boldsymbol{d}_\ell\cdot(\boldsymbol{x}-\boldsymbol{x}_K)}, a_\ell \in \mathbb{C}\} \tag{4.5}$$

is the plane wave space, that we know from Equation (3.37), with a shift to the element center $\boldsymbol{x}_K$. Clearly, $\dim(V_{p_K}) = n_K \cdot p_K$ and by choosing $a_{j\ell} = a_\ell e^{i\omega \boldsymbol{d}_\ell\cdot(\boldsymbol{v}_j-\boldsymbol{x}_K)}$ we get $V^*_{p_K}(K) \subset V_{p_K}(K)$.

The reason for choosing only polynomials of degree 1 is that they form a partition of unity and therefore our PW-VEM space is a PUFEM space introduced in [19], allowing us to apply the helpful approximation result stated there, later on. To see that we have a partition of unity notice that, since all φ_j are linear on each edge, we have for $f = \sum_{j=1}^{n_K} \varphi_j$ that $f(\boldsymbol{x}) = 1,\ \forall \boldsymbol{x} \in \partial K$. Since we also require that $\Delta f = 0$ in K is follows that $f \equiv 1$, thus $\{\varphi_j\}_{j=1}^{n_K}$ is indeed a partition of unity.

To get a better grip on the basis functions we introduce the notation

$$\pi_\ell(\boldsymbol{x}) = e^{i\omega \boldsymbol{d}_\ell \cdot (\boldsymbol{x} - \boldsymbol{x}_K)}, \qquad \pi_{j\ell}(\boldsymbol{x}) = e^{i\omega \boldsymbol{d}_\ell \cdot (\boldsymbol{x} - \boldsymbol{v}_j)}$$
$$\psi_r(\boldsymbol{x}) = \varphi_j(\boldsymbol{x})\pi_{j\ell}(\boldsymbol{x}) = \varphi_j(\boldsymbol{x}) e^{i\omega \boldsymbol{d}_\ell \cdot (\boldsymbol{x} - \boldsymbol{v}_j)} \qquad \text{with } r = (j-1)p_K + \ell.$$

Finally, we set $p_K = p$ and use the same directions $\{\boldsymbol{d}_\ell\}_{\ell=1}^{p}$ for all $K \in \mathcal{T}_h$. We define the global PW-VEM space as

$$V_p(\mathcal{T}_h) = \{v \in C^0(\bar{\Omega}) : v|_K \in V_p(K),\ \forall K \in \mathcal{T}_h\}, \tag{4.6}$$

notice that we enforce continuity across inter-element boundaries. On the other hand, we introduce the global plane wave space

$$V_p^*(\mathcal{T}_h) = \prod_{K \in \mathcal{T}_h} V_p^*(K), \tag{4.7}$$

which allows discontinuities along element boundaries, thus $V_p^*(\mathcal{T}_h) \nsubseteq V_p(\mathcal{T}_h)$. The space dimension given by $\dim(V_p^*) = p$ times the numbver of elements in the mesh.

For each $K \in \mathcal{T}_h$ the local version of the bilinear form given in Equation (2.4), reads

$$a^K(u, v) = \int_K \nabla u \cdot \overline{\nabla v}\, dV - \omega^2 \int_K u \bar{v}\, dV. \tag{4.8}$$

4.2 Virtual Element Method

We follow [25] in the construction of the PW-VEM for the homogeneous Helmholtz equation. A crucial step in defining the method is the definition of a projection operator that links the spaces V_p and V_p^*. After defining said operator in the next section, we are ready to present the main idea and formulation of the VEM in Section 4.2.2.

4.2.1 The projection operator Π

In any VEM the general requirements for the space that we are projecting onto are

- good approximation properties for the solution of the problem and
- allowing exact computation of the bilinear form whenever one of the two entries belongs to that space.

As for our case of plane waves the first criterion is fulfilled, as we know from Section 3.3. The second criterion also holds true as we will see later on in Remark 4.9.

We define the projection operator $\Pi : V_p(K) \to V_p^*(K)$ by the condition

$$a^K(\Pi u, w) = a^K(u, w) \qquad \forall w \in V_p^*(K). \tag{4.9}$$

The condition is sufficient provided that ω^2 is not a Neumann-Laplace eigenvalue on K. This is shown in [25, Sec. 1.3]:

Proposition 4.1 ([25, Proposition 1.3]). *For $K \in \mathcal{T}_h$, let μ_2 be the smallest strictly positive eigenvalue of the Neumann-Laplace operator on K. We assume that*

$$0 < h_K\omega < \sqrt{C_0}\pi,$$

where $0 < C_0 \leq 1$ is the constant fulfilling $C_0\pi^2/h_K^2 < \mu_2$. This constant exists and only depends on the shape of K (see [5]). Then the operator Π is well-defined, and the following local continuity property holds true:

$$\|\Pi u\|_{1,\omega,K} \leq \frac{1}{\beta(h_K\omega)}\|u\|_{1,\omega,K} \qquad \forall u \in V_p(K). \tag{4.10}$$

For $u \in V_p^*(K)$ we clearly have $\Pi u = u$. Furthermore, for $u \in V_p$ and $w \in V_p^*$ we can use that $\Delta w + \omega^2 w = 0$ and integration by parts to write the right hand side of Equation (4.9) as

$$a^K(u, w) = \int_K \nabla u \cdot \overline{\nabla w}\, dV - \omega^2 \int_K u\bar{w}\, dV = \int_{\partial K} u\overline{\nabla w \cdot \nu_K}\, dS. \tag{4.11}$$

Notice how the calculation of Π now only depends on u and $\nabla w \cdot \nu_K$ on ∂K and is independent of the function values in the interior of K.

4.2.2 The PW-VEM formulation

Using the projection operator Π we can rewrite the local bilinear form Equation (4.2) as

$$a^K(u, v) = a^K(\Pi u, \Pi v) + a^K((I - \Pi)u, (I - \Pi)v) + a^K((I - \Pi)u, \Pi v) + a^K(\Pi u, (I - \Pi)v)$$

for all $u, v \in V_p(K)$. Note that the last two terms are zero due to the definition of the Π-operator, Equation (4.9), and a^K being bilinear. Furthermore, we can actually compute the term $a^K(\Pi u, \Pi v)$ exactly using the traces of the shape functions on ∂K only, as discussed in Remark 4.9.

We are left with the term $a^K((I - \Pi)u, (I - \Pi)v)$, which ensures stability, however we cannot calculate it exactly since it requires knowledge of the shape functions on the interior of K. Therefore, we will approximate the term by the stabilization term $s^K(\cdot, \cdot)$, common choices are will be discussed in Section 4.2.4.

The local PW-VEM bilinear form is then given by

$$a_h^K(u, v) = a^K(\Pi u, \Pi v) + s^K((I - \Pi)u, (I - \Pi)v) \tag{4.12}$$

for $u, v \in V_p(K)$.

We say that the first term on the right insures consistency, because $\Pi u^* = u^*$ for all $u^* \in V_p^*(K)$. Hence, the local PW-VEM bilinear form is consistent with plane waves:

$$a_h^K(u^*, v) = a^K(u^*, v) \qquad \forall u^* \in V_p^*(K), v \in V_p(K).$$

To find the global formulation we define

$$a_h(u, v) = \sum_{K \in \mathcal{T}_h} a_h^K(u, v), \tag{4.13}$$

then the left hand side of the global PW-VEM is given by

$$b_h(u, v) = a_h(u, v) + i\omega \int_{\partial\Omega} u\bar{v}\, dS. \tag{4.14}$$

Finally, the complete PW-VEM formulation for the homogeneous Helmholtz problem reads:

$$\text{Find } u_{hp} \in V_p(\mathcal{T}_h) \text{ such that} \quad b_h(u_{hp}, v) = \int_{\partial\Omega} g\bar{v}\, dS \quad \forall v \in V_p(\mathcal{T}_h). \tag{4.15}$$

4.2.3 Convergence Results

Corresponding to the weighted norm defined in Equation (2.5), we now introduce the broken weighted norm for the mesh $\mathcal{T}_h$ given by

$$\|v\|^2_{1,\omega,\mathcal{T}_h} = \sum_{K\in\mathcal{T}_h} \|v\|^2_{1,\omega,K} = \sum_{K\in\mathcal{T}_h} (\|\nabla v\|^2_{0,K} + \omega^2\|v\|^2_{0,K}).$$

For functions in $H^1(\Omega)$ the $\|v\|_{1,\omega,\mathcal{T}_h}$-norm and the $\|v\|_{1,\omega,\Omega}$-norm coincide. However, in general, this is not the case for broken H^1 functions, that is functions in $H^1(\mathcal{T}_h)$. Before we get into the choice of the stabilization term s^K we review convergent results, and take a look at the constraints on the choice of s^K that arise. In [25] it is shown that

Theorem 4.2. *[25, Theorem 2.1] Assume that the local stabilization term $s^K(\cdot,\cdot)$ is chosen such that the following properties hold:*

- *continuity: there exists $\gamma > 0$ such that, for all $u, v \in H^1(\mathcal{T}_h)$*

$$|a_h(u,v)| \leq \gamma\|u\|_{1,\omega,\mathcal{T}_h}\|v\|_{1,\omega,\mathcal{T}_h} \tag{4.16}$$

- *Gårding inequality for the discrete operator: there exists $\alpha > 0$ such that*

$$Re[b_h(v,v)] + 2\omega^2\|v\|^2_{0,\omega} \geq \alpha\|v\|_{1,\omega,\mathcal{T}_h} \qquad \forall v \in V_p(\mathcal{T}_h) \tag{4.17}$$

Well-posedness of the PW-VEM method follows directly (compare Proposition 2.2). Let u be the solution to problem (4.1), and let u_{hp} be the solution to the PW-VEM (4.15). Then, assuming that h is small enough to fulfill

$$\bar{C}(1+\gamma)(1+h\omega)h\omega(1+\omega) \leq \frac{\alpha}{2} \tag{4.18}$$

for a constant $\bar{C} > 0$, the following error estimates hold:

$$\|u-u_{hp}\|_{1,\omega,\mathcal{T}_h} \leq C\frac{1+\alpha+\gamma}{\alpha}\left(\inf_{v_I\in V_p(\mathcal{T}_h)}\|u-v_I\|_{1,\omega,\mathcal{T}_h} + \inf_{v^*_{hp}\in V^*_p(\mathcal{T}_h)}\|u-v^*_{hp}\|_{1,\omega,\mathcal{T}_h}\right) \tag{4.19}$$

$$\|u-u_{hp}\|_{0,\Omega} \leq C\ (1+\gamma)(1+h\omega)h(1+\omega)\left(\|u-u_{hp}\|_{1,\omega,\mathcal{T}_h} + \inf_{v^*_{hp}\in V^*_p(\mathcal{T}_h)}\|u-v^*_{hp}\|_{1,\omega,\mathcal{T}_h}\right) \tag{4.20}$$

with $C > 0$ independent of h, ω and p.

Remark 4.3. Whereas h-convergence of plane waves approximating a homogeneous Helmholtz solution only require ωh to become small (see Theorem 3.20), the assumption (4.18) implies the stronger requirement of $\omega^2 h$ being small enough.

We are left with the task of finding best approximation estimates, which is straight forward thanks to our previous estimation result for plane waves, and handy properties of the PW-VEM space that carry over from PUFEM theory.

Proposition 4.4. *[25, Proposition 2.3] Let $u \in H^{\ell+1}(\Omega)$, $\ell \geq 0$, such that u fulfills $\Delta u + \omega^2 u = 0$ in Ω. We assume the mesh elements to be convex. Then there exist $u^*_{hp} \in V^*_p(\mathcal{T}_h)$ and $u_I \in V_p(\mathcal{T}_h)$, with $p = 2q+1$, such that*

$$\|u-u^*_{hp}\|_{1,\omega,\mathcal{T}_h} \leq C\ \eta(h\omega)\ h^{\min\{m,\ell\}}\|u\|_{\min\{q,\ell\}+1,\omega,\mathcal{T}_h}$$
$$\|u-u_I\|_{1,\omega,\mathcal{T}_h} \leq C\ \eta(h\omega)\ h^{\min\{m,\ell\}}\|u\|_{\min\{q,\ell\}+1,\omega,\mathcal{T}_h}$$

with $C > 0$ independent of h, ω and u and

$$\eta(h\omega) = (1+(h\omega)^{q+9})e^{(\frac{7}{4}-\frac{3}{4}\rho)h\omega}$$

Proof. The first bound follows by applying Theorem 3.20 to each $K \in \mathcal{T}_h$. For the second bound we use [19, Th. 2.1], which requires the basis $\{\varphi_j\}_{j=1}^{n_K}$ for the space $V(K)$ to be a partition of unity, i.e. that $\|\varphi_j\|_{0,K} \leq C$ and $\|\nabla\varphi_j\|_{0,K} \leq \frac{C}{h_k}$ holds for some $C > 0$ and all basis functions. For convex elements, the basis $\{\varphi_j\}_{j=1}^{n_K}$ satisfies the assumptions of [19, Th. 2.1]. □

Combining the two previous results we find the following convergence properties:

Corollary 4.5. *[25, Corollary 2.4] Under the assumptions of Theorem 4.2, if the solution u to $\Delta u + \omega u = 0$ belongs to $H^{m+1}(\Omega)$, $m \geq 0$, then the following error estimate holds:*

$$\|u - u_{hp}\|_{1,\omega,\mathcal{T}_h} \leq C\frac{1+\alpha+\gamma}{\alpha}\eta(h\omega)\ h^{\min\{q,m\}}\|u\|_{\min\{q,m\}+1,\omega,\Omega} \tag{4.21}$$

with $C > 0$ independent of h, ω and $p = 2q + 1$ and $\eta(h\omega)$ as in Proposition 4.4.

Remark 4.6. We can use the above result to bound the L^2-error estimate given in Equation (4.20). We have assumed in Equation (4.18) that ωh is small enough. In fact, the assumption tells us in particular, that $h\omega^2 \leq C$ and therefore the factors on the right hand side of (4.20) can be reduced to a factor of $h^{\frac{1}{2}}$, contributing to the L^2-norm. Thus, under the assumptions of Theorem 4.2 we can conclude

$$\|u - u_{hp}\|_{0,\Omega} = O(h^{\min\{q,m\}+\frac{1}{2}}),$$

4.2.4 Choice for the Stabilization Term

For the convergence results to work the stabilization term needs to fulfil the continuity property and Gårding inequality, as we have seen in the conditions for Theorem 4.2. The following proposition, proved in [25, Prop. 3.2.], states a sufficient condition on the stabilization term to guarantee the Gårding inequality.

Proposition 4.7. *[25, Proposition 3.2] If the stabilization term satisfies*

$$s^K((I-\Pi)v,(I-\Pi)v) \geq \|\nabla(I-\Pi)v\|_{0,K}^2 \qquad \forall K \in \mathcal{T}_h,\ \forall v \in V_p(K) \tag{4.22}$$

then the Gårding inequality for the discrete operator, Equation (4.17)*, holds true.*

This proposition motivates the following choice for the stabilization term

$$s^K((I-\Pi)u,(I-\Pi)v) = \int_K \nabla(I-\Pi)u \cdot \overline{\nabla(I-\Pi)v}\ dV \tag{4.23}$$

as it satisfies Equation (4.22) with equality. Of course, to satisfy the conditions of Theorem 4.2, we need to show continuity for our choice. We start by estimating the local PW-VEM bilinear form:

$$\begin{aligned}
|a_h^K(u,v)| &= \left|\omega^2\int_K \Pi u\ \overline{\Pi v}\ dV + \int_K \nabla\Pi u\ \overline{\nabla v}\ dV + \int_K \nabla u\ \overline{\nabla\Pi v}\ dV\right| \\
&\leq \omega^2\|\Pi u\|_{1,\omega,K}\|\Pi v\|_{1,\omega,K} + \|\Pi u\|_{1,\omega,K}\|v\|_{1,\omega,K} + \|u\|_{1,\omega,K}\|\Pi v\|_{1,\omega,K} \\
&\overset{(4.10)}{\leq} (\omega^2\beta^{-2} + 2\beta^{-1})\|u\|_{1,\omega,K}\|v\|_{1,\omega,K}
\end{aligned}$$

where $\beta > 0$ depends on $h_K\omega$. Therefore, the global PW-VEM form fulfills Equation (4.16) with $\gamma \geq \beta_{\min}^{-2} + 2\beta_{\min}^{-1}$ where $\beta_{\min} = \min_{K\in\mathcal{T}_h}\beta(h_K\omega)$.

Unfortunately, the right-hand side of Equation (4.23) is not computable and we need to approximate it, see Section 4.2.5 below.

4.2.5 Matrix Representation

For every $K \in \mathcal{T}_h(\Omega)$ we will show how to assemble the local matrix, which summed up, as in Equation (4.13), gives the global matrix representation.

For $u \in V_p(K)$ its image under Π is an element in $V_p^*(K)$ and therefore can be expressed in the basis $\{\varphi_\ell\}_{\ell=1}^p$, thus

$$\Pi u = \sum_{\ell=1}^{p} s_\ell \pi_\ell. \tag{4.24}$$

Using this expression for the projection in Equation (4.9), and choosing basis functions as test functions gives

$$\sum_{\ell=1}^{p} s_\ell \; a^K(\pi_\ell, \pi_j) = a^K(v, \pi_j) \qquad j = 1, \dots, p. \tag{4.25}$$

This linear system of equations can be written as

$$\begin{bmatrix} a^K(\pi_1,\pi_1) & a^K(\pi_2,\pi_1) & \cdots & a^K(\pi_p,\pi_1) \\ a^K(\pi_1,\pi_2) & a^K(\pi_2,\pi_2) & \cdots & a^K(\pi_p,\pi_2) \\ \vdots & \vdots & \ddots & \vdots \\ a^K(\pi_1,\pi_p) & a^K(\pi_2,\pi_p) & \cdots & a^K(\pi_p,\pi_p) \end{bmatrix} \begin{bmatrix} s_1 \\ s_2 \\ \vdots \\ s_p \end{bmatrix} = \begin{bmatrix} a^K(v,\pi_1) \\ a^K(v,\pi_2) \\ \vdots \\ a^K(v,\pi_p). \end{bmatrix}$$

Let us denote the elements in the above equation with G for the $p \times p$ matrix

$$G(j,\ell) := a^K(\pi_\ell, \pi_j) \qquad j = 1, \dots, p, \;\; \ell = 1, \dots, p$$

and the vectors $s = [s_1, \dots, s_p]^t$ and $b = [a^K(v,\pi_1), \dots, a^K(v,\pi_p)]^t$.

We continue by computing the projection of the basis functions $\{\psi_k\}_{k=1}^{np}$ of $V_p(K)$ under Π. To this end, we define $s^k = [s_1^k, \dots, s_p^k]^t$ as the coefficients of $\Pi\psi_k$ in the basis $\{\pi_j\}_{j=1}^p$. From the linear system in Equation (4.25) we get

$$s^k = G^{-1} b^k,$$

where $b^k = [a^K(\psi_k,\pi_1), \dots, a^K(\psi_k,\pi_p)]^t$ denotes the corresponding right hand side with $v = \psi_j$. We combine the right hand side vectors b^k into one $p \times np$ matrix, defining

$$B := [b^1, \dots, b^{np}] = \begin{bmatrix} a^K(\psi_1,\pi_1) & a^K(\psi_2,\pi_1) & \cdots & a^K(\psi_{np},\pi_1) \\ a^K(\psi_1,\pi_2) & a^K(\psi_2,\pi_2) & \cdots & a^K(\psi_{np},\pi_2) \\ \vdots & \vdots & \ddots & \vdots \\ a^K(\psi_1,\pi_p) & a^K(\psi_2,\pi_p) & \cdots & a^K(\psi_{np},\pi_p) \end{bmatrix}.$$

Therefore the matrix representation of the operator Π acting from $V_p \to V_p^*$ in the basis $\{\pi_j\}_{j=1}^p$ is given by $G^{-1}B$.

Finally, we need the inclusion of Πu into the space V_p. Since φ_j are a partition of unity we have that

$$\pi_\ell = e^{i\omega \boldsymbol{d}_\ell \cdot (\boldsymbol{x} - \boldsymbol{x}_K)} = \sum_{j=1}^{n} e^{i\omega \boldsymbol{d}_\ell \cdot (\boldsymbol{v}_j - \boldsymbol{x}_K)} e^{i\omega \boldsymbol{d}_\ell \cdot (\boldsymbol{x} - \boldsymbol{v}_j)} \varphi_j(\boldsymbol{x}) = \sum_{j=1}^{n} e^{i\omega \boldsymbol{d}_\ell \cdot (\boldsymbol{v}_j - \boldsymbol{x}_K)} \psi_{(j-1)p+\ell}(\boldsymbol{x}).$$

Thus the change of basis matrix D of size $np \times p$ is given by

$$D((j-1)p + \ell, \ell) := e^{i\omega \boldsymbol{d}_\ell \cdot (\boldsymbol{v}_j - \boldsymbol{x}_K)} \qquad j = 1, \dots, n, \;\; \ell = 1, \dots, p$$

and the matrix representation P, with size $np \times np$, of the operator Π followed by the inclusion from V_p^* into V_p is given by

$$P = DG^{-1}B.$$

We calculate a matrix representation for the first term, with the help of Equation (4.24) we get

$$a^K(\Pi\psi_\ell, \Pi\psi_m) = \sum_{i,j=1}^{p} s_i^\ell \bar{s}_j^m a^K(\pi_i, \pi_j) = \sum_{i,j=1}^{p} (G^{-1}B)_{i\ell}\overline{(G^{-1}B)}_{jm} G_{ji}.$$

Hence, matrix representation A_Π of the above is given by

$$A_\Pi = \overline{B}^T \overline{G}^{-1} B.$$

Similarly, we can find the matrix expression for the stabilization term (4.23) to be

$$(\overline{I-P})^t A(I-P).$$

with the following matrices involved: I denotes the identity matrix of size pn_K, P denotes the matrix introduced above, and A holds the integral

$$A(r,s) = \int_K \nabla\psi_s \cdot \overline{\nabla\psi}_r \; dV.$$

Since we do not know the explicit form of the $V_p(K)$ basis functions on the inside of K we resort to approximating this integral. Since

$$\begin{aligned}\nabla\psi_r &= (\nabla\varphi_j + \varphi_j \; i\omega \boldsymbol{d}_\ell)\pi_{j\ell} \\ \nabla\psi_s &= (\nabla\varphi_\kappa + \varphi_\kappa \; i\omega \boldsymbol{d}_m)\pi_{\kappa m}\end{aligned}$$

the product inside the integral is

$$\nabla\psi_s \cdot \overline{\nabla\psi}_r = \left(\nabla\varphi_\kappa \cdot \nabla\varphi_j + i\omega\varphi_\kappa \boldsymbol{d}_m \cdot \nabla\varphi_j - i\omega\varphi_j \boldsymbol{d}_\ell \cdot \nabla\varphi_\kappa + \omega^2 \varphi_\kappa\varphi_j \boldsymbol{d}_m \cdot \boldsymbol{d}_\ell\right) \pi_{\kappa m}\overline{\pi}_{j\ell}.$$

We have already established that $\|\nabla\varphi_j\|_{L^\infty(K)} \leq C_G/h_K$ (compare proof of Proposition 4.4), and therefore the first term in the brackets scales with h_K^{-2}. Thus for small mesh sizes we can neglect the other terms in the bracket and replace the first one by $\delta_{\kappa j}/h_K^2$. The new matrix representation S_K for the approximated stabilization term is

$$S_K = \overline{(I-P)}^t M(I-P), \tag{4.26}$$

where the $pn_K \times pn_K$ dimensional mass matrix M is the approximation of A with the entries

$$M(r,s) = \int_K \frac{\delta_{\kappa j}}{h_K^2} \pi_{\kappa m}\overline{\pi}_{j\ell} \; dV \quad \text{where} \quad r = (j-1)p + \ell, \; s = (\kappa-1)p + m.$$

In terms of V_p^* basis functions this integral can be written as

$$\int_K \frac{\delta_{\kappa j}}{h_K^2} \pi_{\kappa m}\overline{\pi}_{j\ell} \; dV = \frac{\delta_{\kappa j}}{h_K^2} e^{i\omega \boldsymbol{d}_m(\boldsymbol{x}_K - \boldsymbol{v}_j)} e^{-i\omega \boldsymbol{d}_\ell(\boldsymbol{x}_K - \boldsymbol{v}_\kappa)} \int_K \pi_m \overline{\pi}_\ell \; dV$$

where the integral on the right is computable as we see in Remark 4.9.

Remark 4.8. Exploring different choices for the stabilization term s^K could still improve the PW-VEM method. Especially the approximation leading to S_K could be subject of improvement, as suggested by the discussion in Section 6.1.

We still need to address the boundary integral in Equation (4.14), that is $i\omega \int_{\partial\Omega\cap\partial K} u\overline{v}\ dS$. We define the matrix

$$R(r,s) = i\omega \int_{\partial\Omega\cap\partial K} \psi_s \overline{\psi_r}\ dS, \qquad r,s = 1,\dots,n_K p.$$

Combining everything, the complete matrix representation on each element K for the PW-VEM left hand side is given by

$$\boxed{\overline{B}^t \overline{G}^{-1} B + \overline{(I-P)}^t M (I-P) + R.} \tag{4.27}$$

The following remark shows how to actually compute each of the integrals in the matrix entries we used above.

Remark 4.9. First we show that we can calculate integrals of $\pi_m \bar{\pi}_\ell$ on mesh faces F. Let $\boldsymbol{a}, \boldsymbol{b}$ be the start- and endpoint of F, then

$$\int_F e^{i\omega(\boldsymbol{d}_m - \boldsymbol{d}_\ell)\cdot \boldsymbol{x}} dS = |F| e^{i\omega(\boldsymbol{d}_m - \boldsymbol{d}_\ell)\cdot \boldsymbol{a}} \int_0^1 e^{i\omega(\boldsymbol{d}_m - \boldsymbol{d}_\ell)\cdot(\boldsymbol{b}-\boldsymbol{a})t} dt,$$

for the integral on the right recall that

$$\int_0^1 e^{zt} dt = \begin{cases} \frac{e^z - 1}{z} & \text{for } z \neq 0 \\ 1 & \text{for } z = 0 \end{cases}$$

holds for all $z \in \mathbb{C}$.

For the computation of G we need to calculate integrals of the type $\int_K e^{i\omega(\boldsymbol{d}_m - \boldsymbol{d}_\ell)\cdot \boldsymbol{x}}\ dV$. We consider two cases: For $m = \ell$ the integral is simply $|K|$ and for the case $m \neq \ell$ we use integration by parts to find

$$\begin{aligned}
\int_K e^{i\omega(\boldsymbol{d}_m - \boldsymbol{d}_\ell)\cdot \boldsymbol{x}}\ dV &= \frac{-1}{\omega^2 (\boldsymbol{d}_m - \boldsymbol{d}_\ell)\cdot(\boldsymbol{d}_m - \boldsymbol{d}_\ell)} \int_K \nabla \cdot \nabla e^{i\omega(\boldsymbol{d}_m - \boldsymbol{d}_\ell)\cdot \boldsymbol{x}} \\
&= \frac{-1}{\omega^2 (\boldsymbol{d}_m - \boldsymbol{d}_\ell)\cdot(\boldsymbol{d}_m - \boldsymbol{d}_\ell)} \int_{\partial K} \nabla e^{i\omega(\boldsymbol{d}_m - \boldsymbol{d}_\ell)\cdot \boldsymbol{x}} \cdot \boldsymbol{\nu}_K\ dS \\
&= \sum_{F\in\partial K} \frac{(\boldsymbol{d}_m - \boldsymbol{d}_\ell)\cdot \boldsymbol{\nu}_F}{i\omega(\boldsymbol{d}_m - \boldsymbol{d}_\ell)\cdot(\boldsymbol{d}_m - \boldsymbol{d}_\ell)} \int_F e^{i\omega(\boldsymbol{d}_m - \boldsymbol{d}_\ell)\cdot \boldsymbol{x}} dS \qquad \text{for } m \neq \ell
\end{aligned}$$

where $\boldsymbol{\nu}_F$ is the outer normal vector of the face F. We can use our previous result to compute the last integral.

For B we need to compute $a^K(\psi_r, \pi_\ell)$. We can use the argument established in Equation (4.11) to get

$$a^K(\psi_r, \pi_\ell) = \int_K \nabla\psi_r \cdot \overline{\nabla\pi}_\ell\ dV - \omega^2 \int_K \psi_r \overline{\pi}_\ell\ dV = -i\omega \int_{\partial K} \boldsymbol{d}_\ell \cdot \nu_K \psi_r \bar{\pi}_\ell\ dS.$$

The integral on the right is of the type $\int_F \varphi_j(\boldsymbol{x}) e^{i\omega(\boldsymbol{d}_m - \boldsymbol{d}_\ell)\cdot \boldsymbol{x}}\ dS$ and we can compute it exactly. Recall, that the functions φ_j were determined by $\varphi_j(\boldsymbol{v}_i) = \delta_{ij}$ and are linear on each edge. Thus, if $\boldsymbol{v}_j$ is not an endpoint of F we have that φ_j is zero on that edge and therefore the integral is zero. Otherwise, let $\boldsymbol{a}$ be the coordinate vector of $\boldsymbol{v}_j$ and $\boldsymbol{b}$ be the other endpoint of F then

$$\int_F \varphi_j(\boldsymbol{x}) e^{i\omega(\boldsymbol{d}_m - \boldsymbol{d}_\ell)\cdot \boldsymbol{x}}\ dS = |F| e^{i\omega(\boldsymbol{d}_m - \boldsymbol{d}_\ell)\cdot \boldsymbol{a}} \int_0^1 (1-t) e^{i\omega(\boldsymbol{d}_m - \boldsymbol{d}_\ell)\cdot(\boldsymbol{b}-\boldsymbol{a})t}\ dt$$

where we can use the formula

$$\int_0^1 (1-t)e^{zt}\ dt = \begin{cases} \frac{e^z-z-1}{z^2} & \text{for } z \neq 0 \\ \frac{1}{2} & \text{for } z = 0 \end{cases}$$

for the integral on the right.

Finally, for the matrix R, we need to evaluate integrals of the form

$$\int_F \varphi_i(\boldsymbol{x})\varphi_j(\boldsymbol{x})e^{i\omega(\boldsymbol{d}_m-\boldsymbol{d}_\ell)\cdot\boldsymbol{x}}dS.$$

Again, we need to distinguish cases depending on the points $\boldsymbol{v}_i, \boldsymbol{v}_j$ determining the functions φ_i, φ_j. If either $\boldsymbol{v}_i$ or $\boldsymbol{v}_j$ is not an endpoint of F the integral is zero. Otherwise, we have to cases: Either $\boldsymbol{v}_i = \boldsymbol{v}_j$ or $\boldsymbol{v}_i, \boldsymbol{v}_j$ are the opposite endpoints of F.

In the first case we have $i = j$ and denoting $\boldsymbol{a} = \boldsymbol{v}_i = \boldsymbol{v}_j$ and the other endpoint of F by $\boldsymbol{b}$ we get

$$\int_F \varphi_i^2 e^{i\omega(\boldsymbol{d}_m-\boldsymbol{d}_\ell)\cdot\boldsymbol{x}}dS = |F|e^{i\omega(\boldsymbol{d}_m-\boldsymbol{d}_\ell)\cdot\boldsymbol{a}}\int_0^1 (1-t)^2 e^{i\omega(\boldsymbol{d}_m-\boldsymbol{d}_\ell)\cdot(\boldsymbol{b}-\boldsymbol{a})t}\ dt$$

where the integral on the right can be computed with

$$\int_0^1 (1-t)^2 e^{zt}\ dt = \begin{cases} \frac{2(e^z-z-2)-z^2}{z^3} & \text{for } z \neq 0 \\ \frac{1}{3} & \text{for } z = 0 \end{cases}$$

For the second case where $i \neq j$, the endpoints of F are $\boldsymbol{v}_j$ and $\boldsymbol{v}_i$ that we will denote by $\boldsymbol{a}$ and $\boldsymbol{b}$, respectively. Then

$$\int_F \varphi_i\varphi_j e^{i\omega(\boldsymbol{d}_m-\boldsymbol{d}_\ell)\cdot\boldsymbol{x}}dS = |F|e^{i\omega(\boldsymbol{d}_m-\boldsymbol{d}_\ell)\cdot\boldsymbol{a}}\int_0^1 (1-t)te^{i\omega(\boldsymbol{d}_m-\boldsymbol{d}_\ell)\cdot(\boldsymbol{b}-\boldsymbol{a})t}\ dt$$

which is computable using

$$\int_0^1 (1-t)te^{zt}\ dt = \begin{cases} \frac{e^z(z-2)+z+2}{z^3} & \text{for } z \neq 0 \\ \frac{1}{6} & \text{for } z = 0 \end{cases}.$$

Remark 4.10. Using Equation (4.27), we are able to obtain the matrix form of Equation (4.15). Solving the linear system of equations provides us with a solution in the $V_p(\mathcal{T}_h)$-space. Thus we are left with the issue of reconstructing the numerical solution in the element interiors. We discuss possible options in Section 5.1.1.

4.3 Discontinuous Galerkin Method

4.3.1 PW-DG formulation

We derive the Planewave Discontinuous Galerkin method following [14], starting by writing problem (2.6) as a system of first order differential equations, using the auxiliary function $\boldsymbol{\sigma} : \Omega \to \mathbb{R}^2$.

$$\begin{aligned} i\omega\ \boldsymbol{\sigma} &= \nabla u \qquad \text{in } \Omega \\ i\omega\ u - \nabla \cdot \boldsymbol{\sigma} &= 0 \qquad \text{in } \Omega \\ i\omega\ \boldsymbol{\sigma} \cdot \boldsymbol{\nu}_K + i\omega\ u &= g \qquad \text{on } \partial\Omega \end{aligned}$$

Similar as to obtaining the weak formulation, we multiply the first two equations with test functions and integrate over $K \in \mathcal{T}_h$. Using integration by parts we get

$$\begin{aligned} \int_K i\omega\ \boldsymbol{\sigma} \cdot \overline{\boldsymbol{\tau}}\ dV + \int_K u\overline{\nabla \cdot \boldsymbol{\tau}}\ dV - \int_{\partial K} u\overline{\boldsymbol{\tau} \cdot \boldsymbol{\nu}_K}\ dS = 0 \qquad \forall \boldsymbol{\tau} \in \mathbf{H}(div; K) \\ \int_K i\omega\ u\overline{v}\ dV + \int_K \boldsymbol{\sigma} \cdot \overline{\nabla v}\ dV - \int_{\partial K} \boldsymbol{\sigma} \cdot \boldsymbol{\nu}_K \overline{v}\ dS = 0 \qquad \forall v \in H^1(K) \end{aligned}$$

The space that inhabits the test functions for our auxiliary function and is defined by $\mathbf{H}(div; K) := \{u \in L^2(K, \mathbb{R}^2) \mid \nabla u \in L^2(K)\}$.

The next step, is to restrict our search for a solution to our approximating space, which we choose to be the PW space $V_p^*(\mathcal{T}_h)$, given in Equation (4.7), spanned by $p \in \mathbb{N}$ plane waved. Therefore, we replace u, v and $\boldsymbol{\sigma}, \boldsymbol{\tau}$ by $u_p, v_p \in V_p^*(\mathcal{T}_h)$ and $\boldsymbol{\sigma}_p, \boldsymbol{\tau}_p \in V_p^*(\mathcal{T}_h)^2$, respectively. Furthermore, we replace $u, \boldsymbol{\sigma}$ in the boundary integral by *numerical fluxes* $\hat{u}_p, \hat{\boldsymbol{\sigma}}_p$. The choice of those is non-trivial. They not only have to approximate the traces across inter-element boundaries, but also take care of the inhomogeneous boundary conditions. We will give one possible definition of the numerical fluxes later on.

$$\begin{aligned} \int_K i\omega\ \boldsymbol{\sigma}_p \cdot \overline{\boldsymbol{\tau}}_p\ dV + \int_K u_p\overline{\nabla \cdot \boldsymbol{\tau}_p}\ dV - \int_{\partial K} \hat{u}_p\overline{\boldsymbol{\tau}_p \cdot \boldsymbol{\nu}_K}\ dS = 0 \qquad \forall \boldsymbol{\tau}_p \in V_p^*(K)^2 \\ \int_K i\omega\ u_p\overline{v}_p\ dV + \int_K \boldsymbol{\sigma}_p \cdot \overline{\nabla v_p}\ dV - \int_{\partial K} \hat{\boldsymbol{\sigma}}_p \cdot \boldsymbol{\nu}_K \overline{v_p}\ dS = 0 \qquad \forall v_p \in V_p^*(K) \end{aligned} \tag{4.28}$$

Next, we aim to get rid of the volume integrals. We start by integrating by parts the first equation of (4.28) and get

$$\int_K \boldsymbol{\sigma}_p \cdot \overline{\boldsymbol{\tau}_p}\ dV = \frac{1}{\omega}\int_K \nabla u_p \cdot \overline{\boldsymbol{\tau}_p}\ dV - \frac{1}{i\omega}\int_{\partial K} (u_p - \hat{u}_p)\overline{\boldsymbol{\tau}_p \cdot \boldsymbol{\nu}_K}\ dS. \tag{4.29}$$

It is easy to see that $\nabla_h V_p^*(\mathcal{T}_h) \subseteq V_p^*(\mathcal{T}_h)^2$, where ∇_h denotes the element wise application of ∇. Therefore we can choose for $\boldsymbol{\tau}_p = \nabla v_p$ in the above equation, allowing us to substitute it for the second term of the second equation in (4.28). We get

$$\int_K (\nabla u_p \cdot \overline{\nabla v_p} - \omega^2 u_p \overline{v_p})\ dV - \int_{\partial K} (u_p - \hat{u}_p)\overline{\nabla v_p \cdot \boldsymbol{\nu}_K}\ dS - \int_{\partial K} i\omega\hat{\boldsymbol{\sigma}}_p \cdot \boldsymbol{\nu}_K\ \overline{v_p}\ dS = 0. \tag{4.30}$$

Note that any solution u_p of Equation (4.30) will also be a solution for Equation (4.28), however we need Equation (4.29) to recover the $\boldsymbol{\sigma}_p$ solution component. Integrating the first term by parts once more, the boundary integral over u_p cancels, giving

$$\int_K \overline{(-\Delta v_p - \omega^2 v_p)}\ u_p dV + \int_{\partial K} \hat{u}_p\overline{\nabla v_p \cdot \boldsymbol{\nu}_K}\ dS - \int_{\partial K} i\omega\hat{\boldsymbol{\sigma}}_p \cdot \boldsymbol{\nu}_K\ \overline{v_p}\ dS = 0.$$

Recall that $v_p \in V_p^*(\mathcal{T}_h)$ solves the homogeneous Helmholtz equation and therefore the volume integral vanishes. Thus we are left with

$$\int_{\partial K} \hat{u}_p\overline{\nabla v_p \cdot \boldsymbol{\nu}_K}\ dS - \int_{\partial K} i\omega\hat{\boldsymbol{\sigma}}_p \cdot \boldsymbol{\nu}_K\ \overline{v_p}\ dS = 0. \tag{4.31}$$

We are left with the task of defining the numerical fluxes. We first review some standard DG notation. For any two elements $K^+, K^- \in \mathcal{T}_h$ sharing (part of) an edge let u^+, u^- be the extension onto the edge of the function u, respectively from the side of K^+ and K^-. Furthermore, let us denote $\boldsymbol{\nu}_K^+, \boldsymbol{\nu}_K^-$ for the exterior norm vectors of K^+ and K^- on their shared edge. For piecewise smooth function $u_p : \mathbb{R}^2 \to \mathbb{R}$ and vector field $\boldsymbol{\sigma}_p : \mathbb{R}^2 \to \mathbb{R}^2$ we now define

$$\begin{aligned} \text{the averages:} \quad & \{\!\{u_p\}\!\} := \frac{1}{2}(u_p^+ + u_p^-) \quad , \quad \{\!\{\boldsymbol{\sigma}_p\}\!\} := \frac{1}{2}(\boldsymbol{\sigma}_p^+ + \boldsymbol{\sigma}_p^-) \\ \text{the jumps:} \quad & [\![u_p]\!]_N = u_p^+ \boldsymbol{\nu}_K^+ + u_p^- \boldsymbol{\nu}_K^- \quad , \quad [\![\boldsymbol{\sigma}_p]\!]_N := \boldsymbol{\sigma}_p^+ \cdot \boldsymbol{\nu}_K^+ + \boldsymbol{\sigma}_p^- \cdot \boldsymbol{\nu}_K^- \end{aligned}$$

We will denote with $\mathcal{F}_h = \cup_{K \in \mathcal{T}_h} \partial K$ the skeleton of the mesh, which can be split into exterior faces $\mathcal{F}_h^B = \mathcal{F}_h \cap \partial\Omega$ and interior faces $\mathcal{F}_h^I = \mathcal{F}_h \setminus \mathcal{F}_h^B$.

The numerical flux on interior faces is defined by

$$\begin{cases} \hat{\boldsymbol{\sigma}}_p = \dfrac{1}{i\omega} \{\!\{\nabla_h u_p\}\!\} - \alpha [\![u_p]\!]_N, \\ \hat{u}_p = \{\!\{u_p\}\!\} - \beta \dfrac{1}{i\omega} [\![\nabla_h u_p]\!]_N \end{cases} \tag{4.32}$$

and on boundary faces by

$$\begin{cases} \hat{\boldsymbol{\sigma}}_p = \dfrac{1}{i\omega} \nabla_h u_p - (1-\delta) \left(\dfrac{1}{i\omega} \nabla_h u_p + u_p \boldsymbol{\nu}_K - \dfrac{1}{i\omega} h \boldsymbol{\nu}_K \right), \\ \hat{u}_p = u_p - \delta \left(\dfrac{1}{i\omega} \nabla_h u_p \cdot \boldsymbol{\nu}_K + u_p - \dfrac{1}{i\omega} h \right), \end{cases} \tag{4.33}$$

where α, β and δ are the *flux parameters*, yet to be chosen. Note that the averages and jumps are symmetric in the sense that we can exchange K^+ and K^- with no effect on the results. The same goes for our definition of the numerical fluxes. Thus, summing (4.31) over all elements $K \in \mathcal{T}_h$ gives

$$\int_{\mathcal{F}_h^I} \left(\hat{u}_p [\![\overline{\nabla_h v_p}]\!]_N - i\omega \hat{\boldsymbol{\sigma}} \cdot [\![\overline{v_p}]\!]_N \right) \, dS + \int_{\mathcal{F}_h^B} \left(\hat{u}_p \overline{\nabla_h v_p \cdot \boldsymbol{\nu}_K} - i\omega \hat{\boldsymbol{\sigma}} \cdot \boldsymbol{\nu}_K \overline{v_p} \right) \, dS = 0. \tag{4.34}$$

Substituting the definition for the fluxes the PW-DG method reads: find $u_p \in V_p(\mathcal{T}_h)$ such that, for all $v_p \in V_p(\mathcal{T}_h)$,

$$\mathcal{A}_h(u_p, v_p) = \ell_h(v_p) \tag{4.35}$$

where

$$\begin{aligned} \mathcal{A}_h(u, v) = & \int_{\mathcal{F}_h^I} \left(\{\!\{u\}\!\} + i\omega^{-1} \beta [\![\nabla_h u]\!]_N \right) [\![\overline{\nabla_h v}]\!]_N - \left(\{\!\{\nabla_h u\}\!\} + i\omega\alpha [\![u]\!]_N \right) \cdot [\![\bar{v}]\!]_N \, dS \\ & + \int_{\mathcal{F}_h^B} \left((1-\delta)u + i\omega^{-1}\delta \, \nabla_h u \cdot \boldsymbol{\nu}_K \right) \overline{\nabla_h v \cdot \boldsymbol{\nu}_K} - \left(\delta \, \nabla_h u \cdot \boldsymbol{\nu}_K + i\omega(1-\delta)u \right) \bar{v} \, dS \end{aligned}$$

and

$$\ell_h(v) = i\omega^{-1} \int_{\mathcal{F}_h^B} \delta \, g \, \overline{\nabla_h v \cdot \boldsymbol{\nu}_K} \, dS + \int_{\mathcal{F}_h^B} (1-\delta) \, g \, \bar{v} \, dS. \tag{4.36}$$

Different choices of flux parameters lead to different methods. The original ultra weak variational formulation (UWVF) as introduced in [8] is recovered by choosing

$$\alpha = \beta = \delta = \frac{1}{2}. \tag{4.37}$$

Some error estimates have stronger requirements on the mesh parameters. A dependence on the mesh size h has proven favorable. The choice

$$\alpha = \frac{a}{\omega h}, \qquad \beta = b\omega h, \qquad \delta = d\omega h$$

with $a \geq a_{\min} > 0, b \geq 0$ on $\mathcal{F}_h^I$ and $d > 0$ on $\mathcal{F}_h^B$ is discussed in [13] with error estimates for the non-homogeneous Helmholtz problem. The UWVF does not fulfill the requirements for the estimates given in this paper. A detailed numerical comparison between the UWVF and three PW-DG methods with different choices of a, b, d is recorded in the paper and in the case of the homogeneous problem the UWVF is slightly outperformed by the other methods.

4.3.2 Convergence Results

The DG methods convergence analysis relies on the observation that

$$\begin{aligned}\|v\|_{\mathcal{F}_h}^2 :&= \mathrm{Im}[\mathcal{A}_h(v,v)] \\ &= \omega^{-1}\|\beta^{\frac{1}{2}}[\![\nabla_h v]\!]_N\|_{0,\mathcal{F}_h^I}^2 + \omega\|\alpha^{\frac{1}{2}}[\![v]\!]_N\|_{0,\mathcal{F}_h^I}^2 \\ &\quad + \omega^{-1}\|\delta^{\frac{1}{2}}\nabla_h v \cdot n\|_{0,\mathcal{F}_h^B}^2 + \omega\|(1-\delta)^{\frac{1}{2}} v\|_{0,\mathcal{F}_h^B}^2\end{aligned}$$

defines a norm on the space $V_p(\mathcal{T}_h)$. This is shown, along side with the above equality, quasi-optimality and well-posedness of the method in [14],[7]. Furthermore, the following p-error estimate is derived

Theorem 4.11 ([14], Theorem 3.15)**.** *Let $u \in H^{m+1}(\Omega)$ be the analytical solution to Equation* (2.6) *and let u_p be the PW-DG solution, given in Equation* (4.35)*. Assuming that $p = 2q+1$ is large enough, in particular*

$$m \leq \left\lceil \frac{q+1}{2} \right\rceil \tag{4.38}$$

holds, then

$$\|u - u_p\|_{\mathcal{F}_h} \leq C\ \omega^{-\frac{1}{2}} h^{m-\frac{1}{2}} \left(\frac{\log(p)}{p}\right)^{m-\frac{1}{2}} \|u\|_{m+1,\omega,\Omega} \tag{4.39}$$

$$\|u - u_p\|_{0,\Omega} \leq C\ h^{m-1} \left(\frac{\log(p)}{p}\right)^{m-\frac{1}{2}} \|u\|_{m+1,\omega,\Omega}. \tag{4.40}$$

where there exits a $C > 0$ independent of p and u, but increasing as a function of the product ωh.

Remark 4.12. Note that due to condition (4.38), the above result does not capture the convergence behavior at small p. Following the proofs in [14] with the h-estimate given in Theorem 3.20, which gives information for $q \leq m$, we get $h^{\min(q,m)-1}$ convergence in the L^2 norm, see also [7, Thm. 4.1] and [8, Thm. 3.7]. This under-estimates the actual convergence rate observed in the numerical results carried out in Section 6.

We will see, that a convergence rate similar to the one of the VEM can be expected. The main difference between the derivation of the bounds for the VEM and the DG, is the use of a dual argument for the h-estimate in [25]. h-version estimates with optimal convergence rates for the PW-DG method were derived in [13]. There it was also shown that, in the inhomogeneous case, only low order convergence is achieved, no matter how many plane waves per element are used.

In case of p-convergence we have seen that plane waves are able to approximate the homogeneous Helmholtz solution with exponential rate, if the solution is smooth enough, see Remark 3.22. This carries over to the PW-DG method, as we will see in the numeric examples.

5 Notes on Implementation

5.1 PW-VEM

Let us discuss the implementational details of the PW-VEM. All computations needed to compute the local matrices are stated in Remark 4.9, the pseudo code below will focus on how to assemble the global matrix. Note that we will make use of the fact that G can also be assembled using $G = BD$.

Algorithm 1: `PW-VEM`

Input: mesh, wavelength ω, plain wave degree $p = 2q + 1$, plane wave directions $d_1, \dots, d_p$
Output: approximation u_{hp} in VEM basis

for *each mesh element* K **do**
- Get number of vertices n_K and vertices $\boldsymbol{v}_1, ..., \boldsymbol{v}_{n_K}$ of the element K;
- Assemble local matrices M, B, R^K using remark 4.9;
- Assemble local matrix D;
- Calculate $G = BD$;
- Assemble local right hand side b^K using quadrature;
- Set $A^K = \overline{B}^t \overline{G}^{-1} B \qquad S^K = \overline{(I-P)}^t M (I-P)$;
- **for** *local vertices* $\boldsymbol{v}_i, \boldsymbol{v}_j$ *of* K **do**
  - Let $\mathrm{ind}(\boldsymbol{v}_i)$ denote the index of $\boldsymbol{v}_i$ in the array of mesh vertices;
  - **for** *plane waves* $\ell = 1, \dots, p$ **do**
    - Let $\mathrm{ind}_i = p(\mathrm{ind}(\boldsymbol{v}_i) - 1) + \ell$;
    - Let $\mathrm{ind}_i^{loc} = p(i-1) + \ell$;
    - Insert into global matrices

$$A(\mathrm{ind}_i, \mathrm{ind}_j) = A(\mathrm{ind}_i, \mathrm{ind}_j) + A^K(\mathrm{ind}_i^{loc}, \mathrm{ind}_j^{loc})$$
$$S(\mathrm{ind}_i, \mathrm{ind}_j) = S(\mathrm{ind}_i, \mathrm{ind}_j) + S^K(\mathrm{ind}_i^{loc}, \mathrm{ind}_j^{loc})$$
$$R(\mathrm{ind}_i, \mathrm{ind}_j) = R(\mathrm{ind}_i, \mathrm{ind}_j) + R^K(\mathrm{ind}_i^{loc}, \mathrm{ind}_j^{loc})$$

    and for the global right hand side

$$b(\mathrm{ind}_j) = b(\mathrm{ind}_j) + b^K(\mathrm{ind}_j^{loc})$$

- Calculate $\mathcal{A} = A + S + R$;
- Solve $\mathcal{A} u_{hp} = b$;

5.1.1 Reconstructing the Solution

The solution u_{hp} produced by Algorithm 1 is given in the PW-VEM space basis. If we denote by $ind(K)$ the index of the element K in $\mathcal{T}_h$ we can write the local solution, using the local basis functions ψ_j, as

$$\sum_{j=1}^{n_K p} (u_{hp})_{ind(K)+j} \psi_j.$$

However, we do not know the exact basis functions for V_p, and therefore we are not able to reconstruct a function from u_{hp} in the PW-VEM basis. In the following, we will compare two different methods of reconstructing the solution. Note that the global solution is obtained by summing over all elements $K \in \mathcal{T}_h$. We will keep the analysis local and assume without loss of generality that $ind(K) = 0$.

First, we will use the projection operator Π to project u_{hp} onto the space of plane waves. This can be done using the matrix P, in fact

$$\sum_{j=1}^{n_K p}(u_h)_j \Pi\psi_j = \sum_{j=1}^{n_K p}(u_h)_j \sum_{i=1}^{p}(P)_{ij}\pi_i = \sum_{i=1}^{p}(Pu_h)_i\pi_i.$$

Second, we will present the method used in [25]. Recall that the basis functions can be written as the product $\psi_r = \varphi_j(\boldsymbol{x})\pi_{j\ell}(\boldsymbol{x}),\ r = (j-1)p+\ell$. Since the plane wave functions are computable, another option is to project the VEM basis functions φ_j onto the polynomials of maximal order one. Therefore we use the projection operator $\Pi^\nabla : V(K) \to \mathbb{P}_1(K)$, introduced in [4]. The resulting space

$$V_p^\nabla(K) = \text{span}\{\Pi^\nabla\varphi_j(\boldsymbol{x})\pi_{j\ell}(\boldsymbol{x}) : r = (j-1)p+\ell\}$$

fulfills

$$V_P^*(K) \subset V_p^\nabla(K) \subseteq V_p(K).$$

The projection is given by

$$\Pi^\nabla\varphi_j(\boldsymbol{x}) = \frac{1}{2|K|}(\boldsymbol{x}-\boldsymbol{x}_K)\cdot\boldsymbol{\nu}_j + \frac{1}{n_K},$$

where ν_j is the exterior normal vector of the vector connecting the vertices $\boldsymbol{v}_{j-1}$ and $\boldsymbol{v}_{j+1}$. This projection keeps the important property that

$$\sum_{j}^{n_K}\varphi_j(\boldsymbol{x}) = 1 \qquad \forall\boldsymbol{x}\in K.$$

Finally, note that in the special case where K is a triangle, the basis of V_p are the $\mathbb{P}_1$ hat functions and since the projection is consistent we have $V_p^\nabla(K) = V_p(K)$.

5.2 PW-DG

We present pseudo-code for implementing the PW-DG method, in alg. 2. In the pseudo-code we go through the main steps of assembling the basis functions, calculating the local matrices and right hand side. Finally, inserting the local matrices correctly into the global matrix, to solve the linear system of equations posed by Equation (4.35). The MATLAB functions for computing the local components are given in Appendix A.2.

Algorithm 2: `DG`

Input: mesh $\mathcal{T}_h$, wavelength ω, plain wave degree $p = 2q + 1$, plane wave directions $d_1, \ldots, d_p$

Output: approximation u_h in PW basis

Initialize $(p \cdot \#\mathcal{T}_h) \times (p \cdot \#\mathcal{T}_h)$ matrix A and vector b of size $p \cdot \#\mathcal{T}_h$;

for *each mesh element* $K \in \mathcal{T}_h$ **do**

  Initialize local $p \times p$ matrices A^{K}, A^{κ};

  Get element center x_K and assemble local basis functions

$$\pi_j^K(x) = \begin{cases} e^{i\omega \boldsymbol{d}_j(\boldsymbol{x}-\boldsymbol{x}_K)} & \text{for } x \in K \\ 0 & \text{else} \end{cases} \qquad j = 1, \ldots, p$$

  for *each local edge* e *of* K **do**

    Let $\mathrm{ind}(K)$ denote the index of K in the array of mesh elements $\mathcal{T}_h$, then set $\mathrm{ind}_j^K = p(\mathrm{ind}(K) - 1) + j$ for $j = 1, \ldots, p$;

    if e *is a boundary edge* **then**

      Calculate $A_{j\ell}^{\mathrm{K}} = \mathcal{A}(\pi_\ell^K, \pi_j^K)$ for $j, \ell = 1, \ldots, p$;

      Calculate right hand side $b_j^K = \ell_h(\pi_j^K),\ j = 1, \ldots, p$ using quadrature;

      Insert local into global matrix using index

$$A(\mathrm{ind}_j^K, \mathrm{ind}_\ell^K) = A(\mathrm{ind}_j^K, \mathrm{ind}_\ell^K) + A_{j\ell}^{\mathrm{K}}, \qquad j, \ell = 1, \ldots, p$$

      and for the global right hand side

$$b(\mathrm{ind}_\ell^K) = b(\mathrm{ind}_\ell^K) + b_\ell^K, \qquad \ell = 1, \ldots, p$$

    else if e *is an interior edge* **then**

      Let $\kappa \in \mathcal{T}_h$ be the other mesh element sharing the edge e;

      Assemble basis functions $\pi_j^\kappa(x)$ of the adjecent element (as before);

      Calculate $A_{j\ell}^{\mathrm{K}} = \mathcal{A}(\pi_\ell^K, \pi_j^K)$ and $A_{j\ell}^{\kappa} = \mathcal{A}(\pi_\ell^K, \pi_j^\kappa)$ for $j, \ell = 1, \ldots, p$;

      Insert local into global matrix using index

$$A(\mathrm{ind}_j^K, \mathrm{ind}_\ell^K) = A(\mathrm{ind}_j^K, \mathrm{ind}_\ell^K) + A_{j\ell}^{\mathrm{K}}, \qquad j, \ell = 1, \ldots, p$$

      and for the mixed contribution let $\mathrm{ind}(\kappa)$ denote the index of κ in the array of mesh elements $\mathcal{T}_h$ and set $\mathrm{ind}_j^\kappa = p(\mathrm{ind}(\kappa) - 1) + j$ for $j = 1, \ldots, p$, then

$$A(\mathrm{ind}_j^K, \mathrm{ind}_\ell^\kappa) = A(\mathrm{ind}_j^K, \mathrm{ind}_\ell^\kappa) + A_{j\ell}^{\kappa}, \qquad j, \ell = 1, \ldots, p$$

Solve $Au_h = b$;

6 Numerical Results

In the following we will compare the convergence rates of PW-VEM to the PW-DG with fluxes chosen as in Equation (4.37) (UWVF). Both methods allow us to compute the integrals directly on each mesh element, without any use of a reference element. The main advantage the methods share is that only the integral involving the boundary datum g requires quadrature, all other integrals can be calculated exactly (see Remark 4.9). Moreover, no computation of volume integrals is required.

We will consider the two methods for reconstructing the solution of the PW-VEM, introduced in Section 5.1.1 and will refer to them as VEM Π and VEM Π^∇.

We consider the L^2-error given by

$$\frac{\|u - u_{hp}\|_{0,\Omega}}{\|u\|_{0,\Omega}}$$

for the approximation u_{hp} of the solution u to the homogeneous Helmholtz problem (2.6).

6.1 Effects of approximating the stabilization term in the PW-VEM

Recall that the VEM relies on the approximation of $a^K((I-\Pi)u,(I-\Pi)v)$ by the stabilization term $s^K((I-\Pi)u,(I-\Pi)v)$. We chose s^K in Equation (4.23) and established how to calculate the matrix form of the stabilization term in Section 4.2.5. During the matrix calculation we were forced to do further approximations in order to calculate the integrals involved. We are able to investigate the error during each of the approximation steps on triangular mashes, as the basis functions are fully known and we are able to compute and compare:

- the formulation without the stabilization term, which coincides with the partition of unity method (PUM), see [19],
- the formulation with the stabilization term, (4.23), computed exactly, (GRAD in the following), and
- the VEM with the approximation of the stabilization term.

The meshes divide Ω equally into squares, which are then divided into triangles by their diagonal. We choose the boundary datum g such that the correct solution is given by

$$u(x) = H_0^{(1)}(\omega|x - x_0|), \qquad x_0 = (-0.25, 0) \tag{6.1}$$

where $H_0^{(1)}$ is the zero-th order Hankel function of the first kind.

	PUM		GRAD		PW-VEM		PW-DG	
h	L^2-Error	rate	L^2-Error	rate	L^2-Error	rate	L^2-Error	rate
7.0711e-01	1.9213e-02	-	7.1989e-01	-	4.1548e-01	-	1.4261e-01	-
3.5355e-01	4.0683-04	5.5615	1.5517e-03	8.8577	1.0989e-02	5.2406	1.0633e-03	7.0673
1.7678e-01	3.4126e-06	6.8974	3.3981e-06	8.8349	1.2969e-04	6.4050	9.6063e-06	6.7904
8.8388e-02	4.0163e-08	6.4088	4.0148e-08	6.4033	1.1089e-06	6.8698	8.1903e-08	6.8739

Table 1: L^2-error comparison for $p = 13$ and $\omega = 20$.

The results for h-convergence on meshes with 8, 32, 128 and 512 triangles is reported in Table 1. We see that the formulation of the GRAD stabilization term is sufficient to guarantee an error compareable to that of the PUM. Going from GRAD to VEM, we lose some accuracy, however we keep the convergence rate. Note that GRAD performs much more similar to the PW-DG method. This suggests that there might be some room for improvement on the choice of the approximation of the stabilization term. To get the full picture, a comparison on other meshes would be in order.

[0]I thank A. Russo (University of Milano-Bicocca, Italy) for providing the meshes used in the experiments.

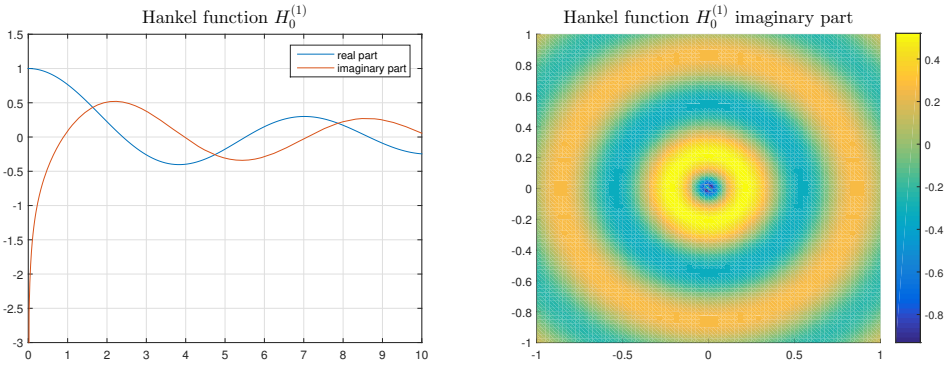

Figure 4: The Hankel function's real and imaginary part in 2D (left) and only the imaginary part in 3D (right).

6.2 The case of Triangular Meshes

We continue our analysis on triangular meshes. Since we are able to compute the VEM basis functions completely on triangles, we have that $V_p^\nabla = V_p$ and therefore $\Pi^\nabla u_{hp} = u_{hp}$, as discussed in Section 5.1.1. This makes for an interesting comparison of the projection Π and its effects on the numeric solution u_h, as we are able to evaluate u_h directly. The results are presented in Figure 5.

Surprisingly, even though $V_p^*(K) \subset V_p(K)$, the VEM Π outperforms the VEM Π^∇. Especially in the case of h-convergence, there is a clear difference in the error performance. It is yet to be discussed why this is the case. It seems that projecting the solution onto a Treffz space shows an advantage in the approximation of homogeneous problems. Furthermore, all methods show the same convergence properties: We have the expected h-convergence speed of 6.5, predicted by Remark 4.6 with $q = 6$. The p-convergence is exponential in all the cases.

On the right hand side in Figure 5, the L^2-error is plotted against the degrees of freedom. We observe that the VEM uses much less degrees of freedom. This is due to the fact that on triangular meshes the number of elements is larger than the number of vertices. Especially

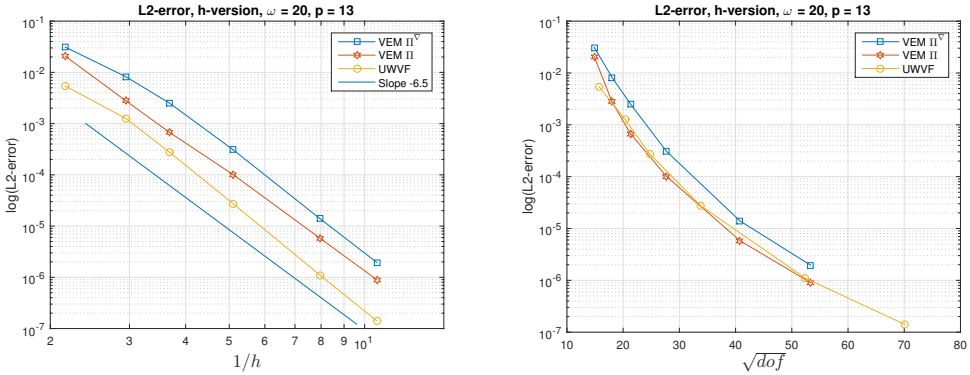

during p-convergence, where the triangular mesh that was used had 1545 elements with only 809 vertices. In the following experiments we will observe the opposite case when we use meshes containing polygons.

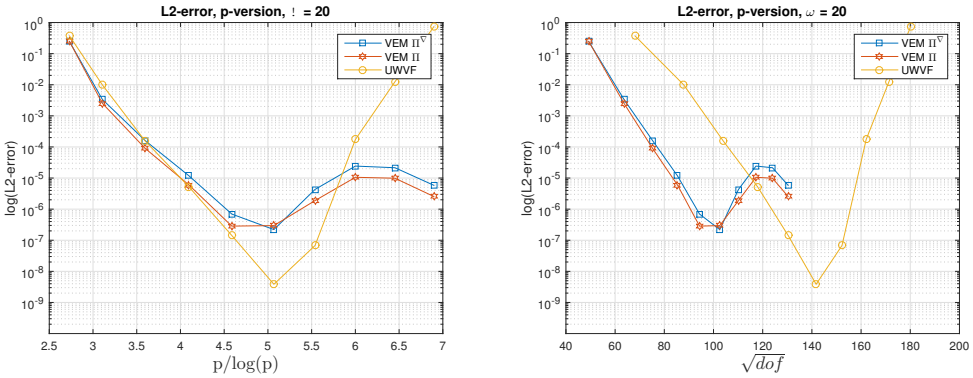

Figure 5: Approximating the smooth part of the Hankel function on triangular meshes.

6.3 The case of Voronoi Meshes

We apply the methods to problem (2.6) on the domain $\Omega = (0,1)^2$. In this section we consider Voronoi meshes made up of random, convex polygons. Two examples with different mesh size are shown in Figure 6. For investigating h-convergence, we fix the number of local plane wave functions to $p = 13$ and use Voronoi meshes with 2^n elements, $3 \leq n \leq 9$.

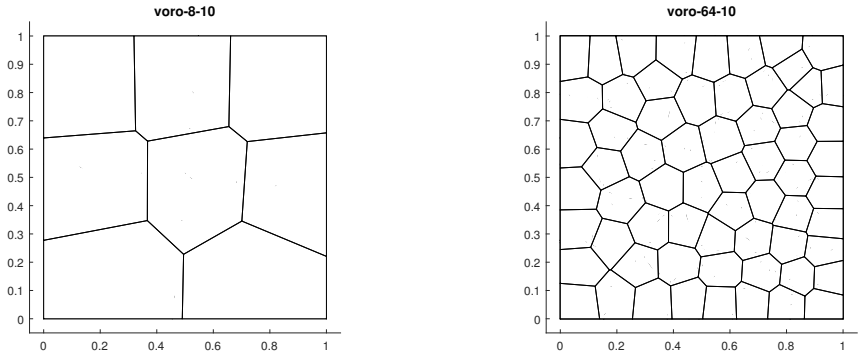

Figure 6: Voronoi mesh with 8 elements (left) and 64 elements (right).

As established, the number of degrees of freedom between the PW-DG method and PW-VEM differ. In case of the PW-DG method the number of degrees of freedom is the number of mesh elements times p, on the other hand for the PW-VEM it is the number of vertices times p. Thus, we will also compare the error versus the number of degrees of freedom. The degrees of freedom govern the matrix size and thus computational effort.

6.3.1 Smooth Solution

We consider the smooth solution given in (6.1), with a singularity outside of the domain.

Let us start with h-convergence analysis. Plotted in Figure 7 is the error with respect to the mesh diameter h. In the case of a small wave number, the projection onto plane waves Π clearly outperforms Π^∇. From Remark 4.6 we expected the convergence rate for the VEM to be $q + 1/2 = 6.5$, for $p = 2q + 1 = 13$. The top left graph in Figure 7 shows the appropriate slope and we see that the VEM reaches the expected convergence rate. In Remark 4.12 we were only able to predicted a convergence rate of $q - 1 = 5$ for the PW-DG method. As discussed in Remark 4.12 there is still room for improvement on the bounds: The PW-DG method exceeds its expected

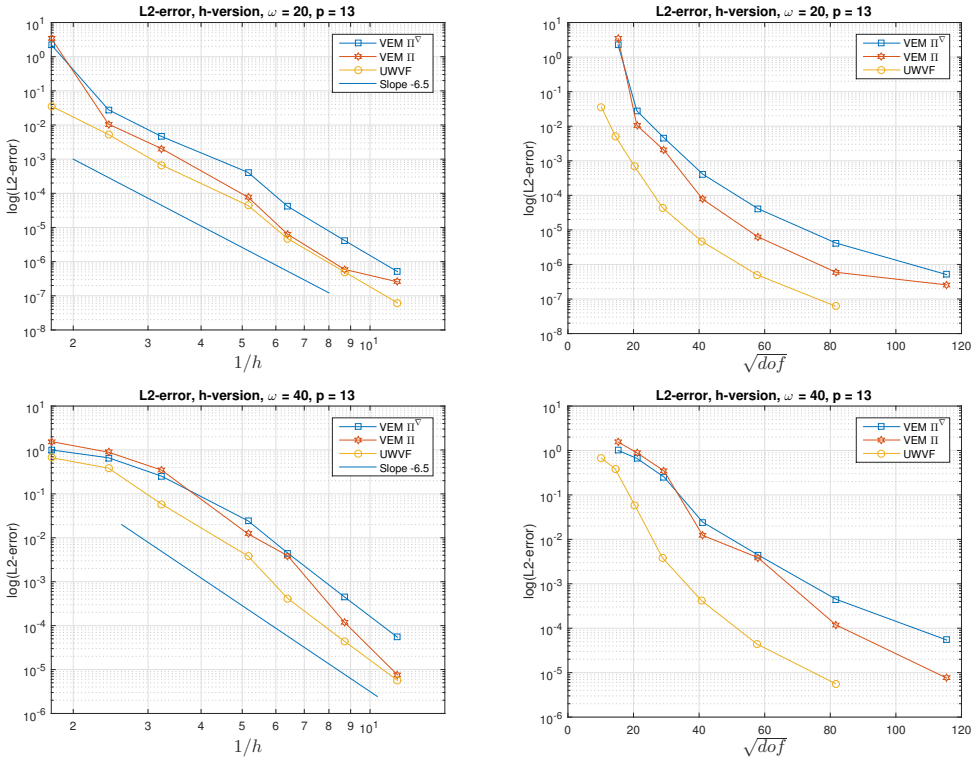

Figure 7: The h-error plotted against the mesh size (left) gives a good error comparison for each mesh, however since the trial spaces vary in size we also plot against the number of degrees of freedom (right). The parameters are chosen as ω=20 and $p = 13$.

rate, converging with a similar rate as the VEM. The PW-DG method produces a slightly smaller error throughout and keeps a better stability.

The figure on the top right reveals another advantage of the PW-DG method: with much less degrees of freedom the PW-DG method produces a better error.

Next, we consider a larger wave number. The overall error is larger than before, which complies with the observations in Remark 3.23, where we have noticed a worse performance of the error bound for larger wave numbers. As before, the PW-DG outperforms the VEM. Similar, the VEM Π performs better than the VEM Π^∇, with the exception of a pre-asymptomatic region. Notice, that we needed three iterations before the threshold condition was reached. Looking back at the previous example with $\omega = 20$, the first iteration of the VEM exhibits a large decrease of error similar to the plot in Figure 3. It appears that the VEM reaches the threshold during this iteration. Obviously, the PW-DG and the VEM have different thresholds, however both seem to abide by the laws established in Remark 3.23.

Let us continue by investigating p-convergence. The L^2-error for p ranging from 3 to 31 and a fixed Voronoi mesh with 16 elements is plotted in Figure 8. We consider the same two cases of wave numbers: $\omega = 20$ and $\omega = 40$. For $\omega = 40$ the pre-asymptotic region is larger then for $\omega = 20$ due to pollution, as expected. During this time the VEM Π^∇ performs worse than the VEM Π.

After the threshold is reached, the graphs reveal exponential convergence for all methods, which ensues from the fact that the solution has a smooth extension outside of the domain, as we have established in Remarks 3.22 and 4.12. As before the VEM Π now outperforms the VEM $\Pi 1\nabla$. The PW-DG keeps a slightly lower error throughout.

Finally, for large p we observe a sudden growth of the error, because the PW-basis suffers

from ill-conditioning. This is especially true for $\omega = 20$, whereas for $\omega = 40$ the basis becomes ill-conditioned slightly later.

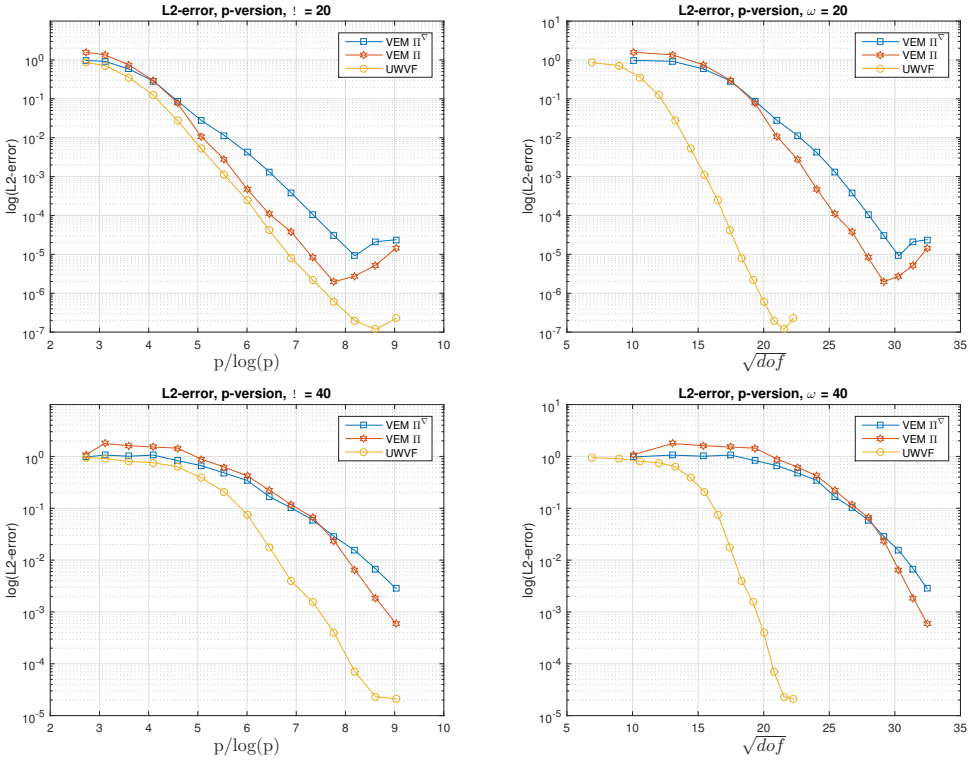

Figure 8: On a fixed mesh with 16 elements we compare the p-error rates for two different wave numbers: $\omega = 20$ (top) and $\omega = 40$ (bottom). On the left we plot the error against the plane wave degree p, on the right we plot against the square root of the degrees of freedom.

6.3.2 Singular Solution

The Hankel function has a singularity in the gradient at $(0, 0)$ as seen in Figure 4. As solution to be approximated we choose the Hankel function, given in (6.1), with $x_0 = (0, 0)$. We get a singularity in the gradient in the origin of our domain Ω. p- and h-convergence are documented for both methods in Figure 9.

The results behave according to the bounds, plotted in Figures 2 and 3 for a solution in H^5. After only a few iterations, the error reaches a lower bound and does not improve further. In the p-convergence case we can see a pre-asymptotic region, only after which the VEM Π catches up with the VEM Π^∇, as before. After the pre-asymptotic region the error stagnates almost instantly. Again, the PW-DG method succeeds with less degrees of freedom needed. All-in-all the methods behave very similar and converge to the same lower bound

The error improves only on a very small margin before seemingly stopping, making observations on the convergence speed difficult. To observe the behavior for non-analytic solutions further, we swap out the Hankel function for another solution.

We choose the boundary conditions, such that the solution u in polar coordinates $\boldsymbol{x} = (r\cos\theta, r\sin\theta)$ is given by

$$u(x) = J_\xi(\omega r)\cos(\xi\theta). \tag{6.2}$$

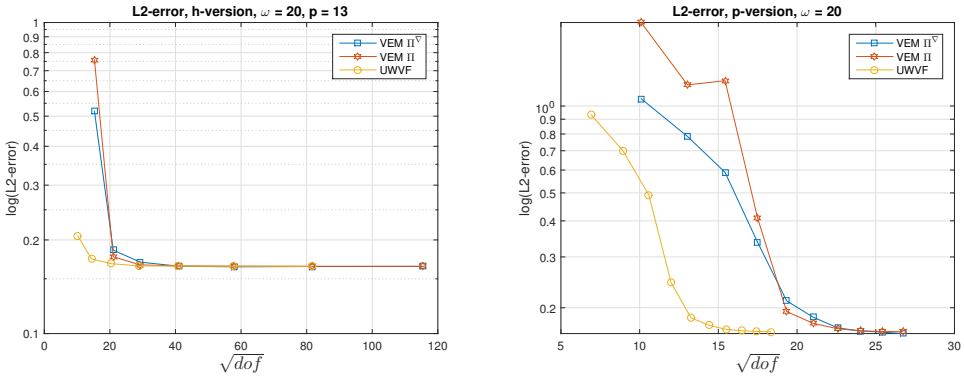

Figure 9: Approximating the Hankel function with a singularity at the origin.

Here, J_ξ denotes the Bessel function of the first kind and order $\xi \geq 0$. The order ξ controls the smoothness of the function: for $\xi \in \mathbb{N}$ the solution u is analytical, whereas if $\xi \notin \mathbb{N}$, its derivatives have a singularity at the origin. Then $u \in H^{\xi+1-\varepsilon}$ for $\varepsilon > 0$.

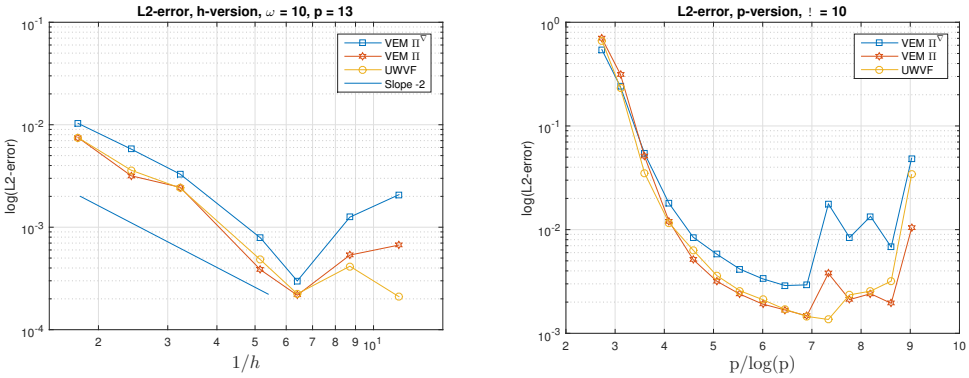

Figure 10: Approximating the Bessel function Equation (6.2) with $\xi = 3/2$.

In Figure 10 we consider the case $\xi = \frac{3}{2}$. To predict the convergence rate in h for the VEM we applying again Remark 4.6. This time the plane wave directions $q = 6$ are larger than the Sobolev space's order, thus Remark 4.6 with $m = \frac{3}{2} - \varepsilon$ predicts an h convergence of $2 - \varepsilon$. In the left graph, showing h-convergence, we have plotted a slope showing convergence speed of 2. Even though the theory predicts a slightly worse convergence speed, the results in this case to not comply, instead the convergence speed seems slightly faster.

In the case of p-convergence, we observe mere algebraic convergence. The solution clearly is not smooth enough to reach the exponential convergence as in the previous example. The error stagnates, reaching lower bound after which numerical error cause instability. This complies with the observation for solutions in lower order Sobolev spaces established in Remark 3.23.

In both cases, h- and p convergence, the basis becomes ill-condition towards the end, and the error behaves accordingly.

Comparing the results to the previous example, where the solution had a singularity in Ω, we notice that even though we still observe a lower bound for the error, the overall performance is much better already. Note, that this time $\omega = 10$ which also helps with the error.

We continue by considering the Bessel function with $\xi = \frac{2}{3}$. Now $u \in H^{\frac{5}{3}-\varepsilon}$ and the results plotted in Figure 11 behave as one would expect. h-convergence is slower and quite unstable. However, it seems to converge with a rate of $\frac{7}{6}$, as predicted by Remark 4.6. For p-convergence, the lowest error is reached after 4 iterations already, and performs worse than in the case $\xi = \frac{3}{2}$

by approximately a factor of 10. The overall error is larger than before, which we are to expect from the discussion in Remark 3.23.

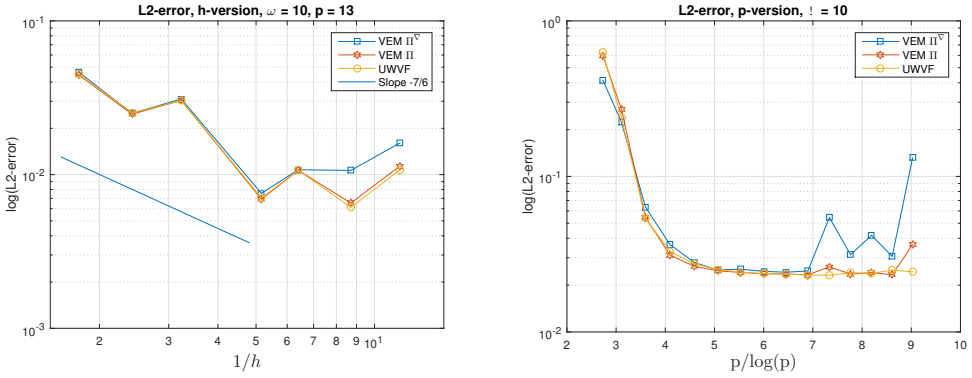

Figure 11: Approximating the Bessel function Equation (6.2) with $\xi = 2/3$.

6.3.3 Pollution Effect

In this section we aim to observe the pollution effect, which occurs if the product $\omega^2 h$ is not small enough to guarantee convergence. Recall that we require ωh to be uniformly bounded for the best approximation error of the plane wave approximation to converge to zero, as discussed in Remark 3.23. We can observe the pollution effect on h-convergence by choosing ω such that $\omega h = 3$ for every mesh. The results are reported in Figure 12: although the best approximation error converges to zero, as ωh is uniformly bounded, the PW-DG method, as well as the PW-VEM, fail to converge in this case. As discussed in Remark 4.3, for the case of the PW-VEM, the convergence of the methods requires the stronger condition of $\omega^2 h$ being small.

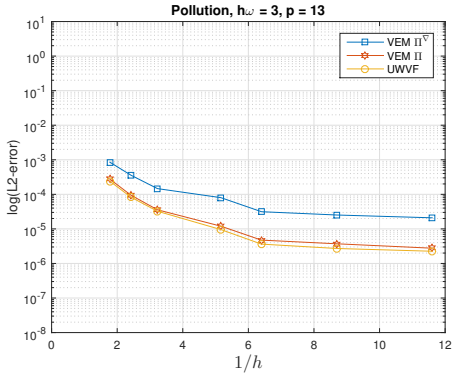

Figure 12: The pollution effect, observed by choosing the wave number such that $h\omega = 3$, for $p = 13$.

Clearly, both methods are affected by pollution in the same way. In the beginning there is some very slow convergence which stagnates quickly. PW-DG and VEM Π behave almost alike, whereas VEM Π^∇ shows a larger error, but the same qualitative behavior.

6.4 Non-Convex Mesh

In Figure 13 the error of approximating the smooth part of the Hankel function on a non convex mesh, and said mesh, are plotted. The results are similar to the one obtained on Voronoi meshes,

note that the better error comes from the fact that for the p-convergence on Voronoi meshes we chose a mesh with only 16 elements, whereas this mesh consists of 100 elements. Instability of the error occurs earlier (at around $q = 10$ for the PW-DG and $q = 8$ for the VEM) than in previous examples, due to the small elements contained in this mesh.

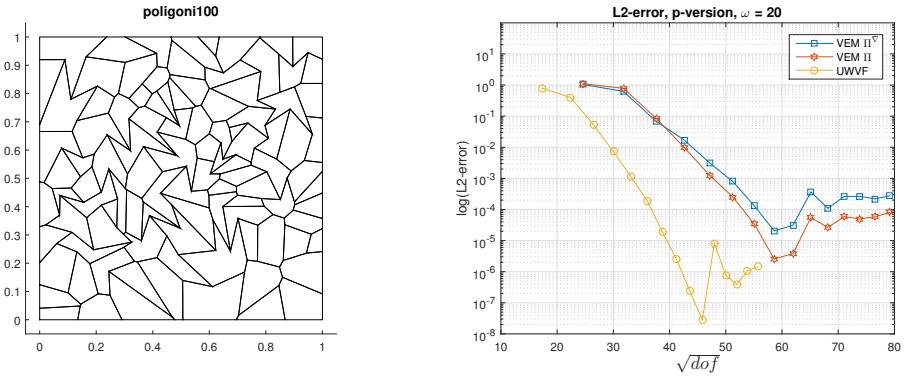

Figure 13: p-convergence results (right) for approximating the smooth part of the Hankel function on a mesh with non-convex polygons (left).

6.5 Escher Mesh

Finally, we consider the mesh shown in Figure 14 approximating the smooth part of the Hankel function. The mesh consists of only 4 elements, however with 225 vertices. We have to restrict $p = 3, \ldots, 11$ because of the heavy computational effort needed for the VEM. As seen in the right Figure 14, the VEM produces a lot mode degrees of freedom, resulting in long computational time. Given the very small p and the large mesh size the performance is as expected.

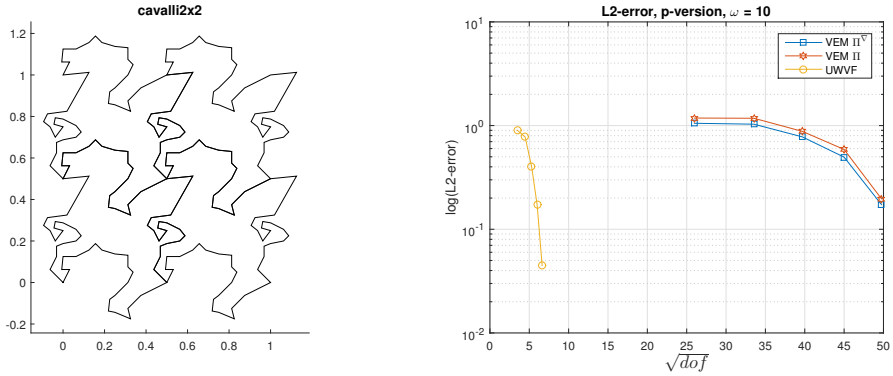

Figure 14: p-convergence (right) for approximating the smooth part of the Hankel function for the mesh on the left.

7 Conclusions

We have presented and compared the PW-VEM and the PW-DG method, setting the DG parameters to mimic the UWVF. The convergence analysis of the PW-VEM covered algebraic h-convergence under the assumption that $\omega^2 h$ is small enough. On the other hand, the convergence analysis for the DG method covered algebraic p-convergence, which turns exponential for solutions that are smooth enough (proven only on graded meshes).

The numeric results clearly back up the theory, as we observed. In general each plot could be split into three regions of behaviour:

- a pre-asymptotic region caused by pollution, matching the requirements from the theory,
- a region of algebraic h- and p-convergence, and exponential p-convergence when choosing a analytical solution, and
- instability due to ill-conditioning of basis and round off errors.

Reviewing the best approximation results for plane waves, and analysing the error bounds, gave another fitting outlook on what to expect from the numeric results.

Furthermore, we were able to compare two methods of evaluating the solution of the PW-VEM. Surprisingly, the simpler method of using the projection onto the (smaller) PW space was able to outperform the projection onto the plane wave space enriched with polynomials. All-in-all the PW-DG method showed better error approximation properties and, due to the need of less degrees of freedom on polynomials meshes, also required less computational time.

On the other hand, there is still room for improvement of the PW-VEM: by designing a better stabilization term or by devising more accurate reconstructions of the numerical solution in the element interiors.

A Appendix

A.1 Properties of the Bessel Function

$$\frac{\partial}{\partial z}J_0(z) = -J_1(z) \qquad \frac{\partial}{\partial z}(zJ_1(z)) = zJ_0(z) \tag{A.1}$$

$$|J_\nu(z)| \leq \frac{e^{|Im(z)|}}{\Gamma(\nu+1)}\left(\frac{|z|}{2}\right)^\nu \qquad \forall \nu > -\frac{1}{2},\ z \in \mathbb{C} \tag{A.2}$$

$$|J_j(t)| \leq 1 \qquad \forall j \in \mathbb{Z},\ t \in \mathbb{R} \tag{A.3}$$

$$\frac{\partial^\ell}{\partial z^\ell}J_n = \frac{1}{2^\ell}\sum_{m=0}^{\ell}(-1)^m \binom{\ell}{m} J_{2m-\ell+n}(z) \tag{A.4}$$

A.2 Matlab Code

Code for calculating interior and boundary matrices for the DG method (compare Section 5.2)

```
function [A_int, A_ext] = assemble_local_interior_matrices( v1, v2, c_int, c_ext,
    ↪ pwdirections, Dati,  alpha, beta  )
% returns two block matrices of size (ndir x ndir)
% corresponding to the interior edge integral over the chosen basis and
% test functions for one element.
% In the globel matrix the rows correspond to the chosen test function
% and the colloms to the basis functions. We sort the output matrices:
%             A_loc = [A_int, A_ext]
% where A_int belongs into A(P_int_block, P_int_block)
%       A_ext belongs into A(P_int_block, P_ext_block)
%

% Note: A_ext has basis fct on P_ext and test fct on P_int
%


    %prepare constants
    ndir = pwdirections.ndirections;
    dir = pwdirections.directions;
    w = Dati.wavenumber;
    im = sqrt(-1);
    normaledge = [ v2(2) - v1(2) ; -v2(1) + v1(1) ] / norm(v2-v1);

    A_int = zeros(ndir);
    A_ext = zeros(ndir);

    for i = 1:ndir
        for j = 1:ndir
            di = dir(:,i);
            dj = dir(:,j);
            d = dj-di;
            %prepare centering for basis functions
            c_i = exp(-im*w*(transpose(d)*c_int));
            c_e = exp(-im*w*( transpose(dj)*c_ext-transpose(di)*c_int ));

            intexp = exp(im*w*dot(d,v1)) * norm(v2-v1) * calc_integral(im*w*dot(d,(
                ↪ v2-v1)));

            A_int(i,j) = ( - 0.5*dot(di,normaledge)...
            - 0.5*dot(dj,normaledge)...
            + alpha ...
            + beta * dot(dj,normaledge)*dot(di,normaledge)...
```

```
            ) * im * w * c_i * intexp;

            A_ext(i,j) = ( - 0.5*dot(di,normaledge)...
            - 0.5*dot(dj,normaledge)...
            - alpha...
            - beta * dot(dj,normaledge) * dot(di,normaledge)...
            ) * im * w * c_e * intexp;
        end
    end

end
```

```
function [B] = assemble_local_boundary_matrices( v1, v2, c, pwdirections, Dati,
    ↪ delta  )
% returns four block matrices of size (ndir x ndir)
% corresponding to the boundary edge integral over the chosen basis and
% test functions.


    %prepare constants
    ndir = pwdirections.ndirections;
    dir = pwdirections.directions;
    w = Dati.wavenumber;
    normaledge = [ v2(2) - v1(2) ; -v2(1) + v1(1) ] / norm(v2-v1);
    im = sqrt(-1);

    B = zeros(ndir);

    for i = 1:ndir
        for j = 1:ndir
            di = dir(:,i);
            dj = dir(:,j);
            d = dj - di;
            %prepare centering for basis functions
            c_int = exp(-im*w*dot(d,c));

            intexp = exp(im*w*dot(d,v1)) * norm(v2-v1) * calc_integral(im*w*dot(d,(
                ↪ v2-v1)));

            B(i,j) = (  - (1-delta)*dot(di,normaledge)...
            - delta*dot(dj,normaledge)...
            + (1-delta)...
            + delta * dot(dj,normaledge)*dot(di,normaledge)...
            )*im*w*c_int*intexp;
        end
    end

end
```

```
function [result] = calc_integral( x )
% this function returns int_0^1 exp(x*t) dt
    if abs(x)>10*eps
        result = (exp(x)-1)/x;
        elseif x~=0 && abs(x)<=10*eps %treat small arguments
        result = expm1(x)/log1p(expm1(x));
    else
        result = 1;
    end
end
```

References

[1] R.A. Adams and J.J.F. Fournier, *Sobolev spaces*, Pure and Applied Mathematics, Elsevier Science, 2003.

[2] B. Ahmad, A. Alsaedi, F. Brezzi, L. D. Marini, and A. Russo, *Equivalent projectors for virtual element methods*, Comput. Math. Appl. **66** (2013), no. 3, 376–391.

[3] L. Beirão da Veiga, F. Brezzi, A. Cangiani, G. Manzini, L. D. Marini, and A. Russo, *Basic principles of virtual element methods*, Mathematical Models and Methods in Applied Sciences **23** (2013), no. 01, 199–214.

[4] L. Beirão da Veiga, F. Brezzi, L. D. Marini, and A. Russo, *The hitchhiker's guide to the virtual element method*, Mathematical Models and Methods in Applied Sciences **24** (2014), no. 08, 1541–1573.

[5] J. H. Bramble and L. E. Payne, *Bounds in the neumann problem for second order uniformly elliptic operators.*, Pacific J. Math. **12** (1962), no. 3, 823–833.

[6] S. Brenner and R. Scott, *The mathematical theory of finite element methods*, Texts in Applied Mathematics, Springer New York, 2007.

[7] A. Buffa and P. Monk, *Error estimates for the ultra weak variational formulation of the Helmholtz equation*, ESAIM: Mathematical Modelling and Numerical Analysis **42** (2008), no. 6, 925–940 (eng).

[8] Olivier Cessenat and Bruno Despres, *Application of an ultra weak variational formulation of elliptic pdes to the two-dimensional Helmholtz problem*, SIAM Journal on Numerical Analysis **35** (1998), no. 1, 255–299.

[9] David Colton and Rainer Kress, *Inverse acoustic and electromagnetic scattering theory, second edition*, 1998.

[10] L.C. Evans, *Partial differential equations*, Graduate studies in mathematics, American Mathematical Society, 2010.

[11] Walter Gautschi, *On inverses of vandermonde and confluent vandermonde matrices iii*, Numerische Mathematik **29** (1978), no. 4, 445–450.

[12] D. Gilbarg and N.S. Trudinger, *Elliptic partial differential equations of second order*, Grundlehren der mathematischen Wissenschaften, Springer, 1998.

[13] Gittelson, Claude J., Hiptmair, Ralf, and Perugia, Ilaria, *Plane wave discontinuous Galerkin methods: Analysis of the h-version*, ESAIM: M2AN **43** (2009), no. 2, 297–331.

[14] R. Hiptmair, A. Moiola, and I. Perugia, *Plane wave discontinuous Galerkin methods for the 2d Helmholtz equation: Analysis of the p-version*, SIAM Journal on Numerical Analysis **49** (2011), no. 1, 264–284.

[15] R. Hiptmair, A. Moiola, and I. Perugia, *Plane wave discontinuous Galerkin methods: Exponential convergence of the hp-version*, Foundations of Computational Mathematics **16** (2016), no. 3, 637–675.

[16] R. Hiptmair and I. Perugia, *Plane wave discontinuous Galerkin methods*, Tech. report, Isaac Newton Institute Cambridge, 2007.

[17] Ralf Hiptmair, Andrea Moiola, and Ilaria Perugia, *A survey of trefftz methods for the Helmholtz equation*, 2015.

[18] R. Leis, *Initial boundary value problems in mathematical physics*, Teubner, 1986.

[19] J. M. Melenk and I. Babuška, *The partition of unity finite element method: Basic theory and applications*, 1996.

[20] J.M. Melenk, *On generalized finite element methods*, University of Maryland at College Park, 1995.

[21] ———, *Operator adapted spectral element methods i: harmonic and generalized harmonic polynomials*, Numerische Mathematik **84** (1999), no. 1, 35–69.

[22] A. Moiola, R. Hiptmair, and I. Perugia, *Plane wave approximation of homogeneous Helmholtz solutions*, Zeitschrift für angewandte Mathematik und Physik **62** (2011), no. 5, 809.

[23] ———, *Vekua theory for the Helmholtz operator*, Zeitschrift für angewandte Mathematik und Physik **62** (2011), no. 5, 779.

[24] Andrea Moiola, Ralf Hiptmair, and Ilaria Perugia, *Approximation by plane waves*, Dipartimento di Matematica, Università di Pavia, IMATI-CNR, Pavia, 2010.

[25] Ilaria Perugia, Paola Pietra, and Alessandro Russo, *A plane wave virtual element method for the Helmholtz problem*, 2015.